Seminario Internacional nanociencia 2010

Computation of local and averaged stresses in nanosize specimens

Alejandro A. Pacheco Sanjuán, Ph.D.

Universidad del Norte

Mechanical Engineering Department, Barranquilla, Colombia.

Materials Processing and Design Group (GIMYP)

CENM ACCEFYN funlaci UNIVERSIDAD DEL NORTE

October 22/ 2010

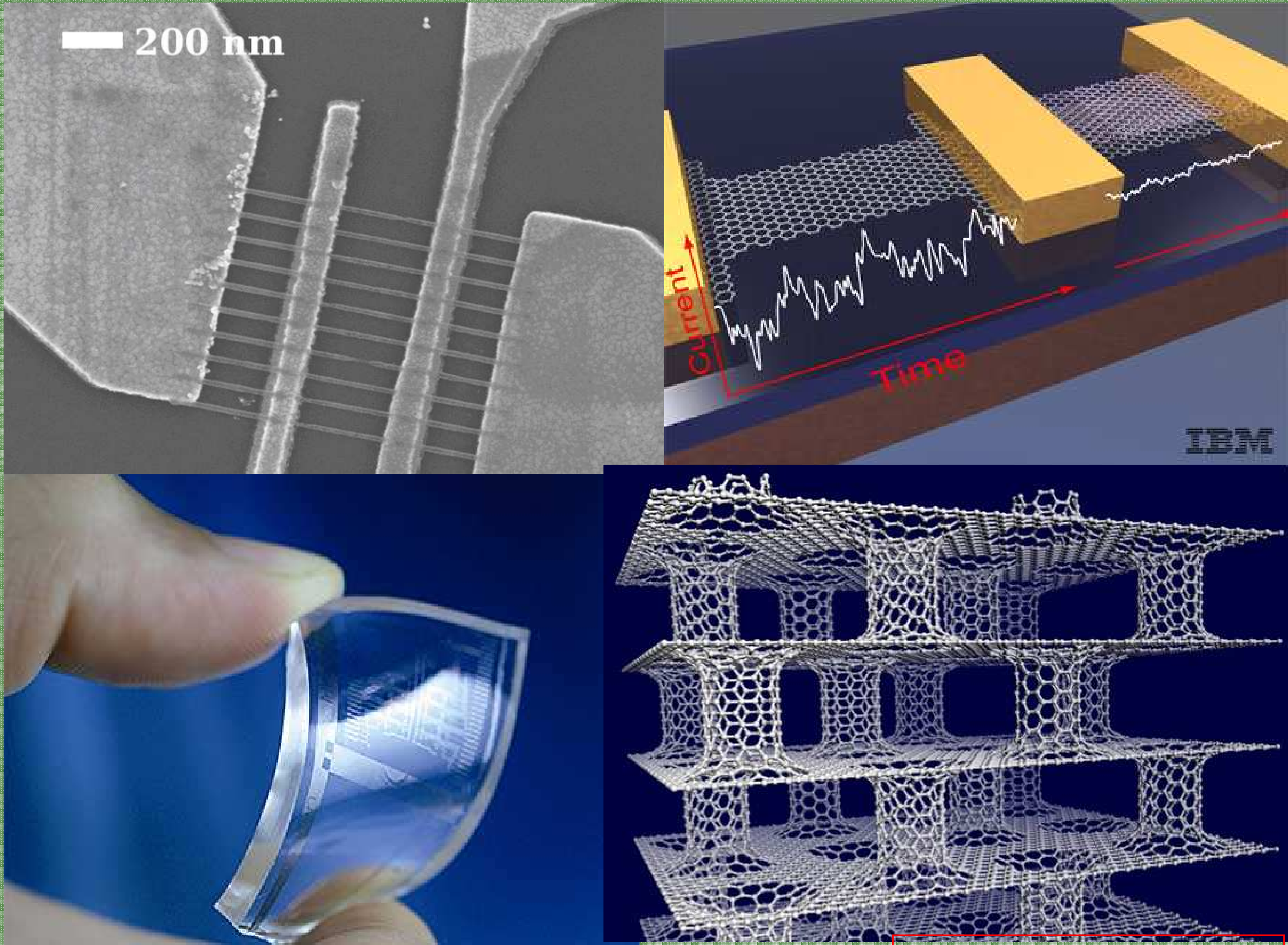

Structures at nanoscale

Nano-structured materials for engineering applications

Young's modulus (E); Tensile yield stress (σ_y).

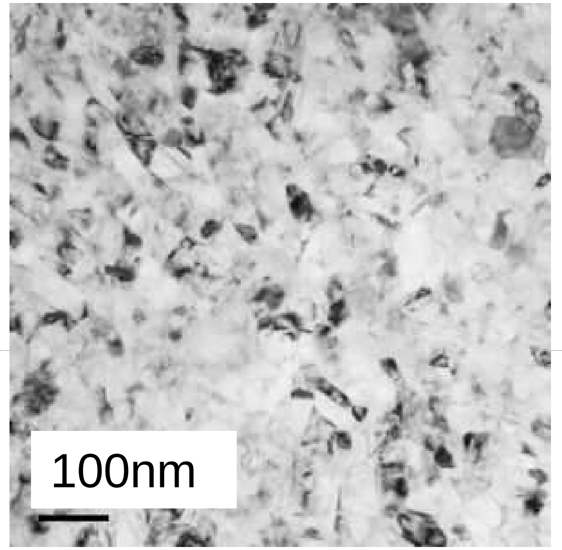

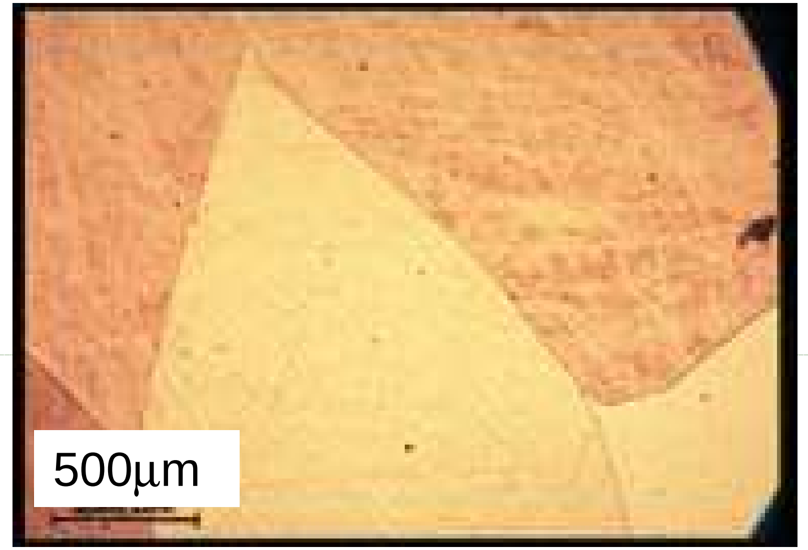

Nano-crystalline copper (Cu)

Average grain size < 100 nm

E ~ 120 GPa

σ_y ~ 0.3 - 1 GPa

Coarse grained Cu

Average grain size ~ 1μm

E ~ 110 - 128 GPa

σ_y ~ 100 MPa

Nano-structured material for engineering applications

Youngn's modulus (E); Tensile yield stress (σ_y)

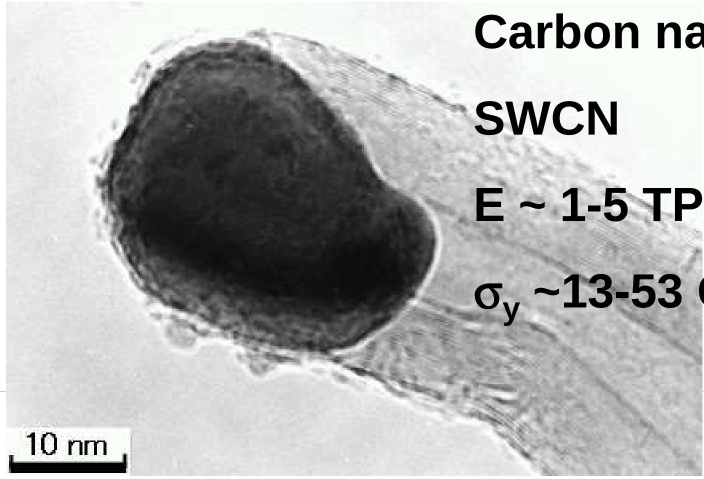

Carbon nanotubes

SWCN

E ~ 1-5 TPa

σ_y ~13-53 GPa

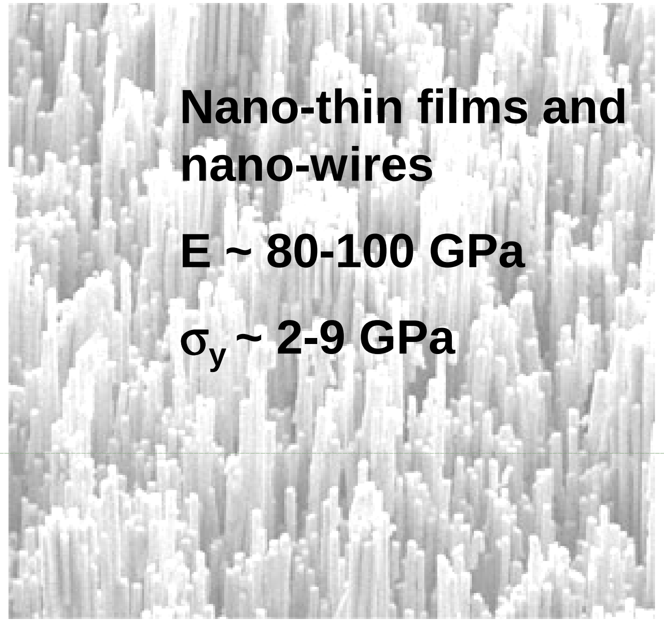

Nano-thin films and nano-wires

E ~ 80-100 GPa

σ_y ~ 2-9 GPa

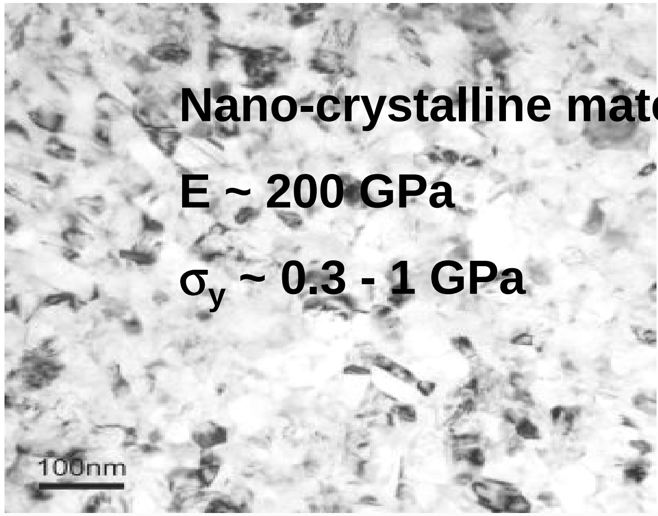

Nano-crystalline materials

E ~ 200 GPa

σ_y ~ 0.3 - 1 GPa

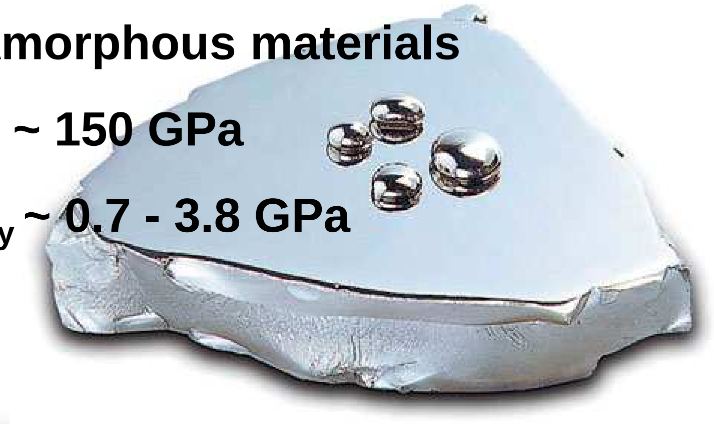

Amorphous materials

E ~ 150 GPa

σ_y ~ 0.7 - 3.8 GPa

Potential benefits of nano-structured materials

- High strength / weight ratio
- High corrosion resistance
- Noise damping
- Reduce manufacturing costs
- Improve recyclability

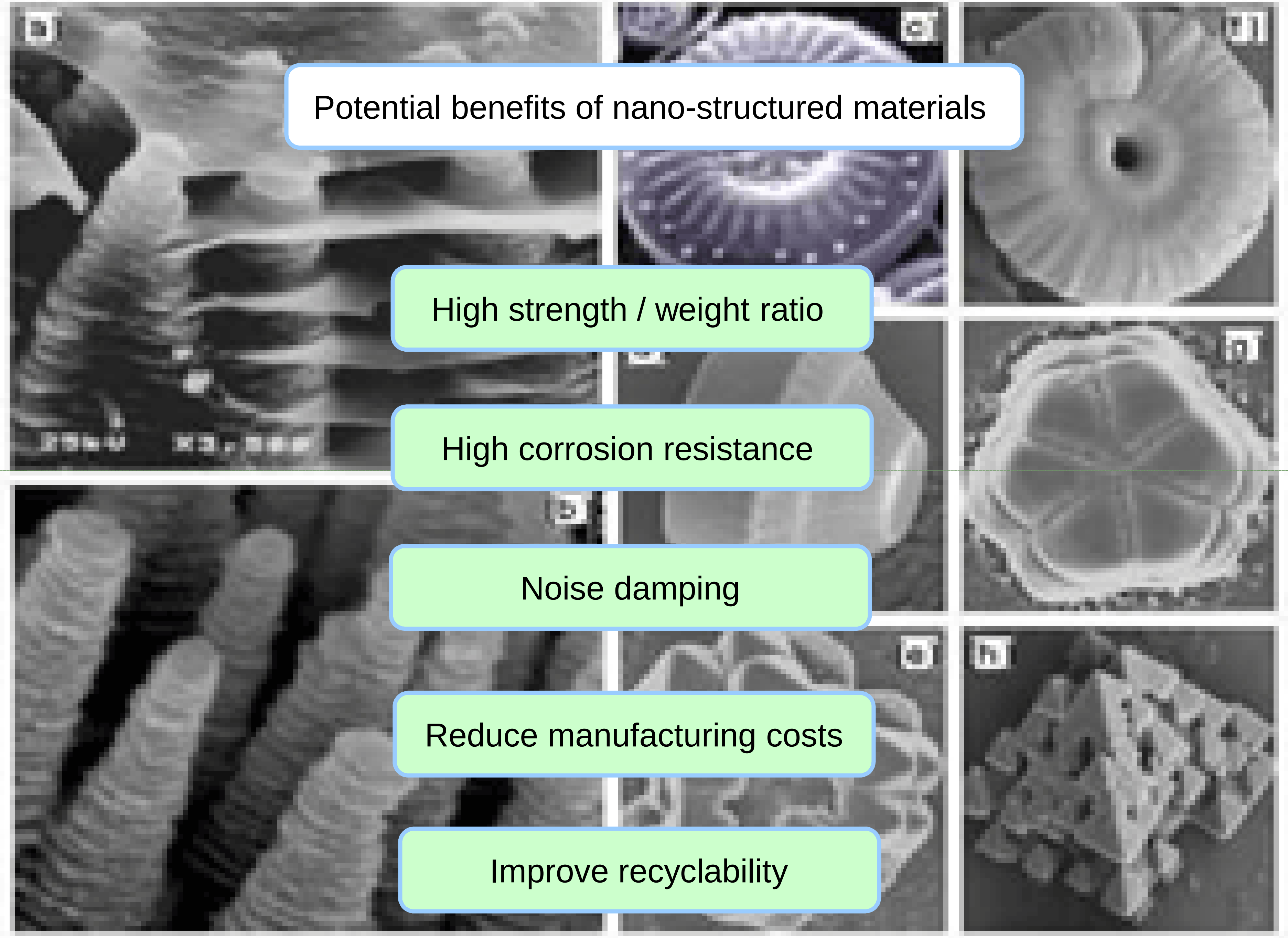

http://www.sandia.gov/news-center/news-releases/2003/mat-chem/nanocrystals.html

Deformation mechanisms at different length scales

Ab-Initio (electrons)

$(1nm)^3$: 0 – 1ps

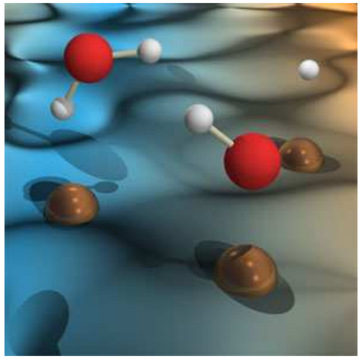

Continuum

(Phenomenological theories)

$(100\ \mu m)^3 – (1m)^3$: ms - h

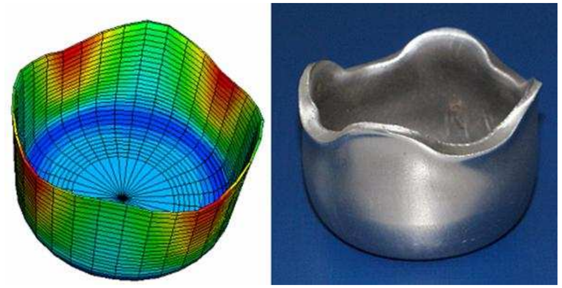

Dislocation dynamics

(defects)

$(\mu m)^3$: ns - s

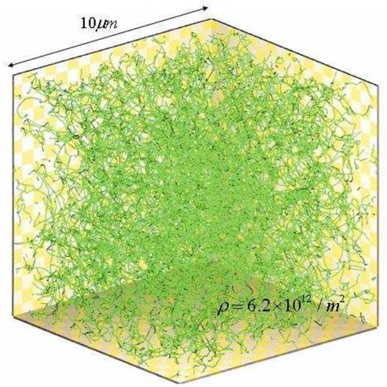

Atomic scale (atoms)

$(1\ nm)^3$ - $(100\ nm)^3$: ns

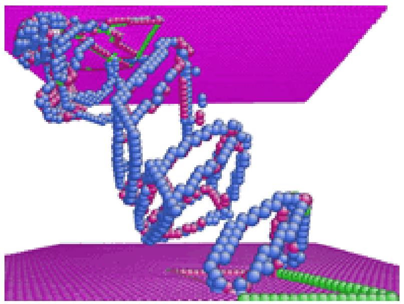

Meso-scale (poly-crystalline materials)

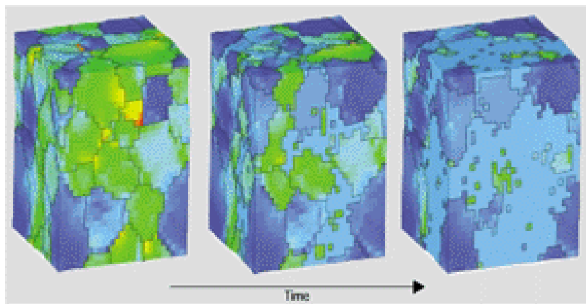

Deformation mechanisms

The mechanical concept of stress

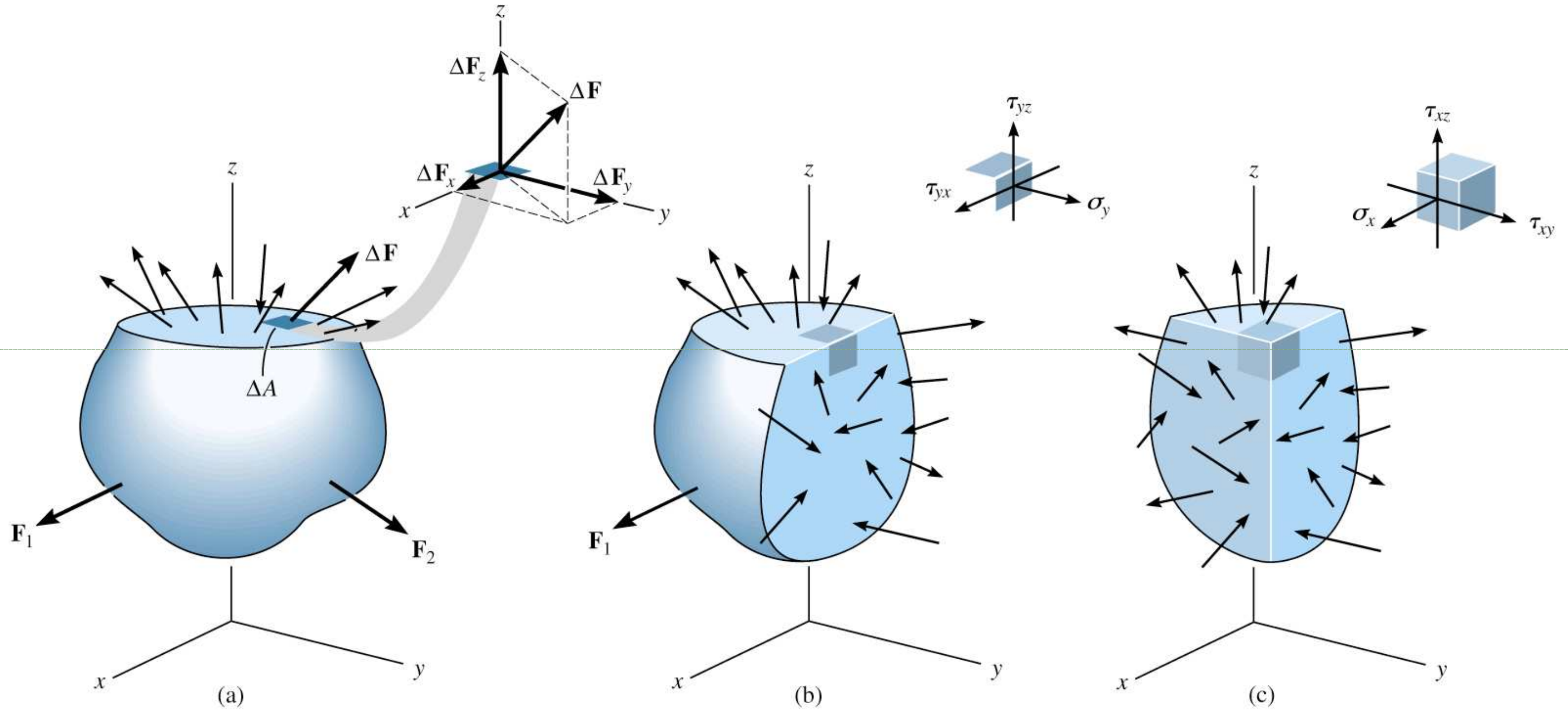

The inertia tensor

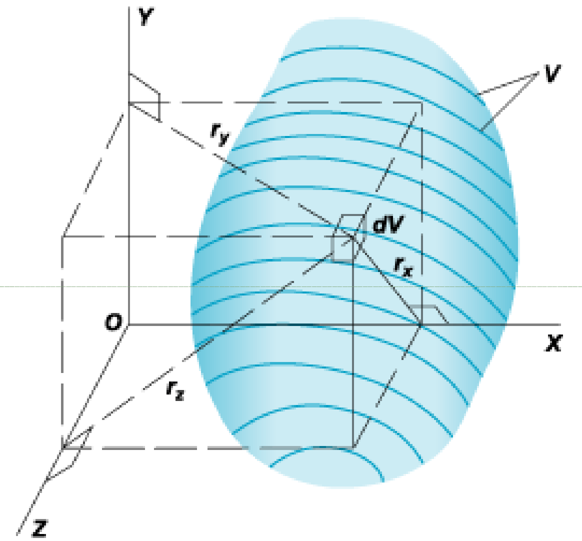

$$I_{\alpha\beta} = \int_{\Omega} \left((\rho x_{\phi} x_{\phi}) \delta_{\alpha\beta} - \rho x_{\alpha} x_{\beta} \right) d\Omega$$

$$\frac{d\left(I_{\alpha\beta}\right)}{dt} = \frac{d}{dt} \int_{\Omega} \left((\rho x_{\phi} x_{\phi}) \delta_{\alpha\beta} - \rho x_{\alpha} x_{\beta} \right) d\Omega$$

The virial of Clausius (1870):

$$G_{\alpha\beta} = \frac{1}{2} \frac{d\left(I_{\alpha\beta}\right)}{dt} = \int_{\Omega} \left(\rho x_{\phi} v_{\phi} \delta_{\alpha\beta} - \frac{1}{2} \rho \left(v_{\alpha} x_{\beta} + x_{\alpha} v_{\beta} \right) \right) d\Omega$$

Conservation laws in continuum mechanics

- Conservation of Mass
- Conservation of Linear Momentum
- Conservation of Angular Momentum
- Conservation of Energy

Conservation of linear momentum

- It requires that the rate of change of the linear momentum, in any part of a body, should equal to the force acting on the part

Linear momentum: $\int \frac{\partial x(X,t)}{\partial t} \rho(X) dV(X)$

Rate of change:

$$\frac{d}{dt}\int \frac{\partial x(X,t)}{\partial t} \rho(X) dV(X) = \int \frac{\partial^2 x(X,t)}{\partial t^2} \rho(X) dV(X)$$

Forces

- Nominal density of body force

$$\boldsymbol{b}(\boldsymbol{x},\boldsymbol{t})=\frac{\text{force in the current state}}{\text{volume in the current state}}$$

- Nominal traction

$$\boldsymbol{t}(\boldsymbol{x},\boldsymbol{t})=\frac{\text{force in the current state}}{\text{area in the current state}}$$

- Conservation of linear momentum

$$\int_{\partial\Omega}\boldsymbol{t}(\boldsymbol{x},\boldsymbol{t})\boldsymbol{dA}+\int_{\Omega}\boldsymbol{b}(\boldsymbol{x},\boldsymbol{t})\boldsymbol{d\Omega}=\frac{\boldsymbol{d}}{\boldsymbol{dt}}\int_{\Omega}\rho(\boldsymbol{x},\boldsymbol{t})\frac{\partial x}{\partial \boldsymbol{t}}\boldsymbol{d\Omega}$$

The virial of Clausius - continuum system

$$\frac{d(G_{\alpha\beta})}{dt} = \frac{d}{dt}\int_{\Omega}\left(\rho x_{\phi} v_{\phi}\delta_{\alpha\beta} - \frac{1}{2}\rho\left(v_{\alpha}x_{\beta} + x_{\alpha}v_{\beta}\right)\right)d\Omega$$

$$\frac{d(G_{\alpha\beta})}{dt} = \int_{\partial\Omega} x_{\phi}t_{\phi}\delta_{\alpha\beta}dA + \int_{\Omega} x_{\phi}\rho b_{\phi}\delta_{\alpha\beta}dA - 1/2\int_{\partial\Omega}\left(t_{\alpha}x_{\beta} + t_{\beta}x_{\alpha}\right)d\Omega\ldots$$

$$-1/2\int_{\Omega}\left(\rho b_{\alpha}x_{\beta} + \rho x_{\alpha}b_{\beta}\right)d\Omega - \boxed{\int_{\Omega}\sigma_{\phi\phi}\delta_{\alpha\beta}d\Omega + \int_{\Omega}\sigma_{\alpha\beta}\,d\Omega\ldots}$$

$$+\int_{\Omega}\left(\rho v_{\phi}v_{\phi}\delta_{\alpha\beta} - \rho v_{\alpha}v_{\beta}\right)d\Omega$$

The virial of Clausius - discrete system

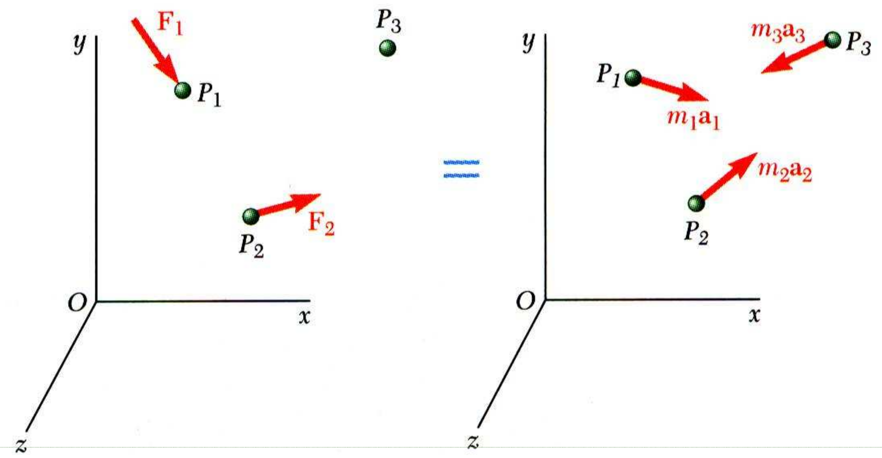

$$I_{\alpha\beta} = \sum_{k=1}^{N} m^{(k)} \left(r_{\phi}^{(k)} r_{\phi}^{(k)} \delta_{\alpha\beta} - r_{\alpha}^{(k)} r_{\beta}^{(k)} \right)$$

$$G_{\alpha\beta} = \frac{1}{2} \frac{dI_{\alpha\beta}}{dt} = \sum_{k=1}^{N} p_{\phi}^{(k)} r_{\phi}^{(k)} \delta_{\alpha\beta} - \frac{1}{2} p_{\alpha}^{(k)} r_{\beta}^{(k)} - \frac{1}{2} r_{\alpha}^{(k)} p_{\beta}^{(k)}$$

Continuum discrete equivalence

$$\sum_{k=1}^{N} p_{\phi}^{(k)} v_{\phi}^{(k)} \delta_{\alpha\beta} \rightarrow \int_{\Omega} \rho v_{\phi} v_{\phi} \delta_{\alpha\beta} d\Omega$$

$$-\sum_{k=1}^{N} p_{\alpha}^{(k)} v_{\beta}^{(k)} \rightarrow -\int_{\Omega} \rho v_{\alpha} v_{\beta} d\Omega$$

$$\sum_{k=1}^{N} {}^{i}f_{\phi}^{(k)} x_{\phi}^{(k)} \delta_{\alpha\beta} \rightarrow -\int_{\Omega} \sigma_{\phi\phi} \delta_{\alpha\beta} d\Omega$$

$$\sum_{k=1}^{N} {}^{e}f_{\phi}^{(k)} x_{\phi}^{(k)} \delta_{\alpha\beta} \rightarrow \int_{\partial\Omega} x_{\phi} t_{\phi} \delta_{\alpha\beta} dA + \int_{\Omega} x_{\phi} \rho b_{\phi} \delta_{\alpha\beta} d\Omega$$

$$-1/2 \sum_{k=1}^{N} {}^{e}f_{\alpha}^{(k)} x_{\beta}^{(k)} + {}^{e}f_{\beta}^{(k)} x_{\alpha}^{(k)} \rightarrow -1/2 \int_{\partial\Omega} \left(x_{\beta} t_{\alpha} + x_{\alpha} t_{\beta} \right) dA \ldots + \int_{\Omega} \left(x_{\beta} \rho b_{\alpha} + x_{\alpha} \rho b_{\beta} \right) d\Omega$$

$$\boxed{-1/2 \sum_{k=1}^{N} {}^{i}f_{\alpha}^{(k)} x_{\beta}^{(k)} + {}^{i}f_{\beta}^{(k)} x_{\alpha}^{(k)} \rightarrow \int_{\Omega} \sigma_{\alpha\beta} d\Omega}$$

The average stress tensor

$$\Omega\bar{\sigma}_{\alpha\beta} = \int_{\Omega} \sigma_{\alpha\beta} d\Omega$$

$$\Omega\bar{\sigma}_{\alpha\beta} = \int_{\partial\Omega} x_\alpha t_\beta dA + \int_{\Omega} \rho b_\beta x_\alpha d\Omega - \frac{d}{dt}\int_{\Omega} \rho v_\beta x_\alpha d\Omega + \int_{\Omega} \rho v_\beta v_\alpha d\Omega$$

$$\langle \ldots \rangle_T = \int_0^T () dt$$

$$\Omega\langle \bar{\sigma}_{\alpha\beta} \rangle_T = \left\langle \int_{\partial\Omega} x_\alpha t_\beta dA \right\rangle_T + \left\langle \int_{\Omega} \rho b_\beta x_\alpha d\Omega \right\rangle_T + \boxed{\left\langle \int_{\Omega} \rho v_\beta v_\alpha d\Omega \right\rangle_T}$$

The average stress tensor - relative motion

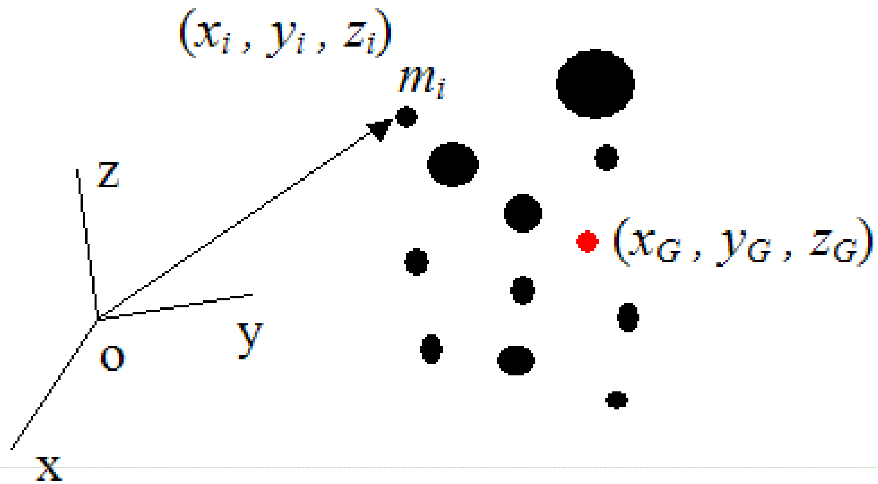

$$\Omega\left\langle \sigma_{\alpha\beta}\right\rangle_T = \left\langle \int_{\partial\Omega} \tilde{x}_\alpha t_\beta dA \right\rangle_T + \left\langle \int_{\Omega} \rho b_\beta \tilde{x}_\alpha d\Omega \right\rangle_T + \left\langle \int_{\Omega} \rho \tilde{v}_\beta \tilde{v}_\alpha d\Omega \right\rangle_T$$

$$\Omega\left\langle \sigma_{\alpha\beta}\right\rangle_T = \left\langle 1/2 \sum_{k=1}^{N} \left({}^e f_\alpha^{(k)} \tilde{x}_\beta^{(k)} + {}^e f_\beta^{(k)} \tilde{x}_\alpha^{(k)} \right) \right\rangle_T + \left\langle \sum_{k=1}^{N} m^{(k)} \tilde{v}_\alpha^{(k)} \tilde{v}_\beta^{(k)} \right\rangle_T$$

The average stress tensor – rotating disk

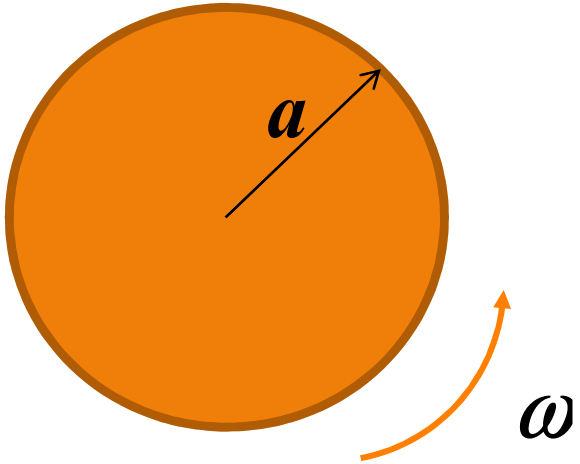

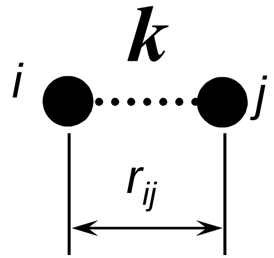

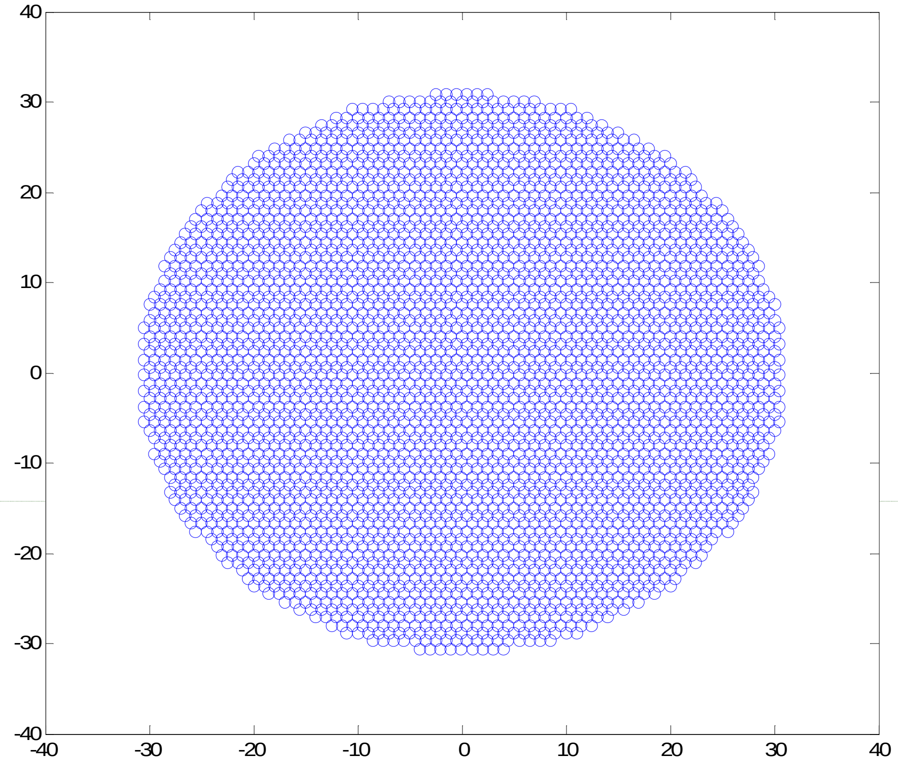

$$U_{Hooke} = \frac{k}{2}\left(\left|r^{(ij)}\right| - d\right)$$

N =3486
m = 1
k = 1
a = 30.9 *units*

The average stress tensor – rotating disk
Linear elasticity solution

$$\lambda = G = \sqrt{3/16k}$$

$$\sigma_{rr}(r) = \frac{\rho\omega^2}{12}\left(5a^2 - 5r^2\right), \quad \sigma_{\theta\theta}(r) = \frac{\rho\omega^2}{12}\left(5a^2 - 3r^2\right)$$

$$\bar{\sigma}_{\alpha\beta} = \frac{\rho\omega^2}{12\pi a^2}\int_0^{2\pi}\int_0^{a}\left(\begin{bmatrix} c\theta & s\theta \\ -s\theta & c\theta \end{bmatrix}^T \begin{bmatrix} 5a^2 - 5r^2 & 0 \\ 0 & 5a^2 - 3r^2 \end{bmatrix}\begin{bmatrix} c\theta & s\theta \\ -s\theta & c\theta \end{bmatrix}\right) r.dr.d\theta$$

$$\bar{\sigma}_{\alpha\beta} = \frac{\rho\omega^2 a^2}{4}\delta_{\alpha\beta} = 0.02774$$

The average stress tensor – rotating disk

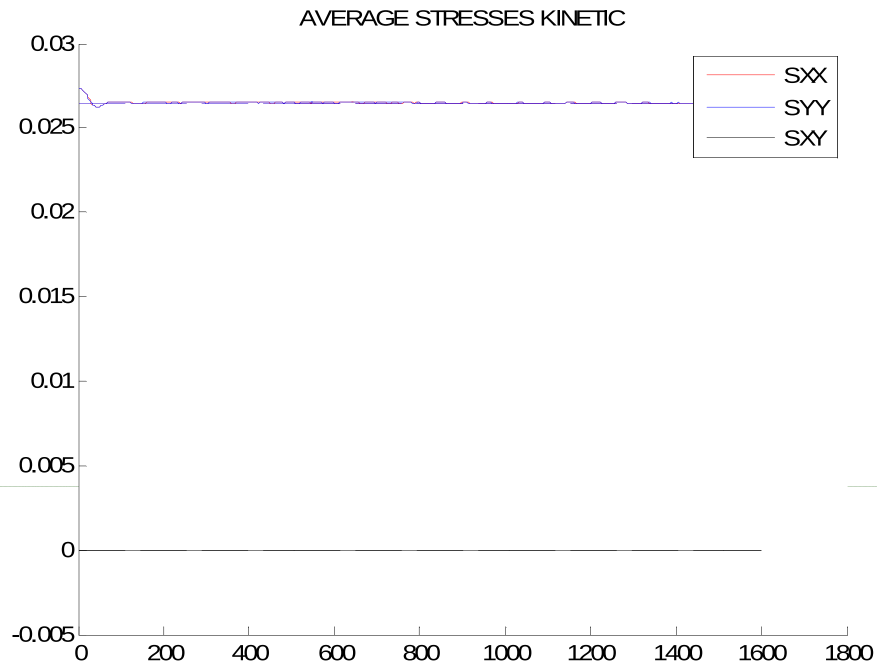

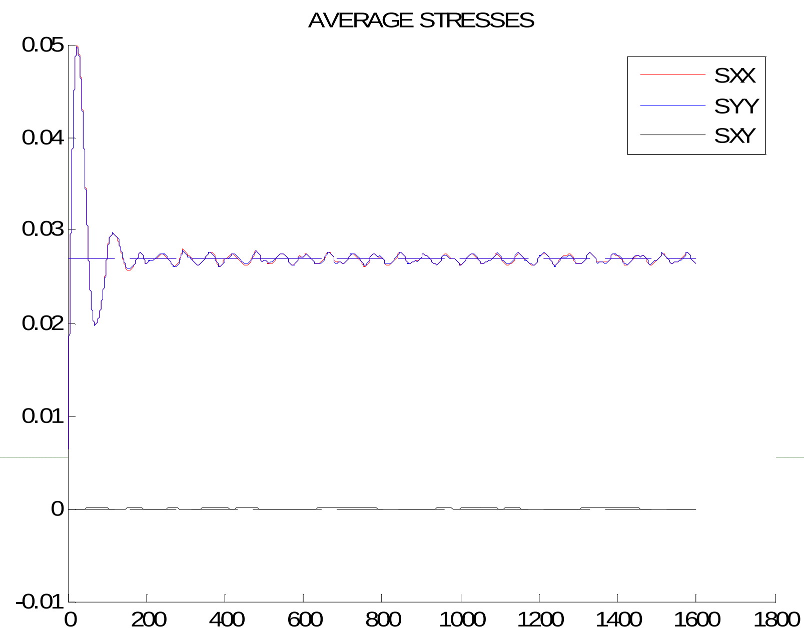

SXX_AVERAGE =0.0269
SYY_AVERAGE = 0.0269
SXY_AVERAGE = -1.2158e-006

SXX_AVERAGEKIN = 0.0265
SYY_AVERAGEKIN = 0.0265
SXY_AVERAGEKIN = 1.0716e-008

ω = 0.01 [rad/sg]
KT = 0.0
(reduced temperature)

$$\varepsilon_r \approx 1.5\%$$

The average stress tensor – rotating disk

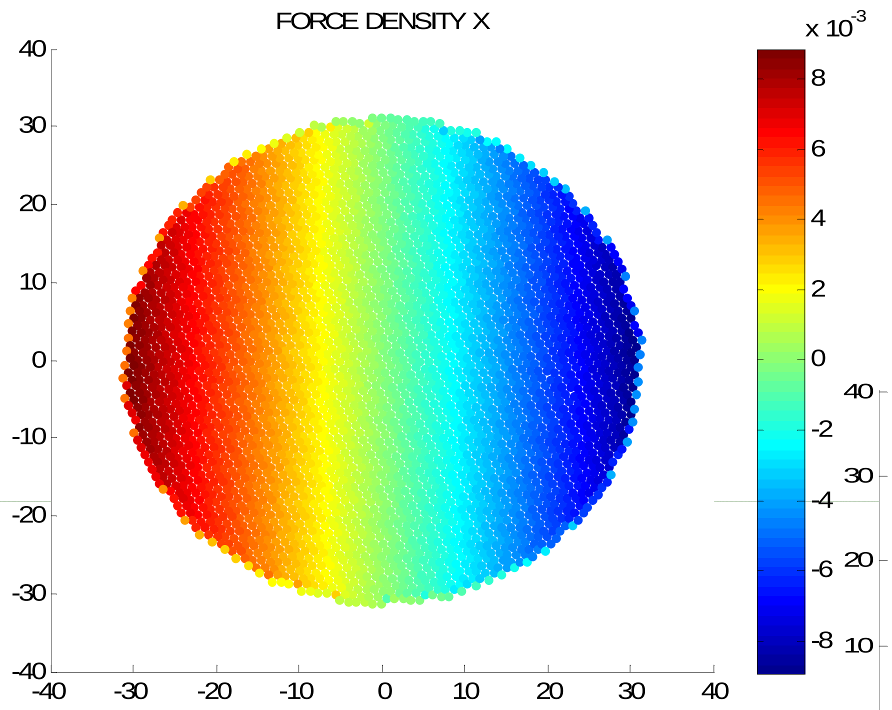

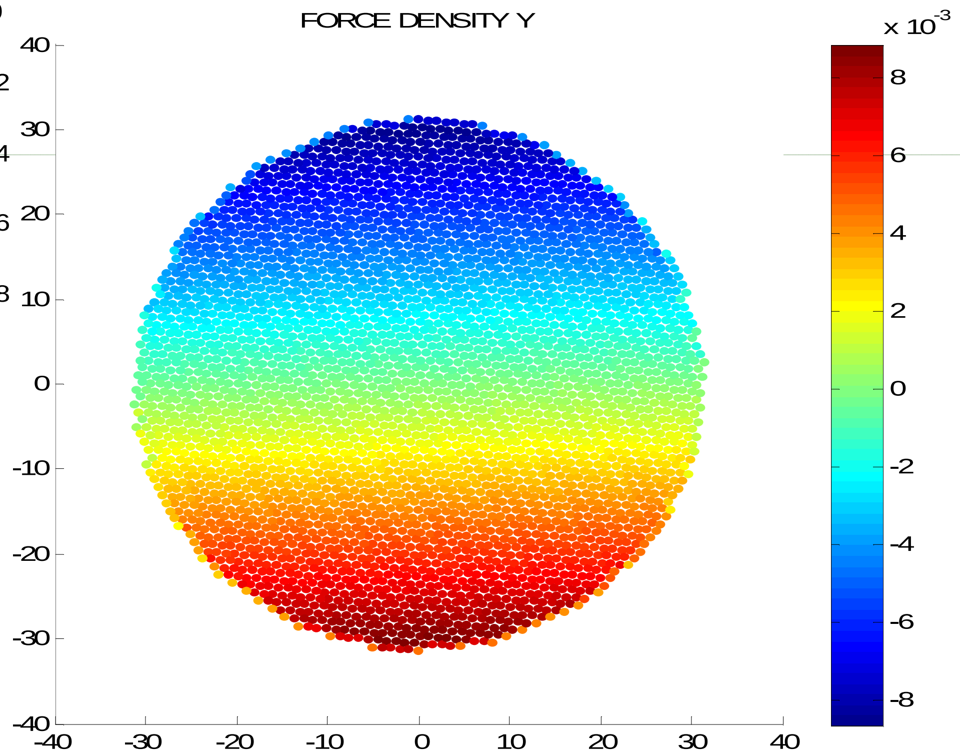

The average stress tensor – rotating disk

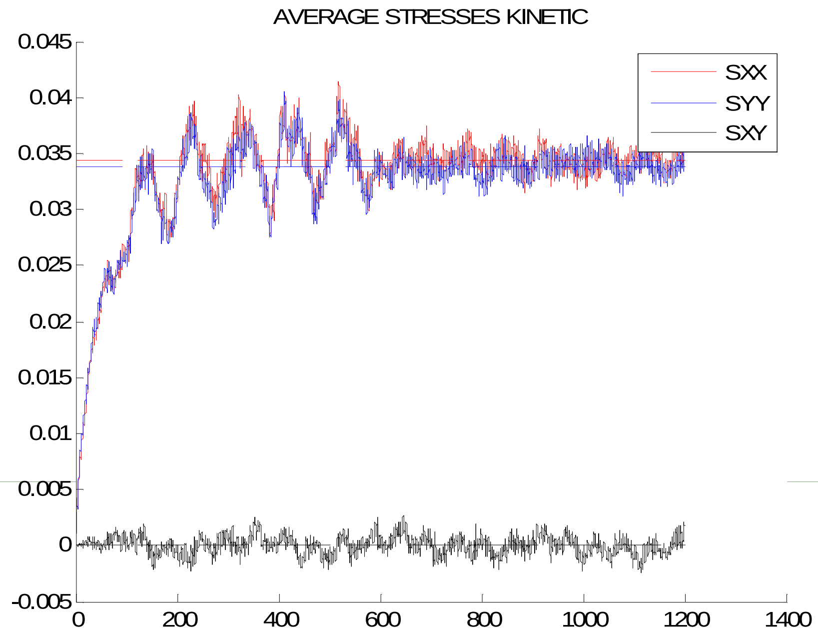

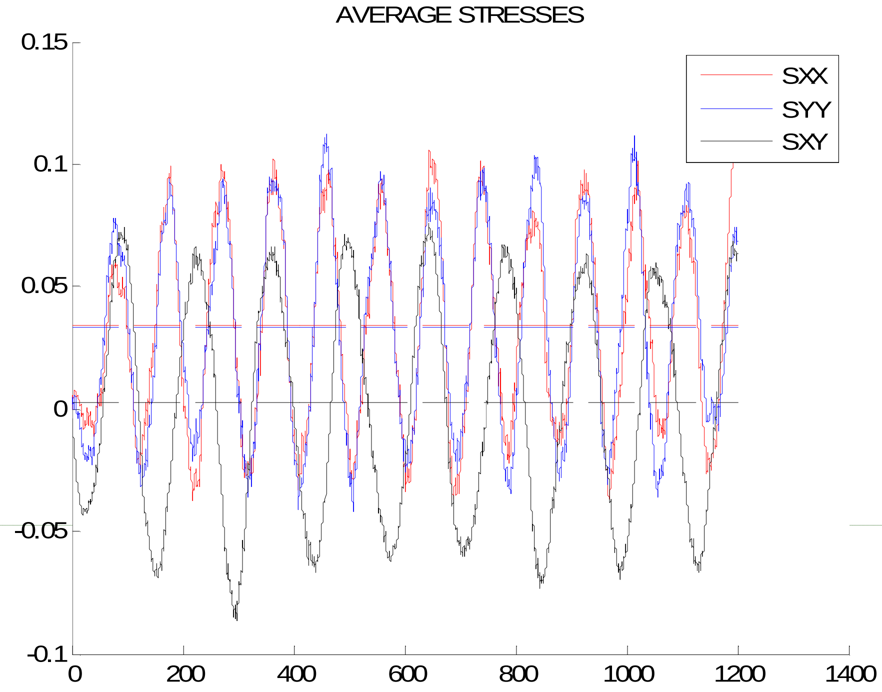

SXX_AVERAGE = 0.0340
SYY_AVERAGE =0.0334
SXY_AVERAGE =0.0028

SXX_AVERAGEKIN = 0.0344
SYY_AVERAGEKIN =0.0338
SXY_AVERAGEKIN = -1.9971e-005

ω = 0.0001 [rad/sg]
KT = 0.03
(reduced temperature)

$$\varepsilon_r \approx 1.2\%$$

The average stress tensor – rotating disk

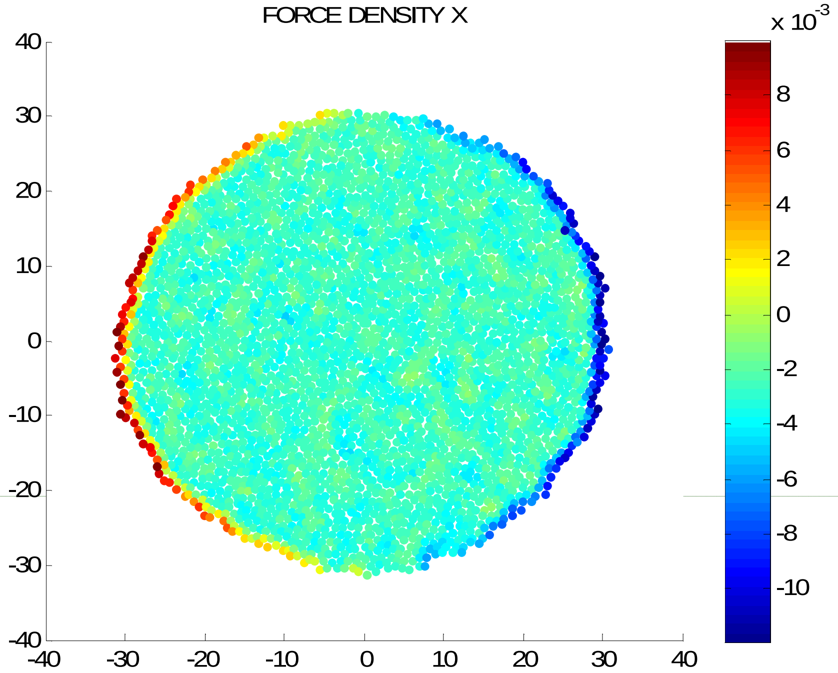

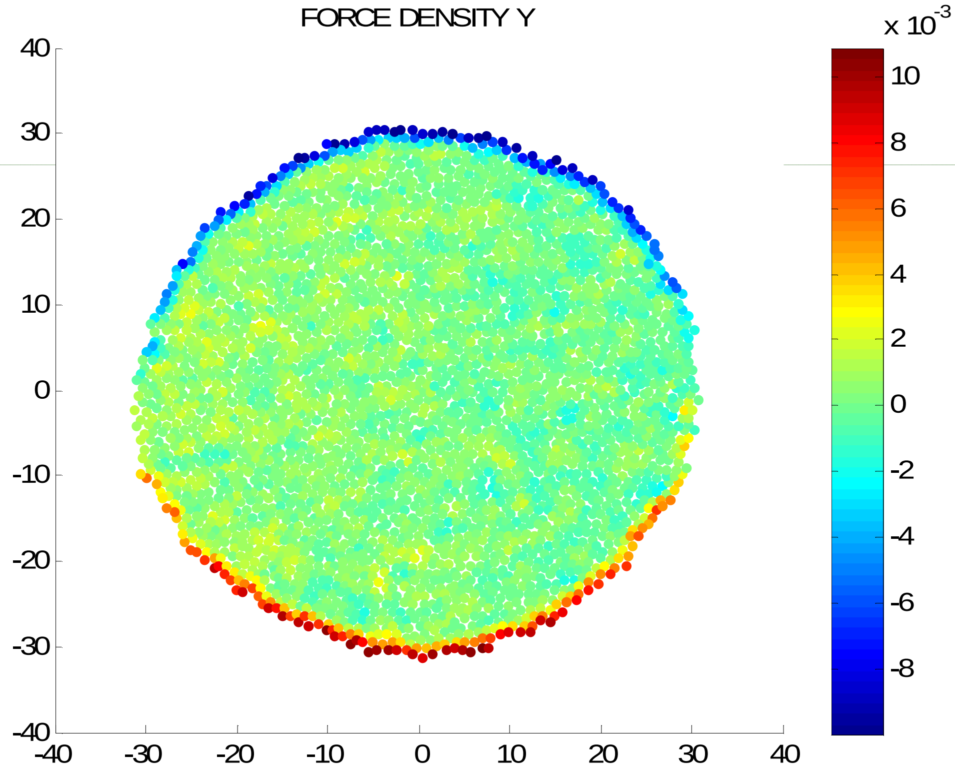

Interatomic potentials

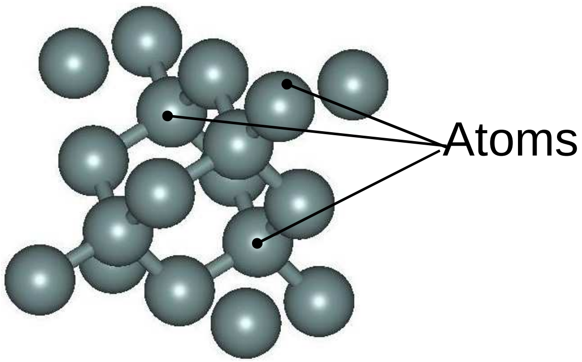

Newton 2nd law

$$m\ddot{\vec{x}}_i = \vec{F}_i = -\vec{\nabla} U$$

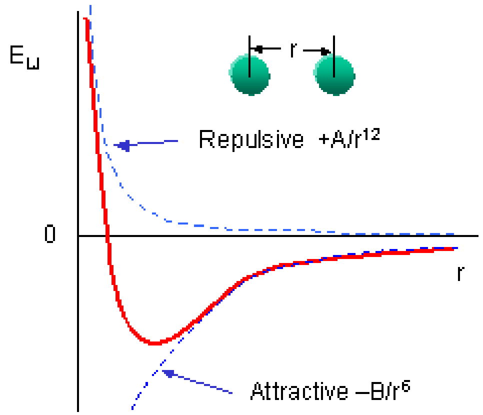

Interatomic potential (general form)

$$U = \phi_1(\vec{x}_i) + \sum_{j\neq i} \phi_2(\vec{x}_i, \vec{x}_j) + \sum_{j\neq i}\sum_{k\neq j} \phi_3(\vec{x}_i, \vec{x}_j, \vec{x}_k) + \ldots$$

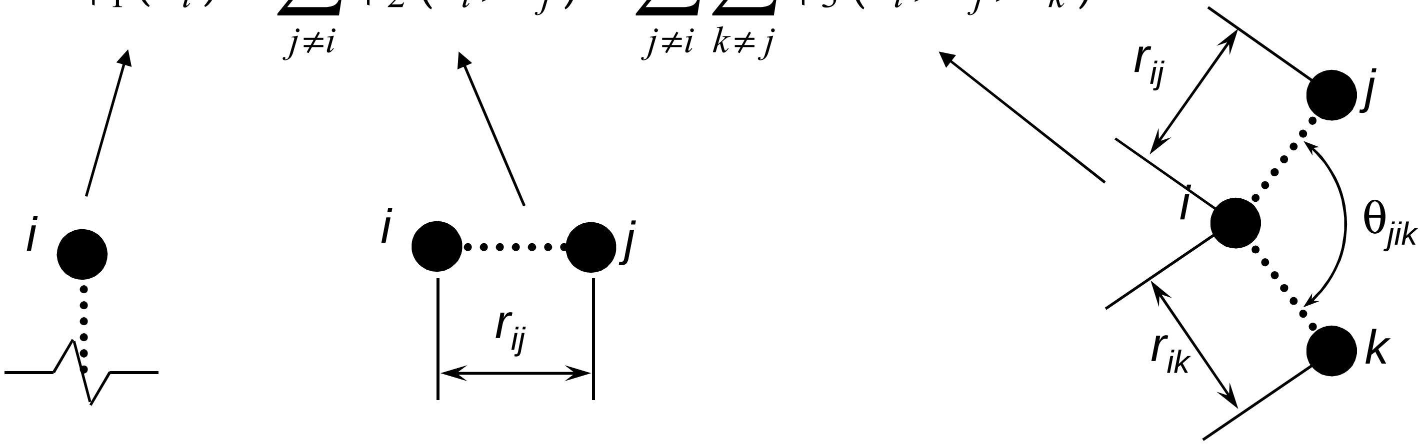

Atomic scale

$(1nm)^3$ - $(100nm)^3$: ns

Inter-atomic potential and inter-atomic forces

Tight-Binding (TB) potential (Cleri and Rosato, 1993)

$$V^{(i)} = -\left(\sum_{\substack{j=1\\ j\neq i}}^{N} \zeta^2 \exp\left(-2D\left(\frac{r^{(ij)}}{r_0}-1\right)\right)\right)^{1/2} + \sum_{\substack{j=1\\ j\neq i}}^{N} M \exp\left(-\tilde{P}\left(\frac{r^{(ij)}}{r_0}-1\right)\right)$$

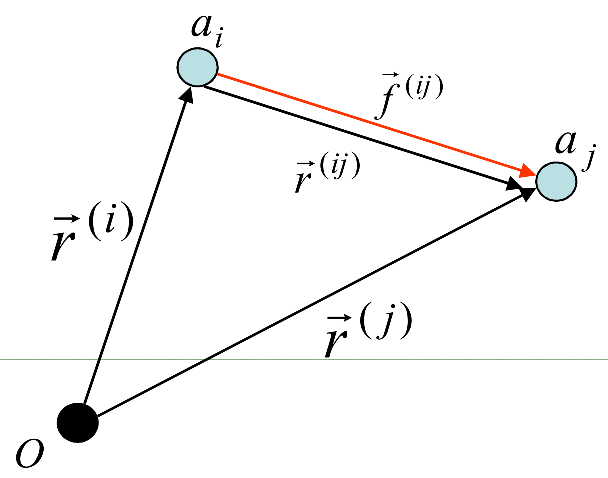

$$V = \sum_{i=1}^{N} V^{(i)}$$

$$f_\alpha^{(ij)} = -\frac{\partial V}{\partial r_\alpha^{(ij)}}$$

$$f_\alpha^{(i)} = -\frac{\partial V}{\partial r_\alpha^{(i)}}$$

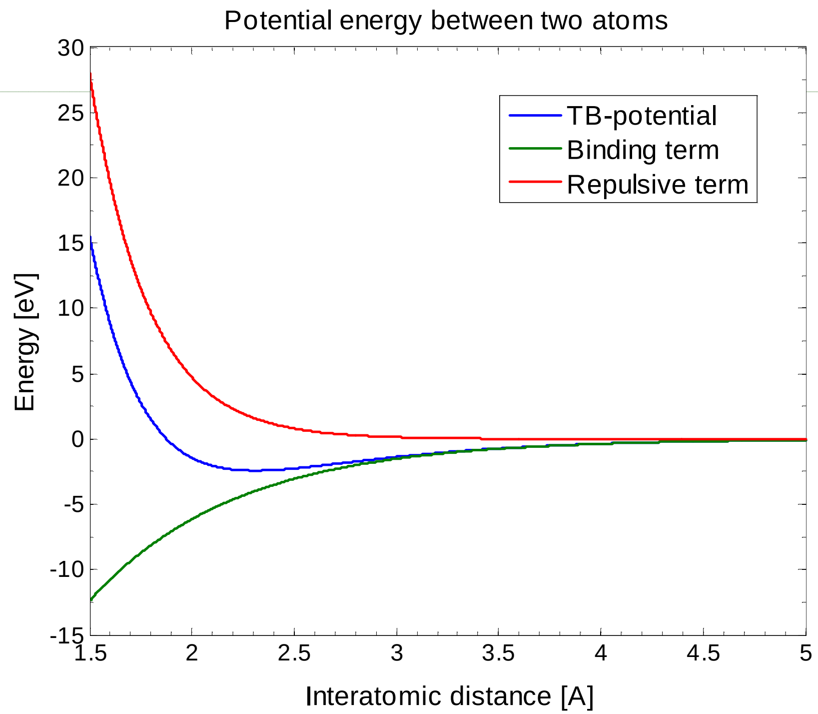

Simulation of mechanical tests

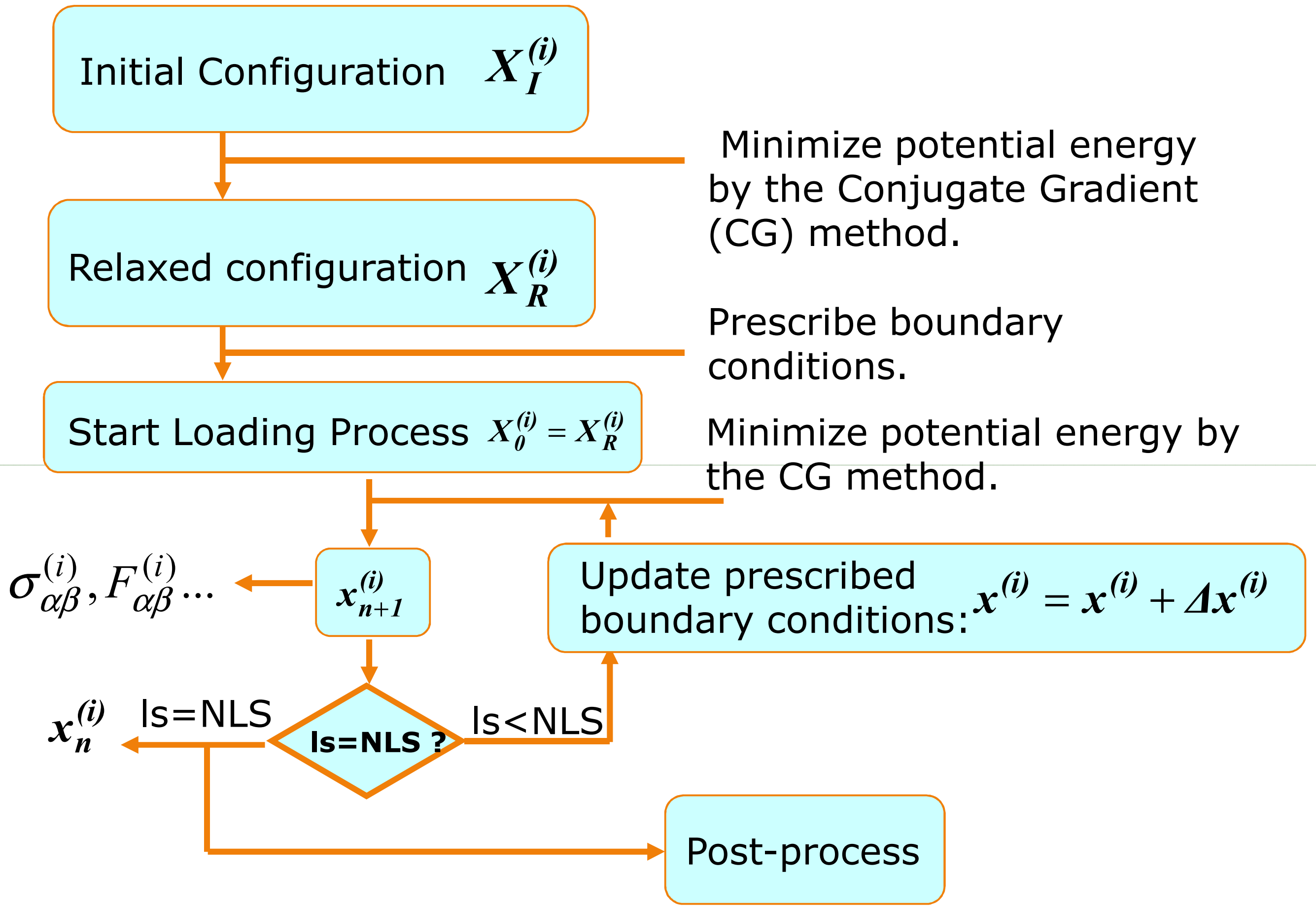

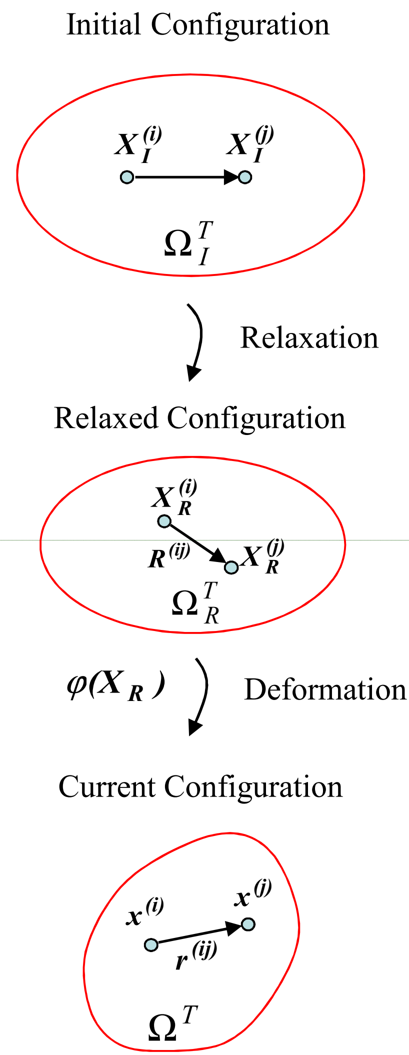

Convergence criterion:

$$\boxed{\max\left\{\frac{\partial V}{\partial q_\beta}\right\} \le 1E-8\,\frac{\text{eV}}{\text{Å}}}$$

Determination of macroscopic stresses

Average stress tensor : $\overline{\sigma}_{\alpha\beta} = \dfrac{1}{\Omega^{T}} \displaystyle\int_{\Omega} \sigma_{\alpha\beta} \, d\Omega$

Global balance of Linear Momentum : $\displaystyle\int_{\partial\Omega} t_{\alpha} dS + \int_{\Omega} g_{\alpha} d\Omega = 0$

Local balance of Linear Momentum : $\sigma_{\beta\alpha,\beta} + g_{\alpha} = 0 \text{ in } \Omega$

$$\overline{\sigma}_{\alpha\beta} = \boxed{\frac{1}{\Omega^{T}} \int_{\partial\Omega} t_{\alpha} x_{\beta} dS} + \frac{1}{\Omega^{T}} \int_{\Omega} g_{\alpha} x_{\beta} d\Omega$$

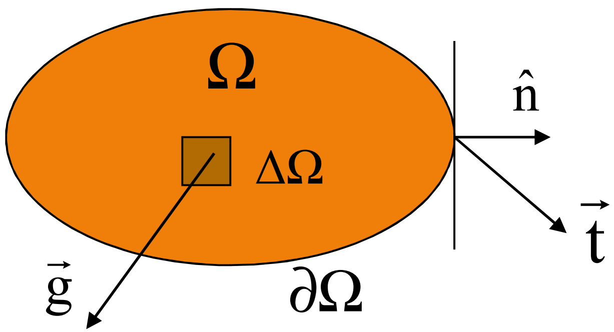

$$\overline{\sigma}_{\alpha\beta} = \frac{1}{\Omega^{T}} \sum_{i=1}^{Nb} x_{\beta}^{(i)} f_{\alpha}^{(i)}$$

Deformation gradient

$\vec{R}^{(i)}$: Position of atom (i) in reference config.

$\vec{r}^{(i)}$: Position of atom (i) in current config.

$\boldsymbol{F}^{(i)}$: Deformation gradient of atom (i)

$$r_\alpha^{(ij)} = F_{\alpha\beta}^{(i)} R_\beta^{(ij)}$$ *No summation in (i)*

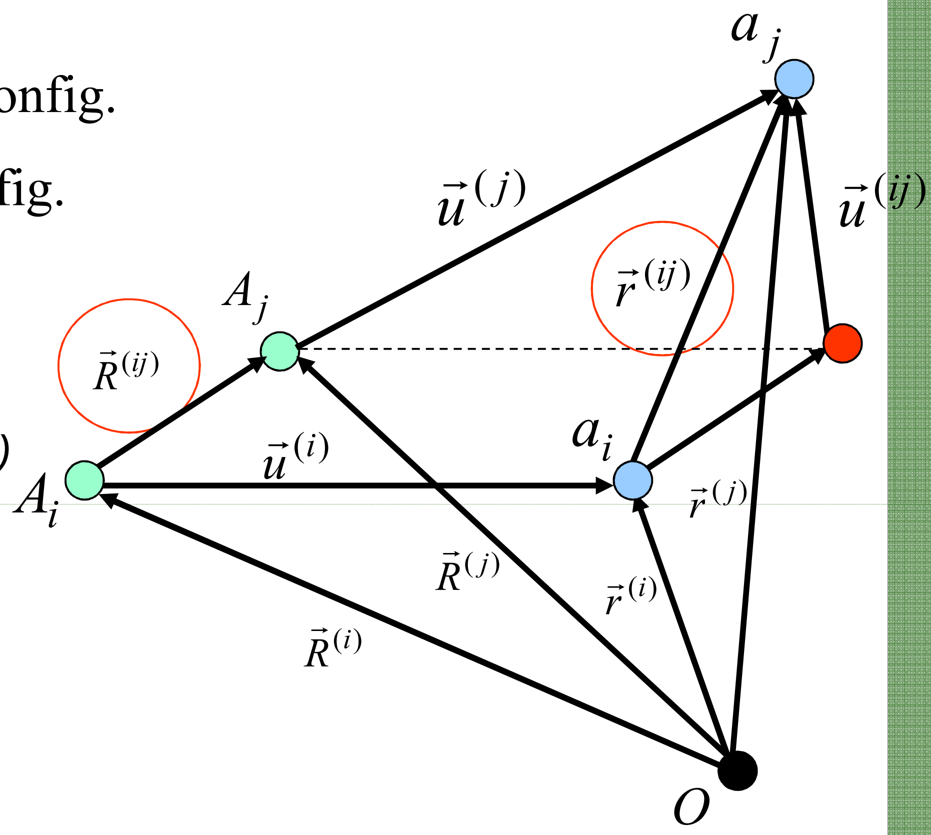

Cauchy-Born rule

Least Squares Method (LSM):

$$F^{(i)} = \left(\sum_j^N \vec{R}^{(ij)} \otimes \vec{R}^{(ij)} \right)^{-1} \left(\sum_j^N \vec{R}^{(ij)} \otimes \vec{r}^{(ij)} \right)$$

(*Zimmerman, 2000; Sunyk and Steinmann, 2003; Li, 2005*)

LSM in conjunction with smoothing functions (*Gullett et al., 2008*)

Determination of macroscopic strains (MSPH – Modified Smoothed Particle Hydrodynamics)

Values $\varphi^{(i)}$ of $\varphi(\boldsymbol{X})$ at N points in domain Ω are known

Taylor series around $\boldsymbol{x}^{(i)}$

$$\varphi(\xi) \approx \varphi\left(X^{(i)}\right) + \frac{\partial \varphi}{\partial X_\alpha^{(i)}}\left(\xi_\alpha - X_\alpha^{(i)}\right) + \frac{1}{2}\frac{\partial^2 \varphi}{\partial X_\alpha^{(i)} \partial X_\beta^{(i)}}\left(\xi_\alpha - X_\alpha^{(i)}\right)\left(\xi_\beta - X_\beta^{(i)}\right)$$

Weight with Kernel function and derivatives of kernel function

$$\left[W; W_{,\gamma}; W_{,\gamma\delta}\right]$$

Integrate over Ω

$$\int_\Omega (\ldots) d\Omega$$

Compute integrals numerically

$$\text{Solve for}: \varphi^{(i)}; \varphi_{,\alpha}^{(i)}; \varphi_{,\alpha\beta}^{(i)}$$

$$\textit{Solve for } x_{\alpha,\beta}^{(i)}$$
$$\textit{and compute } F_{\alpha\beta}^{(i)}$$

(Zhang and Batra, 2004)

Determination of macroscopic strains

Almansi-Hamel strain tensor :

$$\varepsilon_{\alpha\beta}^{(i)} = (1/2)\left(\delta_{\alpha\beta} - \left(F^{-1}\right)_{\phi\alpha}^{(i)} \left(F^{-1}\right)_{\phi\beta}^{(i)} \right)$$

$$\varepsilon = \frac{l^2 - l_0^2}{2l^2}$$

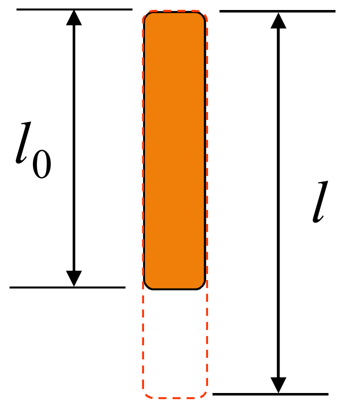

Green-St. Venant strain tensor : $\widetilde{E}_{\alpha\beta}^{(i)} = (1/2)\left(\left(F\right)_{\phi\alpha}^{(i)} \left(F\right)_{\phi\beta}^{(i)} - \delta_{\alpha\beta}\right)$

$$\widetilde{E} = \frac{l^2 - l_0^2}{2 l_0^2}$$

Average strain tensor : $\bar{\varepsilon}_{\alpha\beta} = \dfrac{1}{\Omega^T} \displaystyle\int_{\Omega} \varepsilon_{\alpha\beta}(\boldsymbol{x}) d\Omega = \sum_{i=1}^{N} \frac{\Omega^{(i)}}{\Omega^T} \varepsilon_{\alpha\beta}^{(i)}$

Gold specimens used in the different mechanical tests

Planes parallel to [100], [010] and [001].

L/H	L (Å)	No. atoms	$\frac{\Delta V}{V_I}$ (eV/eV)	$\frac{\Delta\Omega^T}{\Omega_I^T}$ (Å^3/Å^3)	ε (Å/Å)
1	~32	3480	3.763e-3	-2.021e-2	-2.081e-2
1	~50	7813	2.549e-3	-1.486e-2	-1.713e-2
1	~100	58825	1.044e-3	-6.923e-3	-1.036e-2
3	~110	9928	2.616e-3	-1.531e-2	-1.589e-2
5	~188	16787	2.369e-3	-1.518e-2	-1.518e-2
10	~367	32671	2.197e-3	-1.361e-2	-1.469e-2
20	~742	65883	2.105e-3	-1.316e-2	-1.430e-2

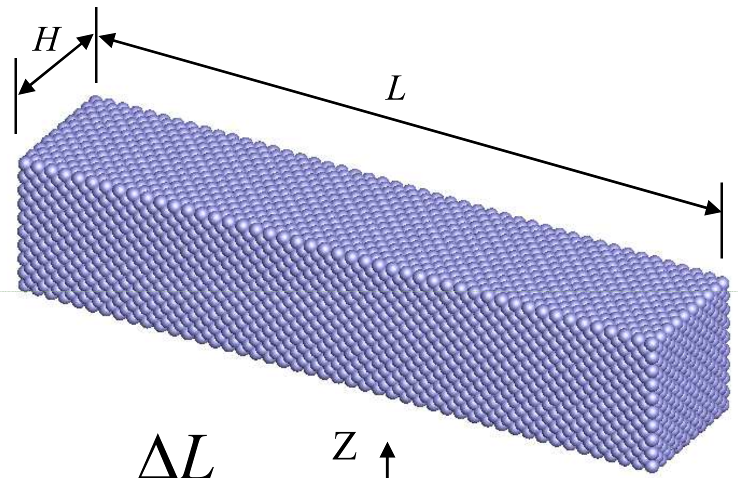

$$\varepsilon = \frac{\Delta L}{L_R}$$

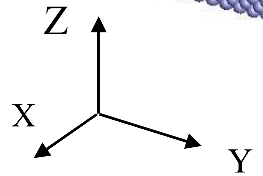

Table: For specimens with different L/H ratios, the change in the total potential energy (*V*), the change in the total volume (Ω^T), and the axial strain (ε) upon relaxation.

Tensile/compressive deformations in gold crystals

Specimens: $1 \le L/H \le 20$

Simple tension/compression

$$u_y = u_y + \Delta u_y$$

Tension/compression with prescribed essential B.C.s. on all bounding surfaces

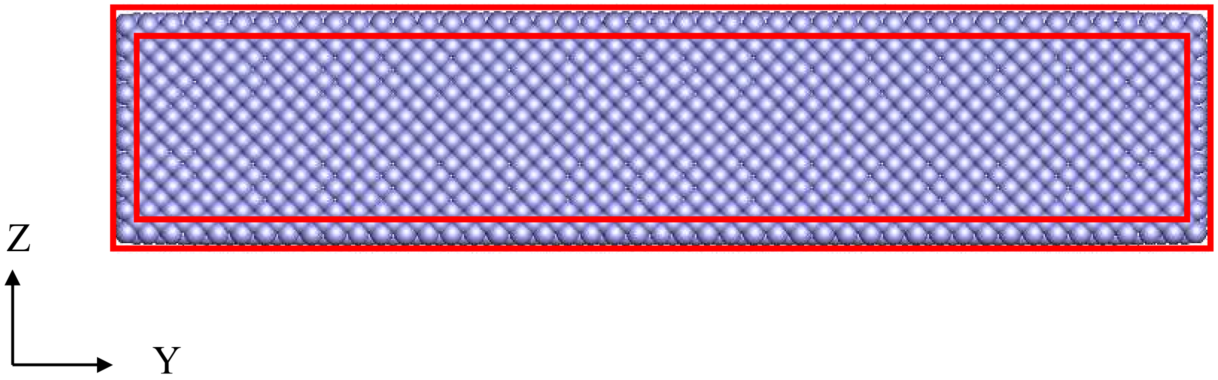

$$\boldsymbol{F} = diag\{\lambda_1, \lambda_2, \lambda_3\}$$

$$\lambda_1 \lambda_2 \lambda_3 = 1$$

$$\lambda_1 = \lambda_3 = 1/\sqrt{\lambda_2}$$

Elastic constants gold crystals
(Young's modulus *E*)

L/H = 10

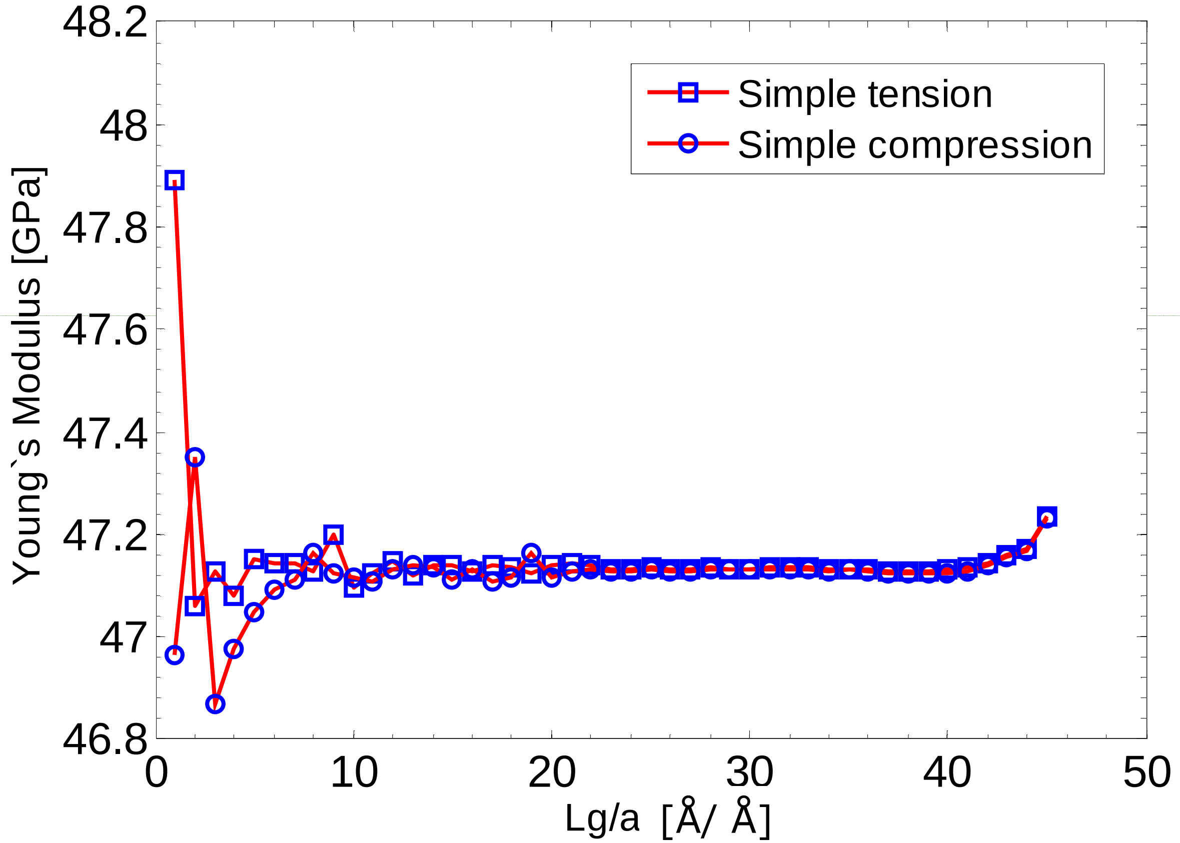

Value from elastic constants:

$$E = \frac{\widetilde{C}_{11}^2 + \widetilde{C}_{12}\widetilde{C}_{11} - 2\widetilde{C}_{12}^2}{\widetilde{C}_{11} + \widetilde{C}_{12}}$$

$$E = 46.5\,[\mathrm{GPa}]$$

L_g: Length of the averaging volume

Elastic constants gold crystals
(Poisson's ratio *ν*)

L/H = 10

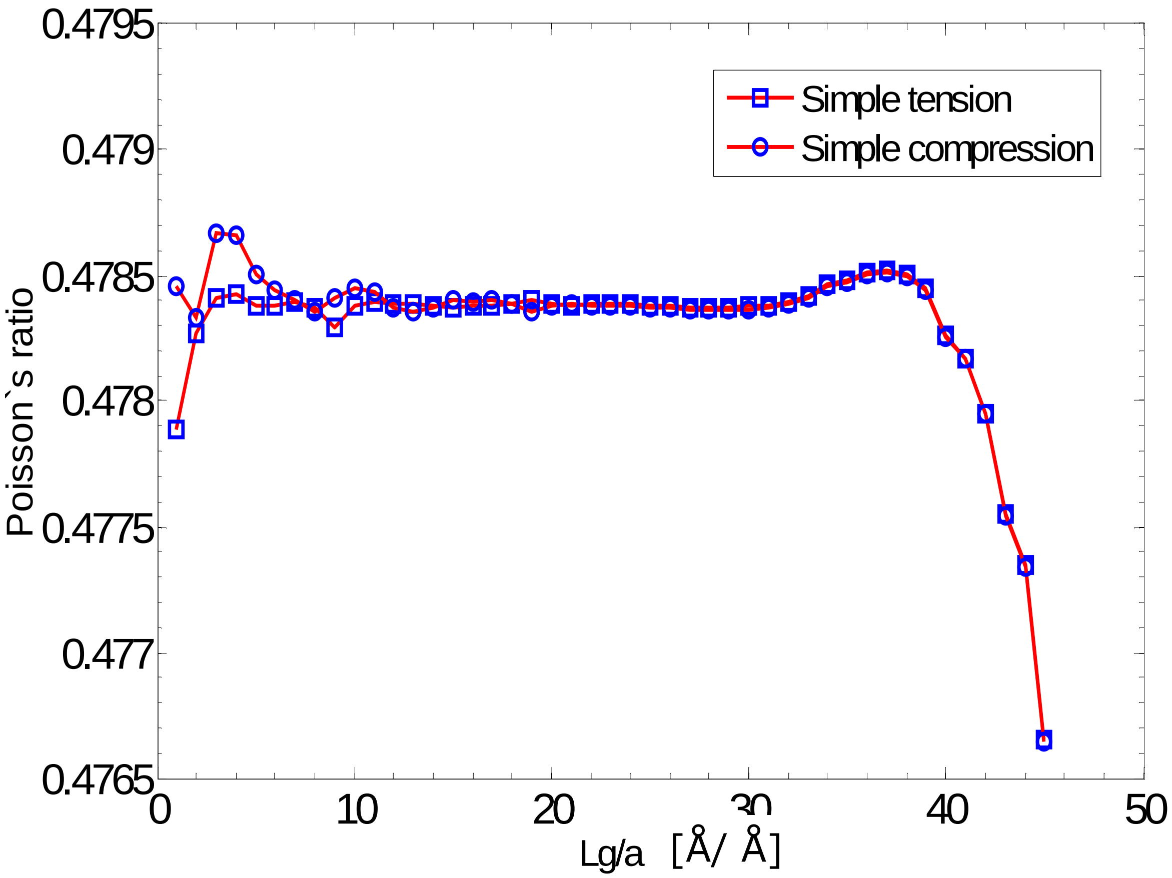

Value from elastic constants:

$$\nu = -\frac{\varepsilon_{xx}}{\varepsilon_{yy}} = \frac{\tilde{C}_{12}}{\tilde{C}_{11} + \tilde{C}_{12}}$$

$$\nu = 0.453$$

L_g: Length of the averaging volume

Stress tensors - Tension/compression with prescribed essential B.C.s. on all bounding surfaces

Strain energy density:

$$W_0(\boldsymbol{F}) = \sum_{i}^{N} \frac{V^{(i)}}{\Omega_R^{(i)}}$$

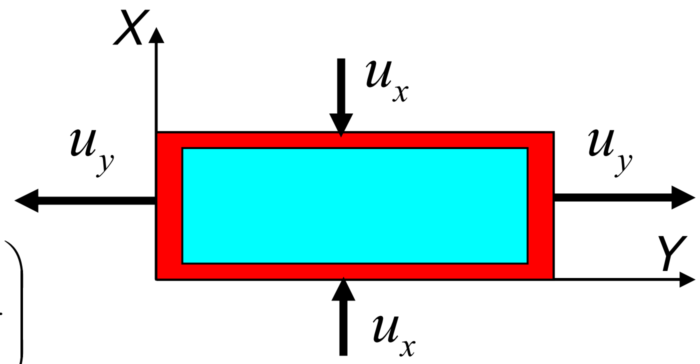

First Piola-Kirchhoff stress tensor:

$$\overline{\boldsymbol{P}} = \frac{\partial W_0}{\partial \boldsymbol{F}} = \frac{\partial}{\partial \boldsymbol{F}}\left(\sum_{i=1}^{N} \frac{V^{(i)}}{\Omega_R^{(i)}}\right)$$

$$[\sigma(\lambda_1,\lambda_2,\lambda_3)] = \sum_{\substack{i,k=1 \\ i\neq k}}^{N} \frac{1}{\Omega^{(i)}} \frac{1}{r^{(ik)}} \frac{\partial V^{(i)}}{\partial r^{(ik)}} [\Theta^{(ik)}(\lambda_1,\lambda_2,\lambda_3)],$$

$$\boxed{\boldsymbol{P} = J\boldsymbol{F}^{-1}\boldsymbol{\sigma}}$$

where

$$[\Theta^{(ik)}(\lambda_1,\lambda_2,\lambda_3)] = \begin{bmatrix} \lambda_1\lambda_1 R_{xx}^{(ik)} & \lambda_1\lambda_2 R_{xy}^{(ik)} & \lambda_1\lambda_3 R_{xz}^{(ik)} \\ \lambda_2\lambda_1 R_{yx}^{(ik)} & \lambda_2\lambda_2 R_{yy}^{(ik)} & \lambda_2\lambda_3 R_{yz}^{(ik)} \\ \lambda_3\lambda_1 R_{xx}^{(ik)} & \lambda_3\lambda_2 R_{zy}^{(ik)} & \lambda_3\lambda_3 R_{zz}^{(ik)} \end{bmatrix}$$

$R_{xx}^{(ik)} = R_x^{(ik)} R_x^{(ik)}$, $R_{xy}^{(ik)} = R_x^{(ik)} R_{y,}^{(ik)}$ and so on.

Comparison of average normal stress components computed by different methods

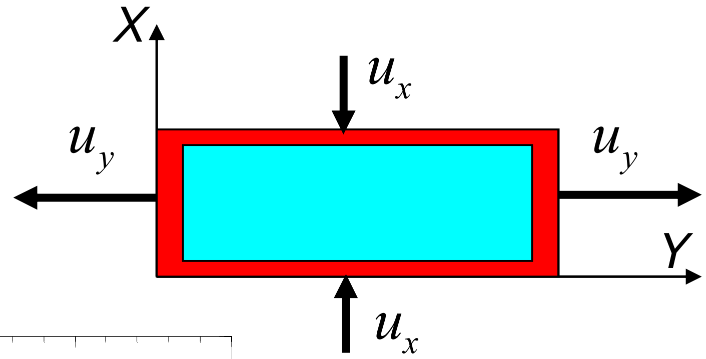

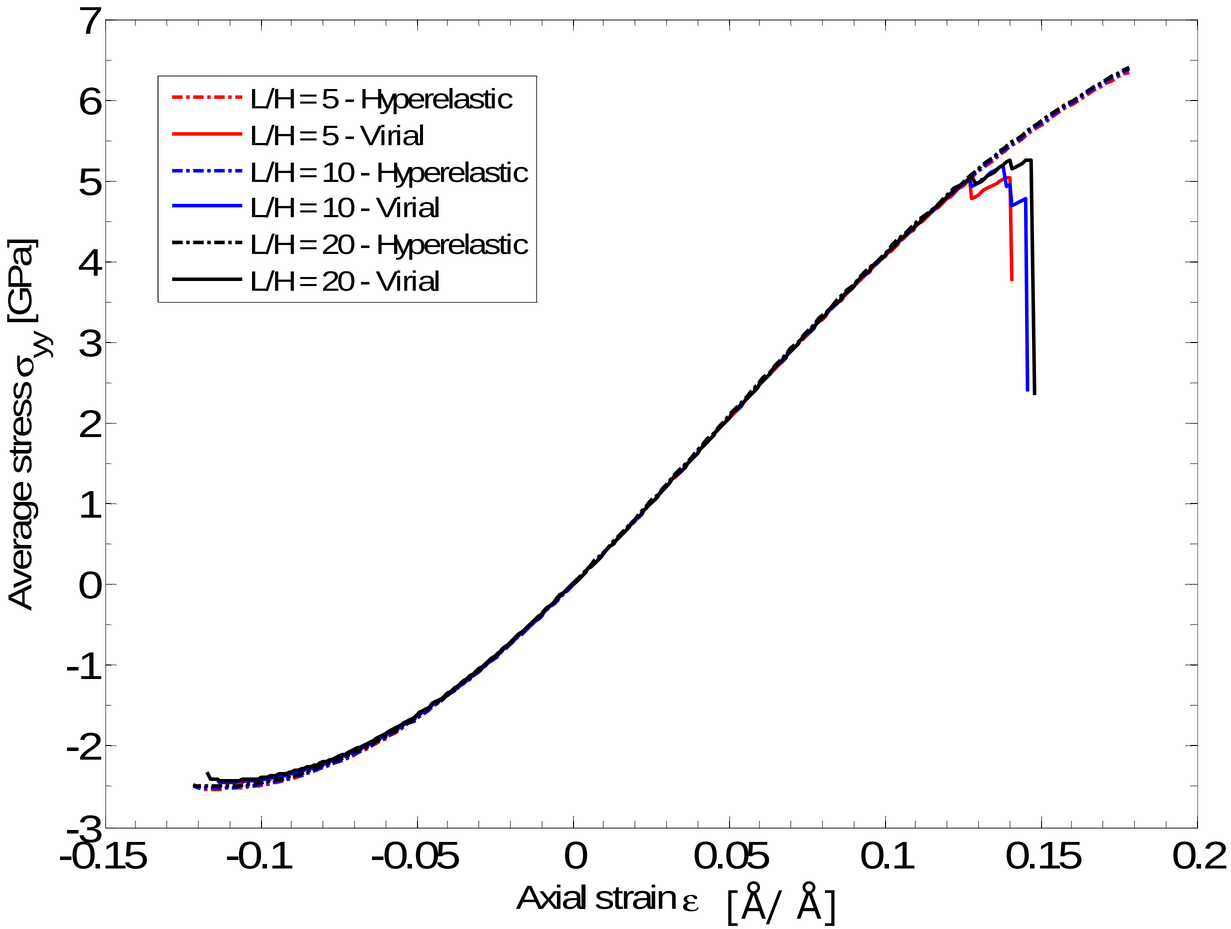

Axial

Tension/compression

L/H = 5, 10, 20

$$\bar{\sigma}_{xx} = \bar{\sigma}_{zz}$$

$$\bar{\sigma}_{xy} = \bar{\sigma}_{xz} = \bar{\sigma}_{yz} = 0$$

Comparison of average normal stress components computed by different methods

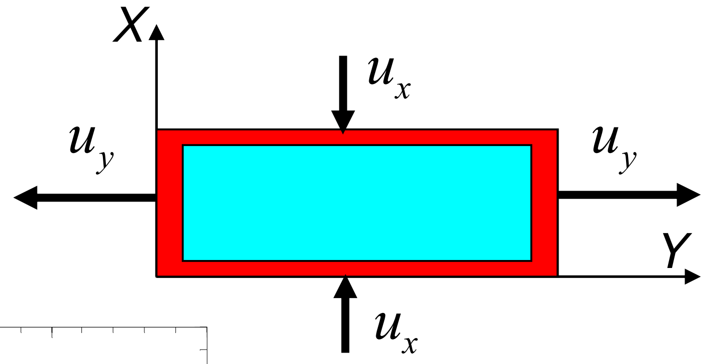

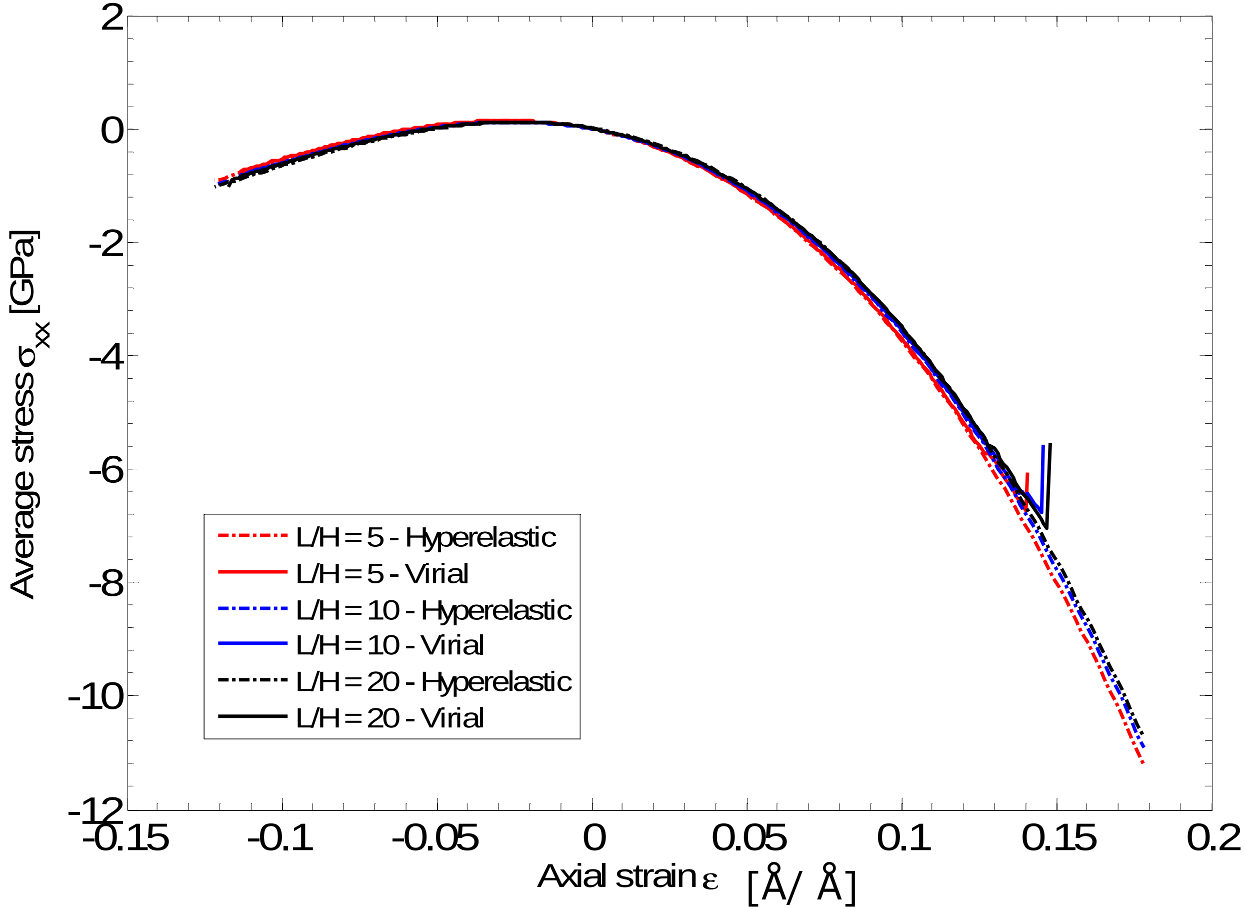

Axial

Tension/compression

L/H = 5, 10, 20

$$\bar{\sigma}_{xx} = \bar{\sigma}_{zz}$$

$$\bar{\sigma}_{xy} = \bar{\sigma}_{xz} = \bar{\sigma}_{yz} = 0$$

Simple tension/compression – Average axial stress

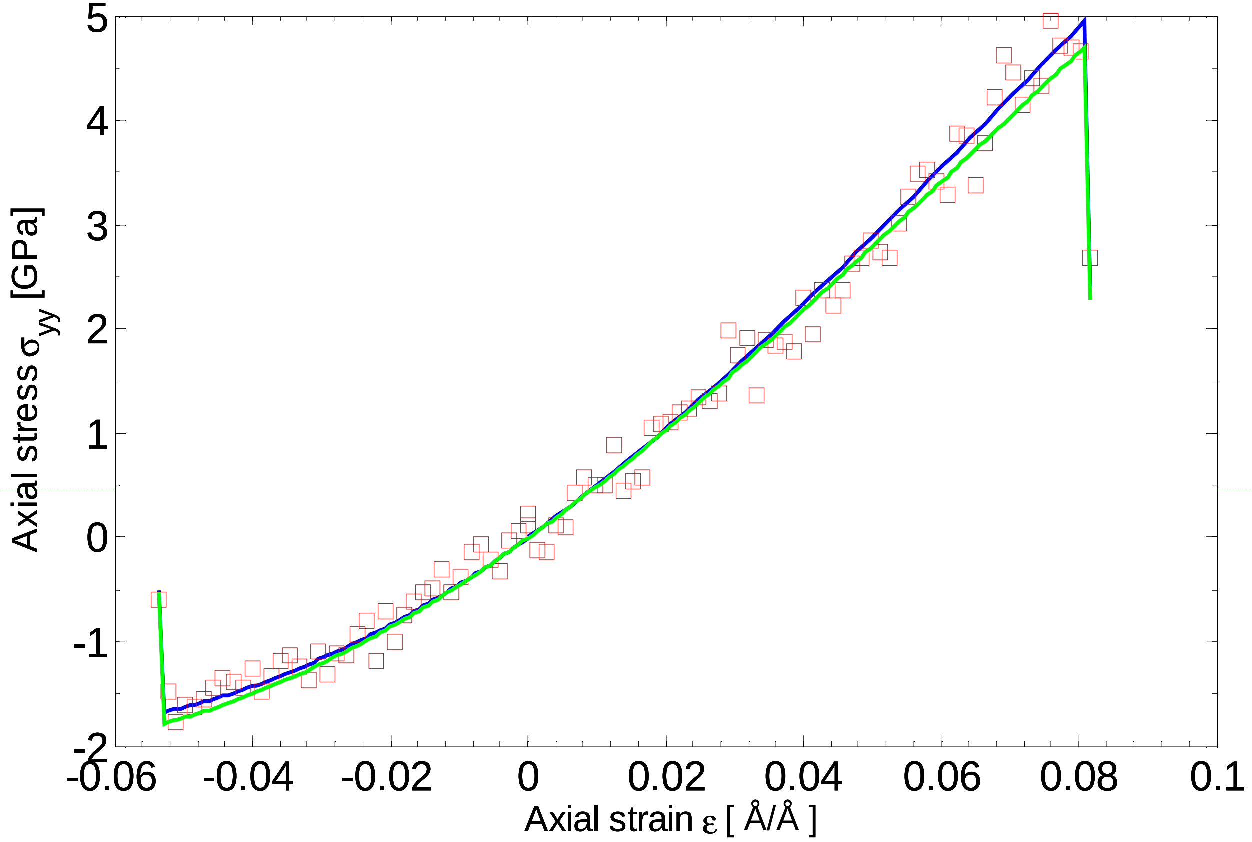

Firsts moment of surface forces

Virial stress

Force/area

L/H = 10

Simple tension test - Loading and unloading paths

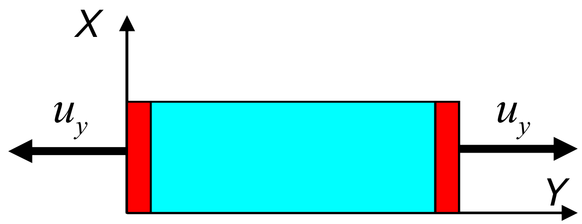

L/H = 10

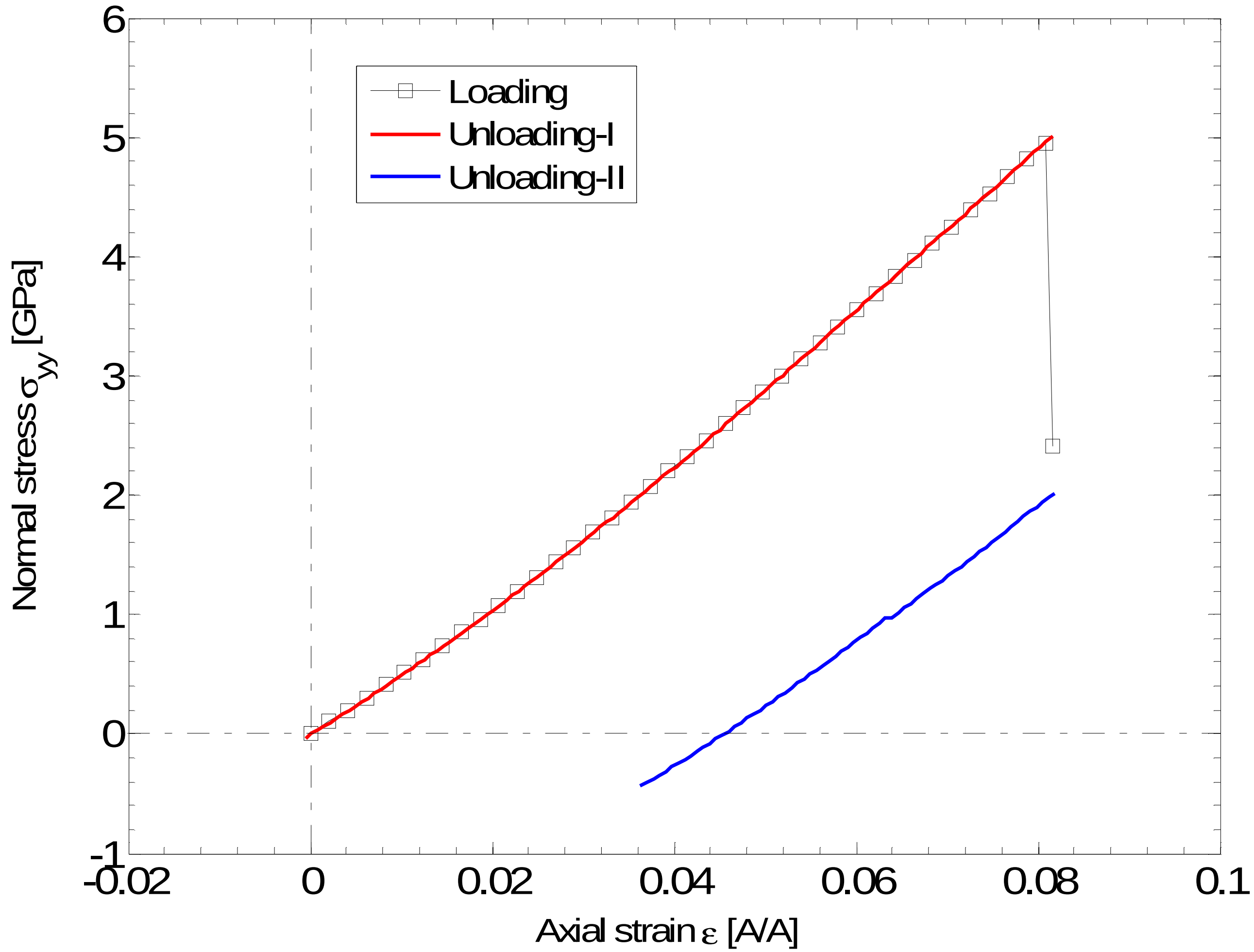

Simple tension/compression – Values of the yield stress

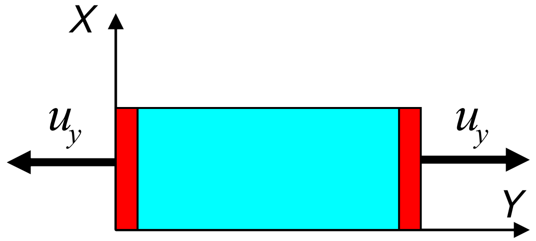

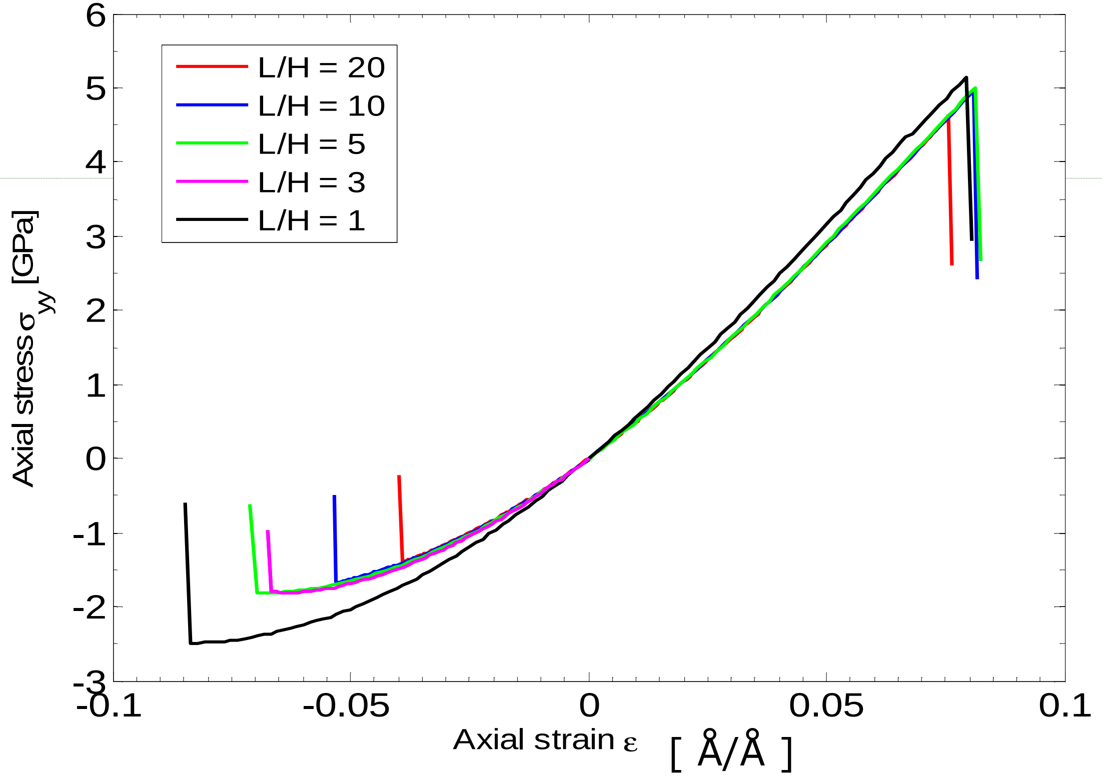

$$\left(\overline{\sigma}_{yy}^{yield}\right)_{tension}$$

L/H = 1: 5.134 GPa

L/H = 3: 5.050 GPa

L/H = 5: 4.996 GPa

L/H = 10: 4.990 GPa

L/H = 20: 4.618 GPa

$$\left(\overline{\sigma}_{yy}^{yield}\right)_{compression}$$

L/H = 1: -2.498 GPa

L/H = 3: -1.784 GPa

L/H = 5: -1.810 GPa

L/H = 10: -1.671 GPa

L/H = 20: -1.387 GPa

Computation of local Cauchy stress tensor

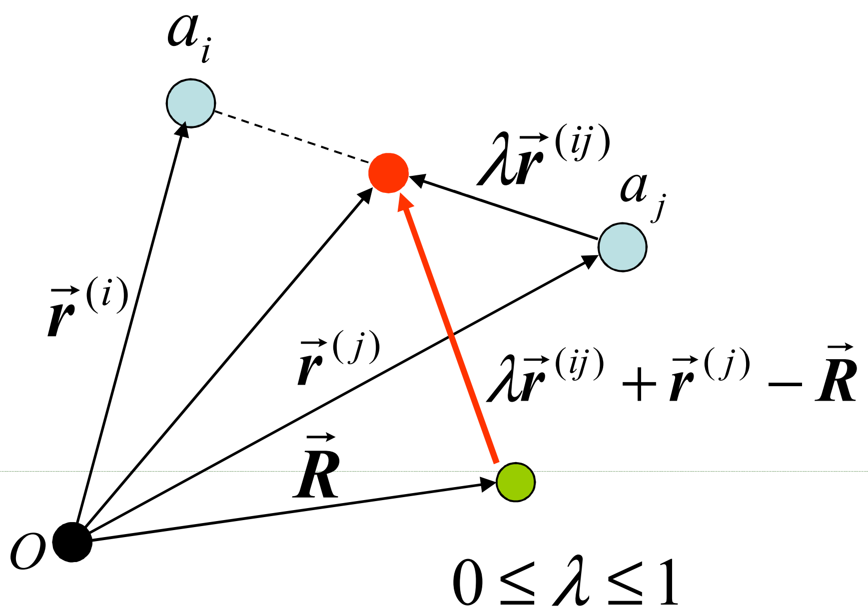

$$div\boldsymbol{\sigma} = \frac{\partial}{\partial \boldsymbol{R}} \cdot \boldsymbol{\sigma} = \sum_{i=1}^{N} \vec{f}^{(i)} \Psi\left(\vec{r}^{(i)} - \vec{R}\right)$$

$$\boldsymbol{\sigma} = \frac{1}{2} \sum_{i=1}^{N} \sum_{\substack{j=1 \\ j \neq i}}^{N} \vec{r}^{(ij)} \otimes \vec{f}^{(ij)} B^{(ij)}(\vec{R})$$

Bond function: $B^{(ij)}\left(\vec{R}\right)$ *(Hardy, 1981)*

$$B^{(ij)}\left(\vec{R}\right) \equiv \int_0^1 \Psi\left(\lambda\vec{r}^{(ij)} + \vec{r}^{(j)} - \vec{R}\right) d\lambda$$

Hardy, R. J. 1981. Formulas for determining local properties in molecular dynamics simulations: shock waves. J. Chem. Phys. 76, 622-628

Stress distribution along centroidal lines

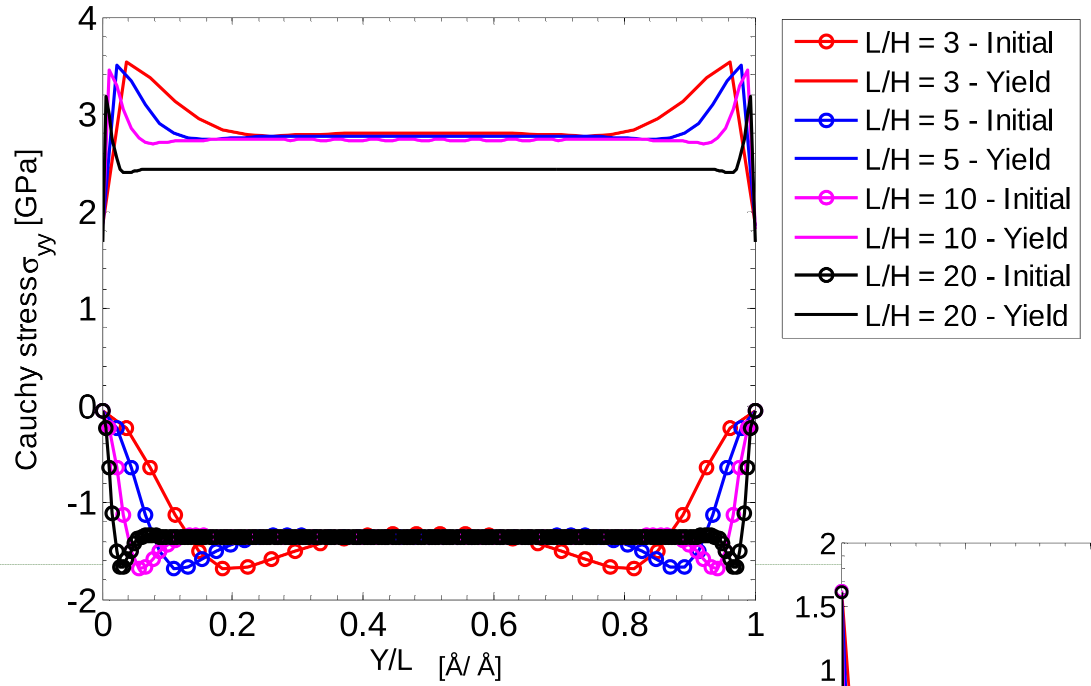

Simple tension

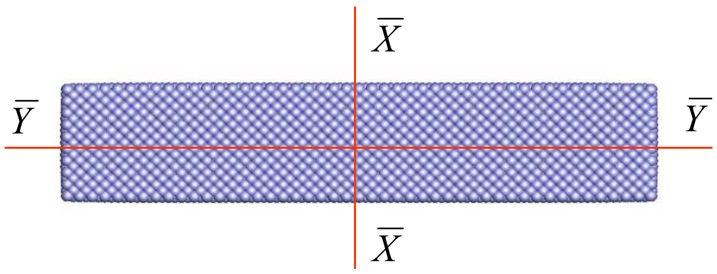

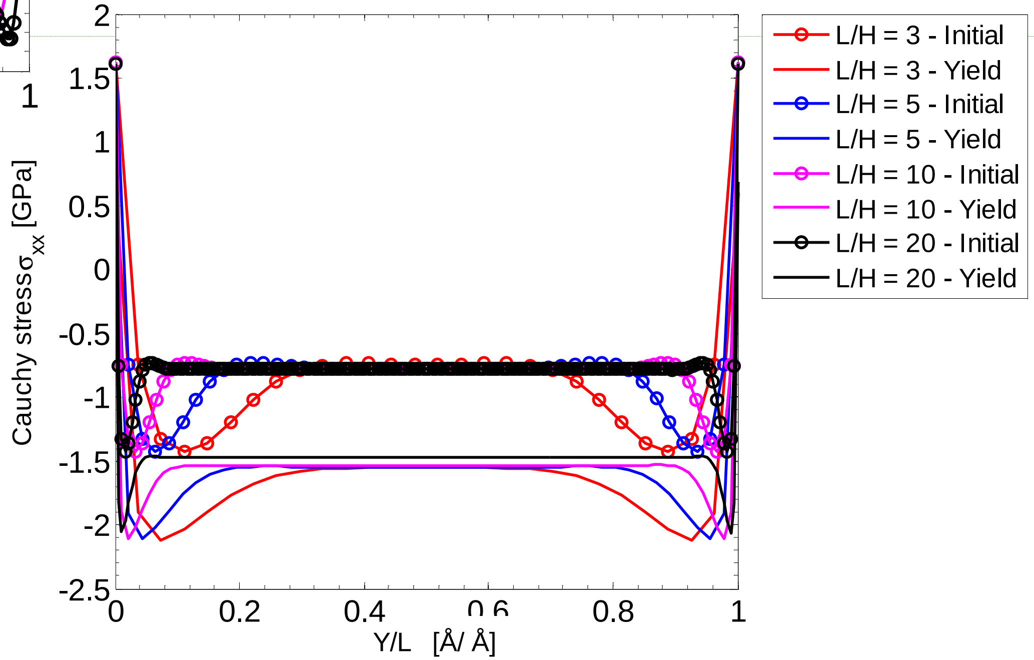

Stress distribution along centroidal lines

Simple compression

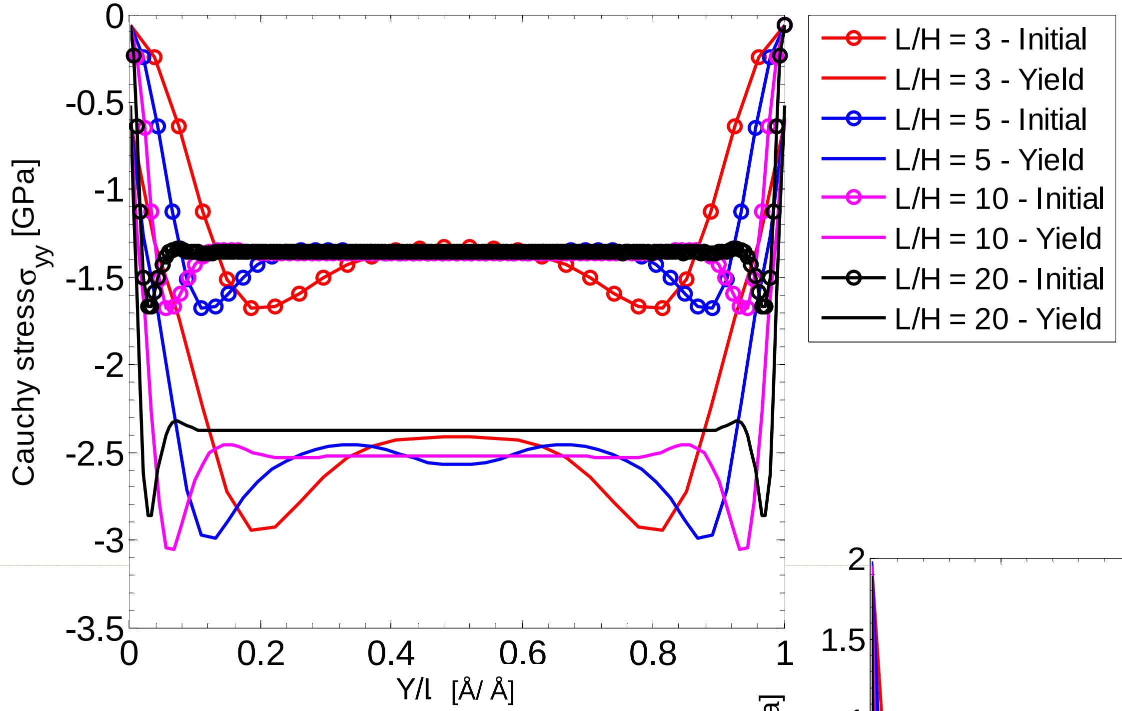

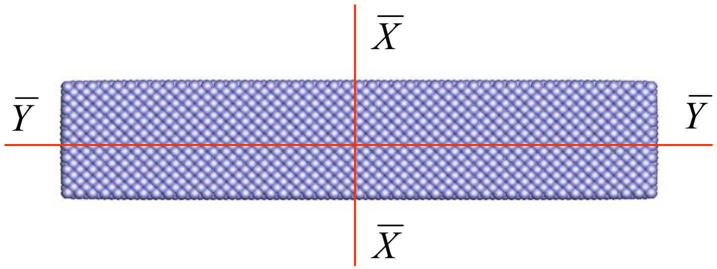

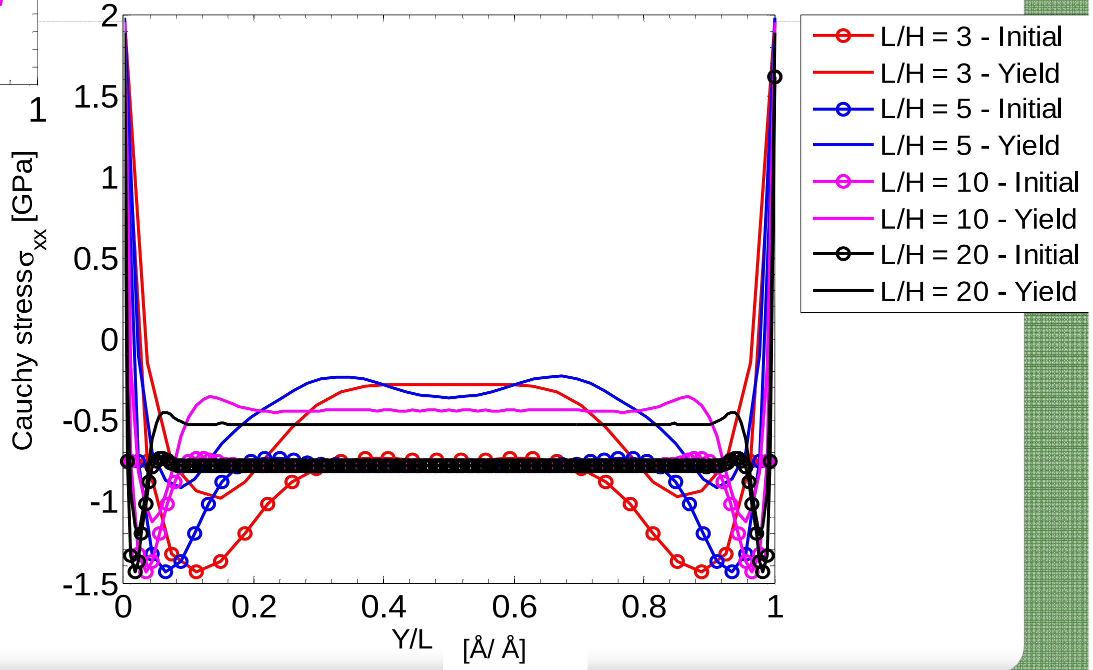

Local instability criteria: Local Hessian, CNP parameter, Second-order gradients

$$H_{jk}^{(i)} = \frac{\partial^2 V^{(i)}}{\partial r^{(ij)} \partial r^{(ik)}}, \quad k, j = 1,2,..N_f$$

$$\text{SRV : Sphere with } R = \left(\sqrt{3}/2\right)a$$

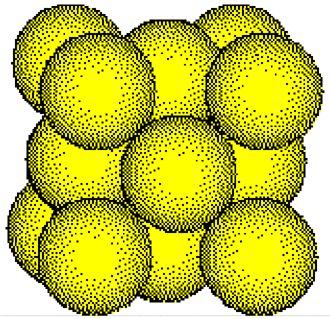

$$CNP^{(i)} = \frac{1}{N_f} \sum_{j=1}^{N_f} \left| \sum_{k=1}^{N_{ij}} \left(\boldsymbol{r}^{(ik)} + \boldsymbol{r}^{(jk)} \right) \right|^2$$

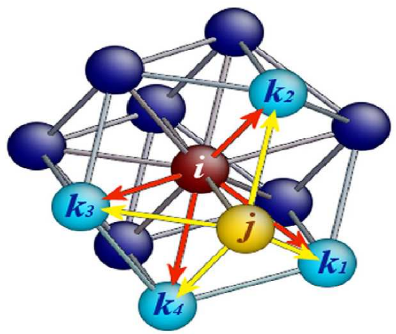

Tsuzuki et al., 2007

$$\|\boldsymbol{G}\| = a \max\left(\left| G_{\alpha\beta\gamma} \right| \right)$$

Comparison of results from the local instability criteria

Simple tension

L/H = 10

ε = 8.08%

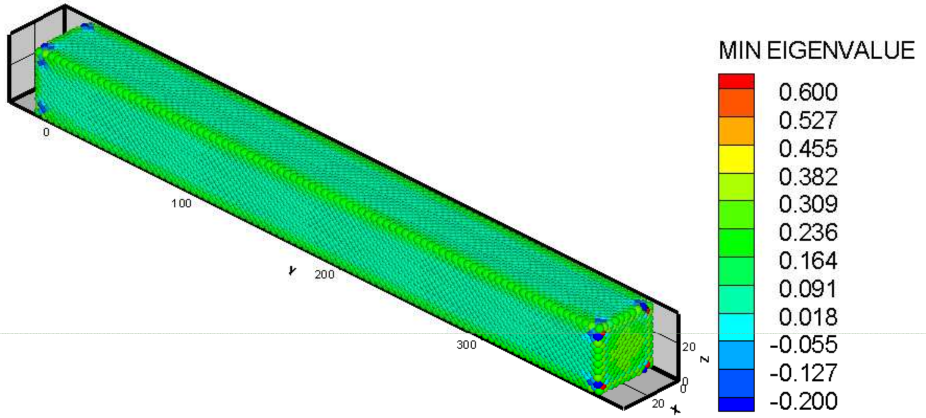

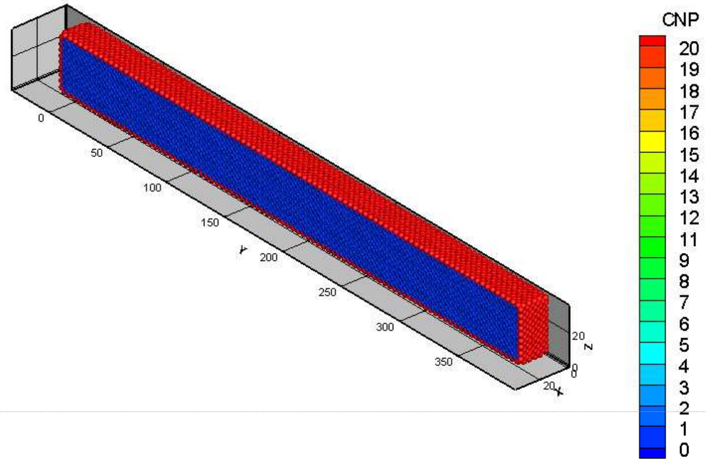

ε = 8.15%

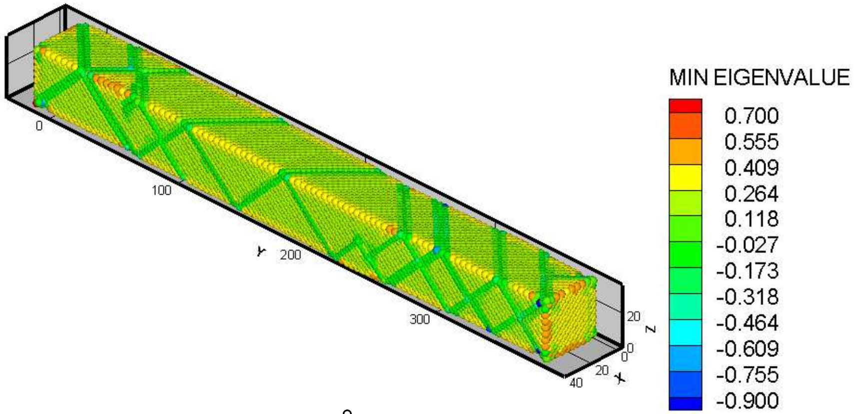

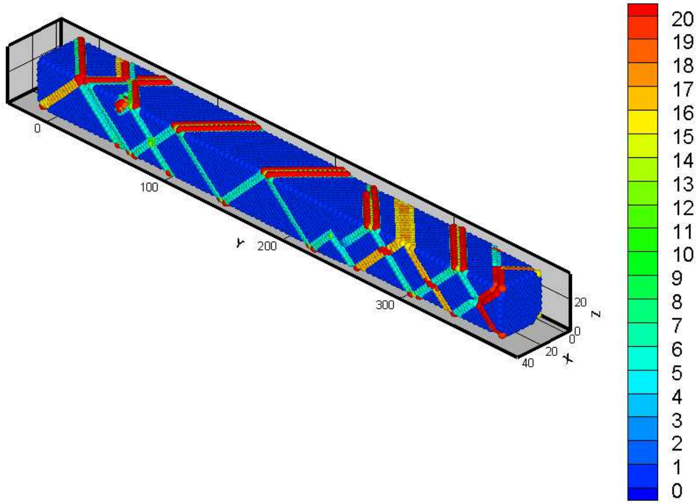

Dimensions in Å

Comparison of results from the local instability criteria

Simple compression **L/H = 10**

ε = -5.15%

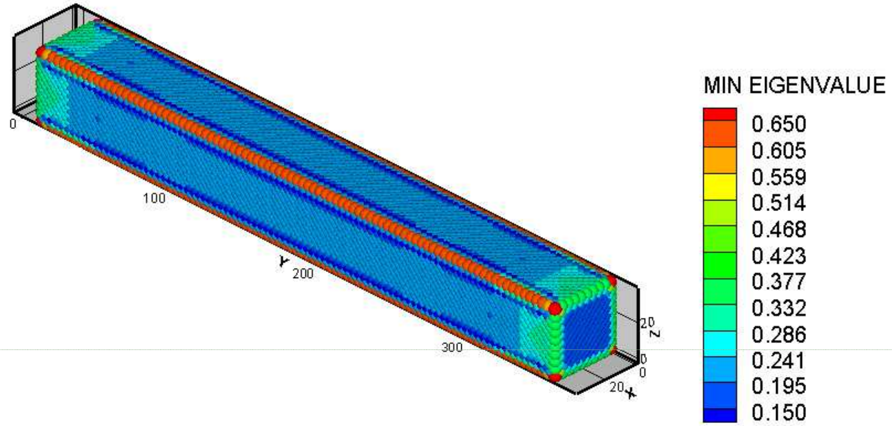

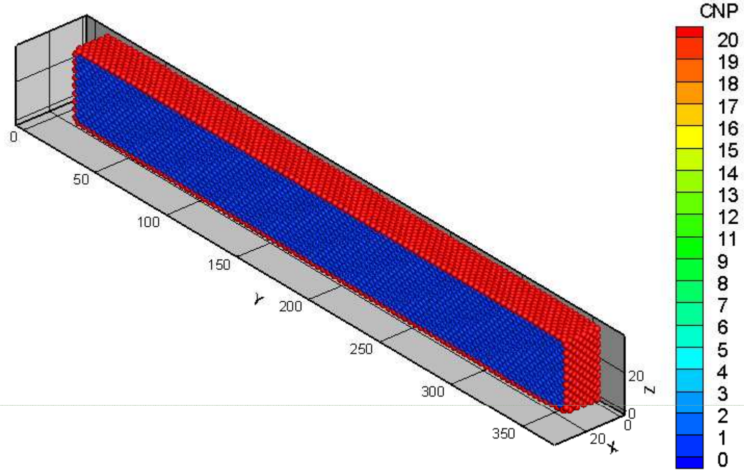

ε = -5.16%

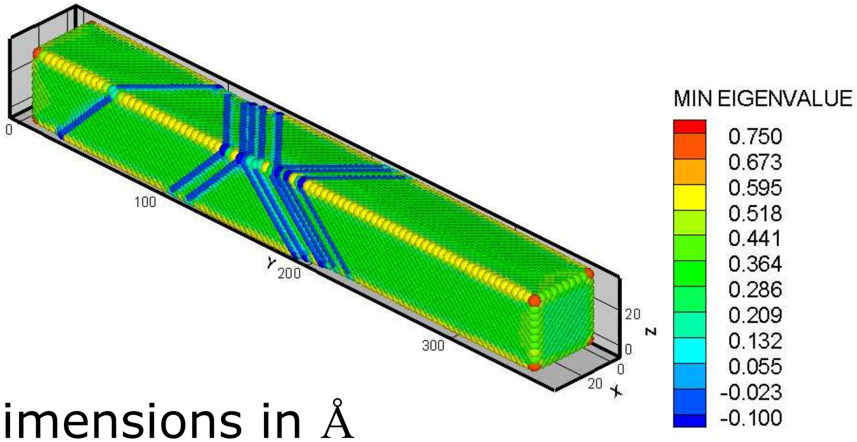

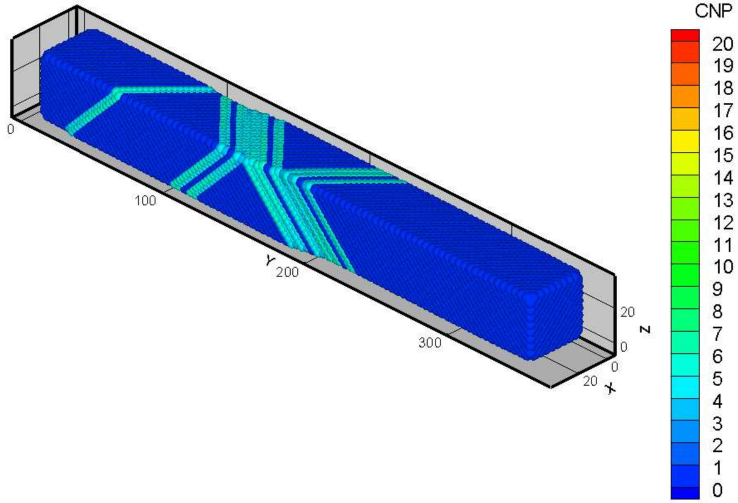

Dimensions in Å

Comparison of results from the local instability criteria

L/H = 10

Simple compression

$\varepsilon = -5.15\%$

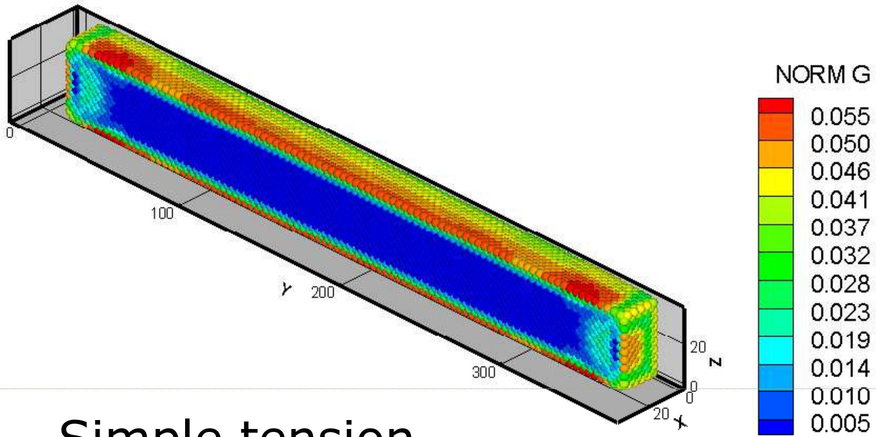

$\varepsilon = -5.16\%$

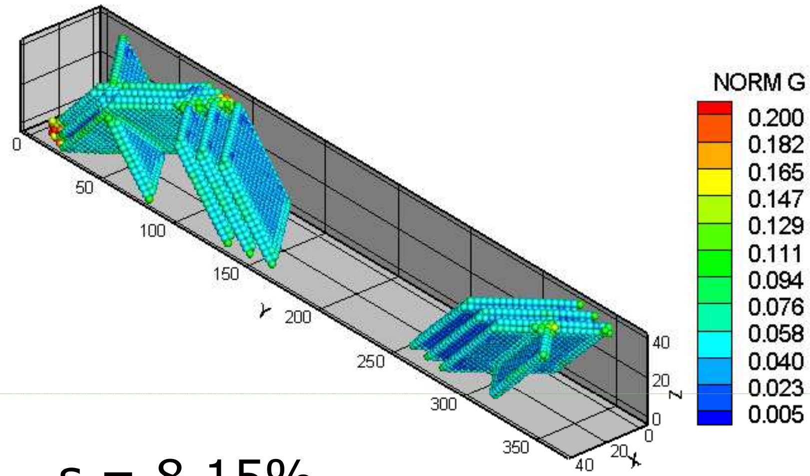

Simple tension

$\varepsilon = 8.08\%$

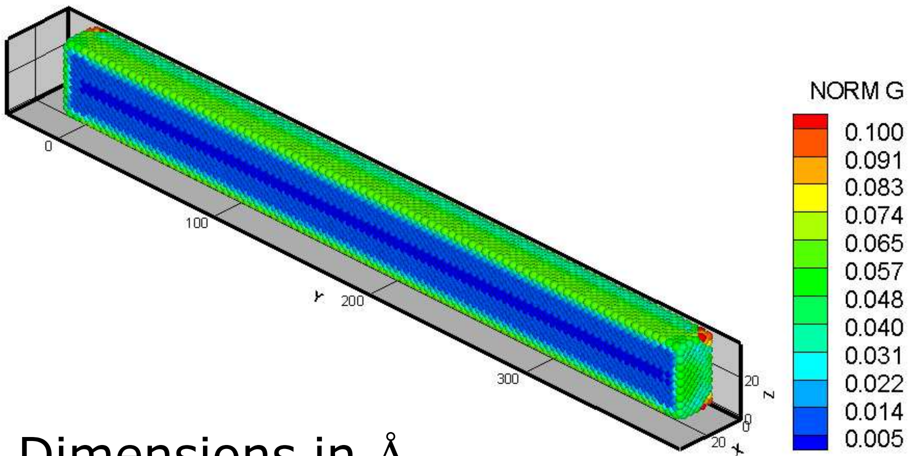

$\varepsilon = 8.15\%$

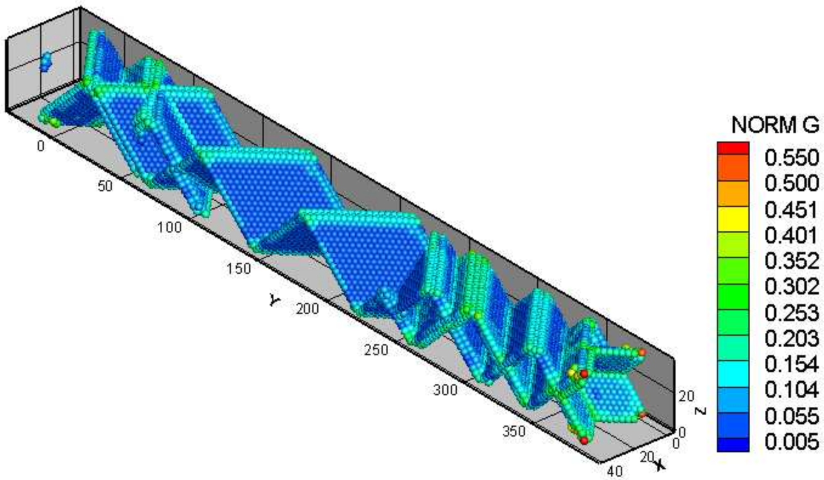

Dimensions in Å

Shear and simple shear tests in gold crystals

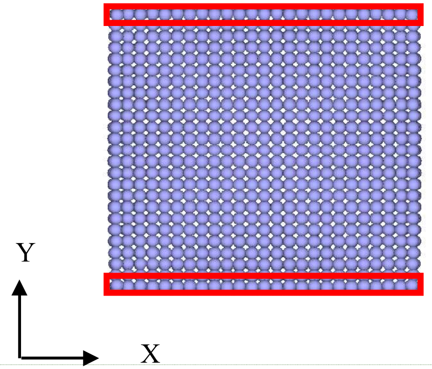

Specimen A: side ~32 Å, 3480 atoms
Specimen B: side ~50 Å, 7813 atoms
Specimen C: side ~100 Å, 58825 atoms.
Planes parallel to [100], [010] and [001].

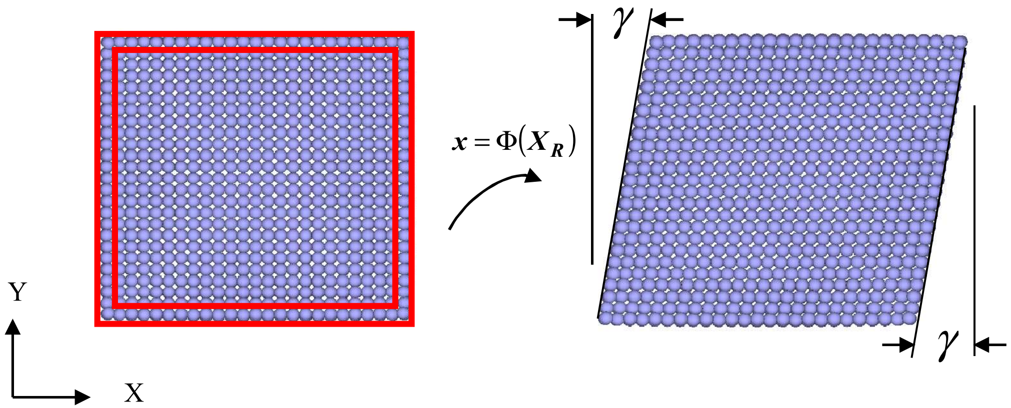

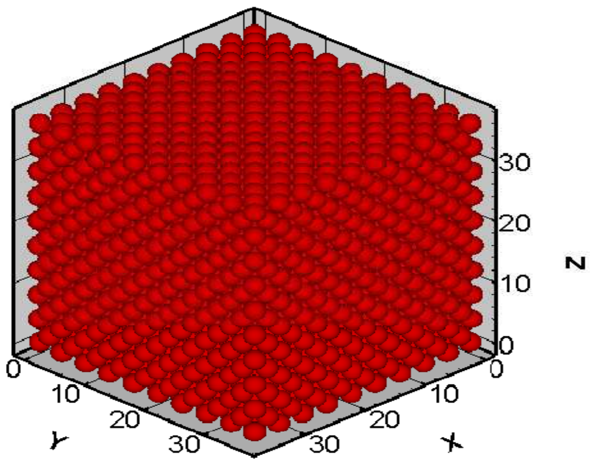

Analysis of simple shear deformations

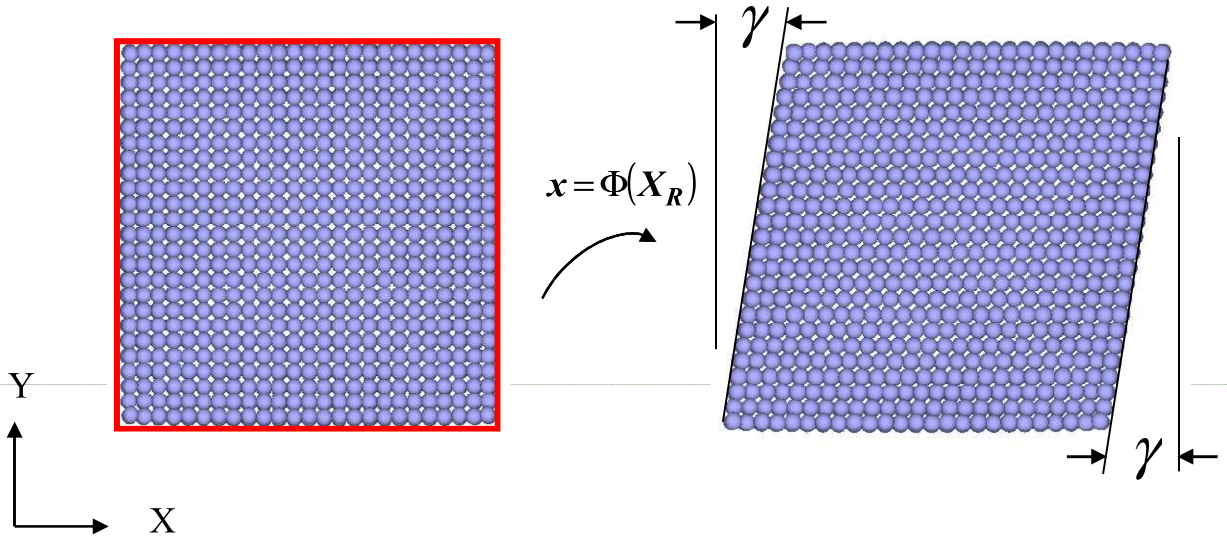

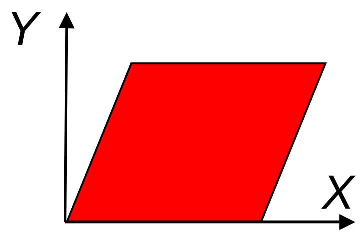

$$k_s = \tan(\gamma)$$

Prescribed displacements :

$x = X + k_s Y$

$y = Y$

$z = Z$

$$[F(k_s)] = \begin{bmatrix} 1 & k_s & 0 \\ 0 & 1 & 0 \\ 0 & 0 & 1 \end{bmatrix},$$

for which

$$[\varepsilon(k_s)] = \begin{bmatrix} 0 & k_s/2 & 0 \\ k_s/2 & k_s^{\,2}/2 & 0 \\ 0 & 0 & 0 \end{bmatrix}$$

Stress tensors for simple shear deformations

Strain energy density: $W_0(\boldsymbol{F}) = \sum_{i}^{N} \frac{V^{(i)}}{\Omega_R^{(i)}}$

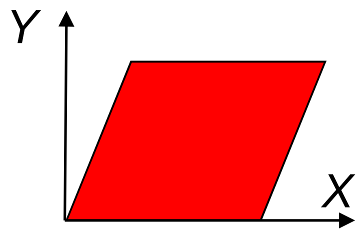

First Piola-Kirchhoff stress tensor: $\overline{\boldsymbol{P}} = \frac{\partial W_0}{\partial \boldsymbol{F}} = \frac{\partial}{\partial \boldsymbol{F}}\left(\sum_{i=1}^{N} \frac{V^{(i)}}{\Omega_R^{(i)}}\right)$

$$\boxed{\boldsymbol{P} = J\boldsymbol{F}^{-1}\boldsymbol{\sigma}}$$

$$[\overline{\sigma}(k_s)] = \sum_{\substack{i,k=1 \\ i \neq k}}^{N} \frac{1}{\Omega^{(i)}} \frac{1}{r^{(ik)}} \frac{\partial V^{(i)}}{\partial r^{(ik)}} [\Theta^{(ik)}(k_s)],$$

where

$$[\Theta^{(ik)}(k_s)] = \begin{bmatrix} R_{xx}^{(ik)} + k_s R_{xy}^{(ik)} + k_s\left(R_{xy}^{(ik)} + k_s R_{yy}^{(ik)}\right) & R_{xy}^{(ik)} + k_s R_{yy}^{(ik)} & R_{xz}^{(ik)} + k_s R_{yz}^{(ik)} \\ R_{yx}^{(ik)} + k_s R_{yy}^{(ik)} & R_{yy}^{(ik)} & R_{yz}^{(ik)} \\ R_{zx}^{(ik)} + k_s R_{zy}^{(ik)} & R_{zy}^{(ik)} & R_{zz}^{(ik)} \end{bmatrix}$$

$R_{xx}^{(ik)} = R_x^{(ik)} R_x^{(ik)}$, $R_{xy}^{(ik)} = R_x^{(ik)} R_{y,}^{(ik)}$ and so on.

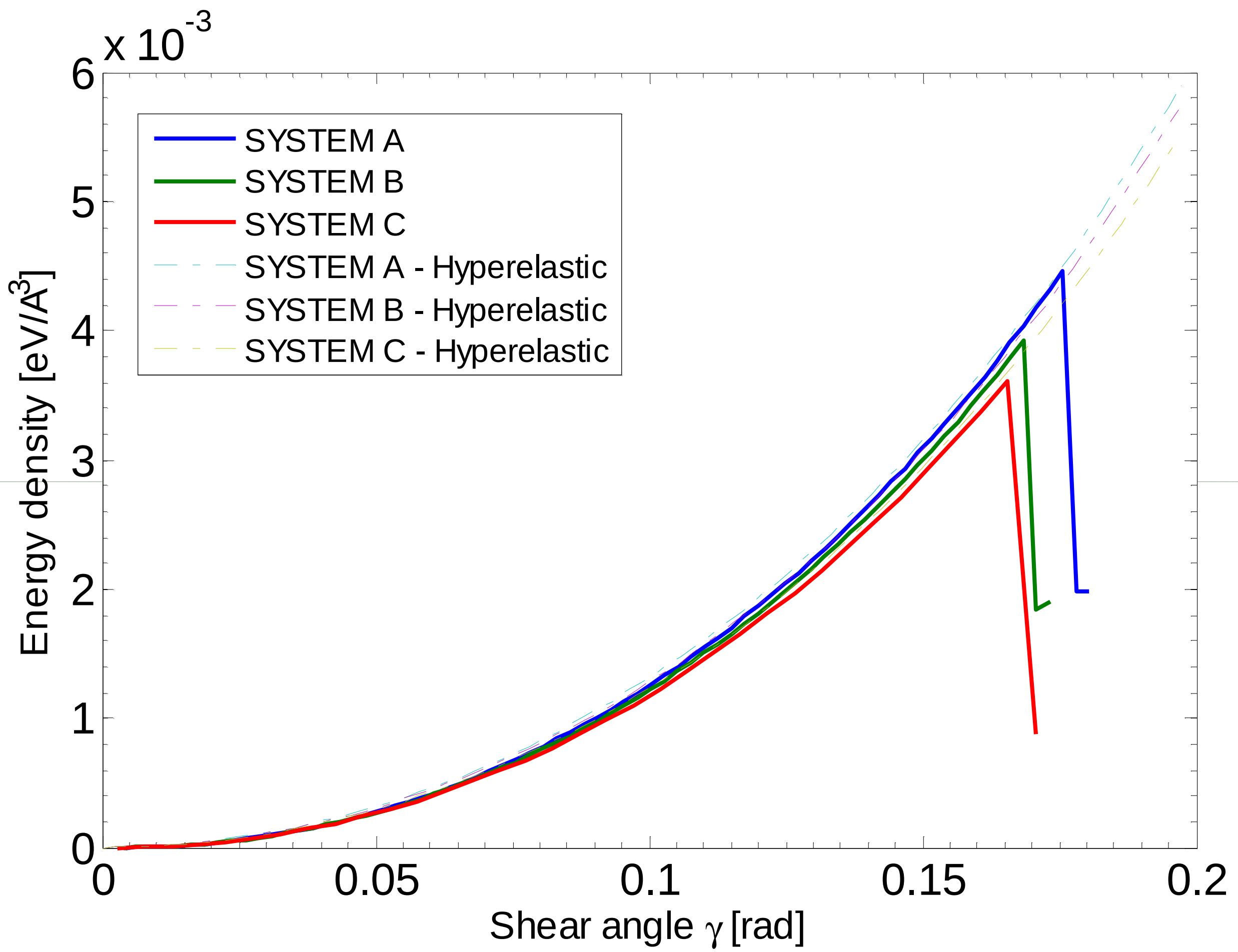

Simple shear tests

Comparison of results from the three local instability criteria

Specimen C

Shear test

$\gamma = 0.1020$

$\|G\|$

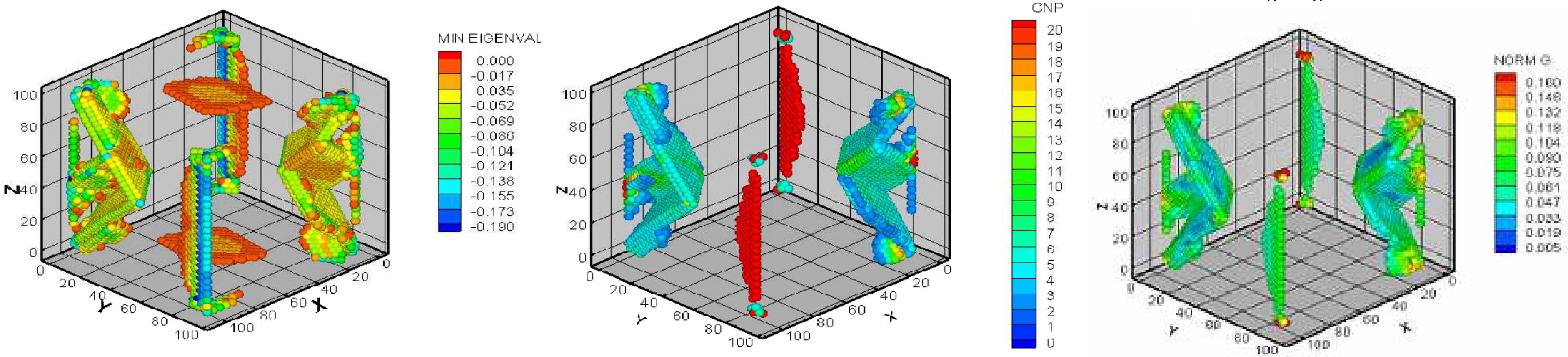

$\gamma = 0.1069$

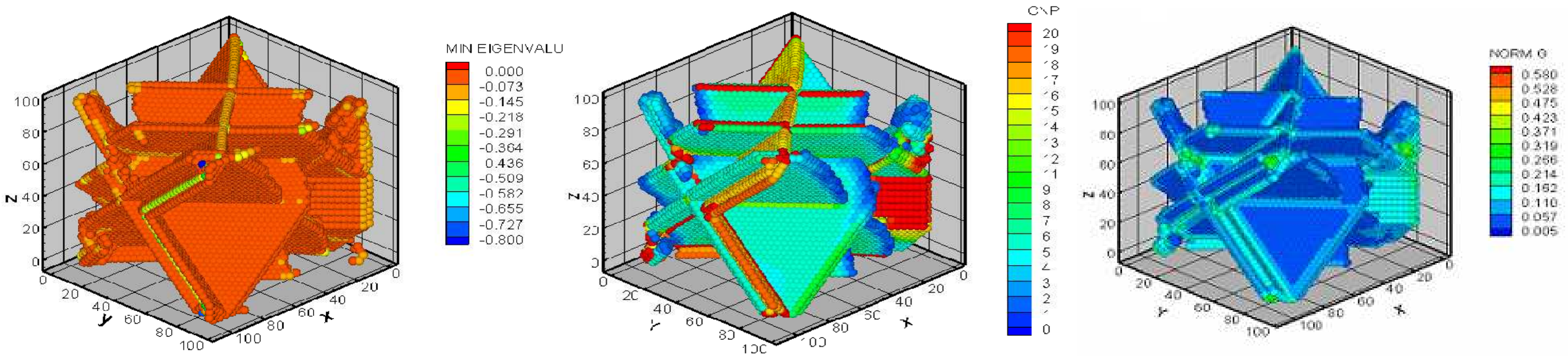

Distributions of the local components of the Cauchy stress tensor in the unloaded relaxed configuration

Specimen C

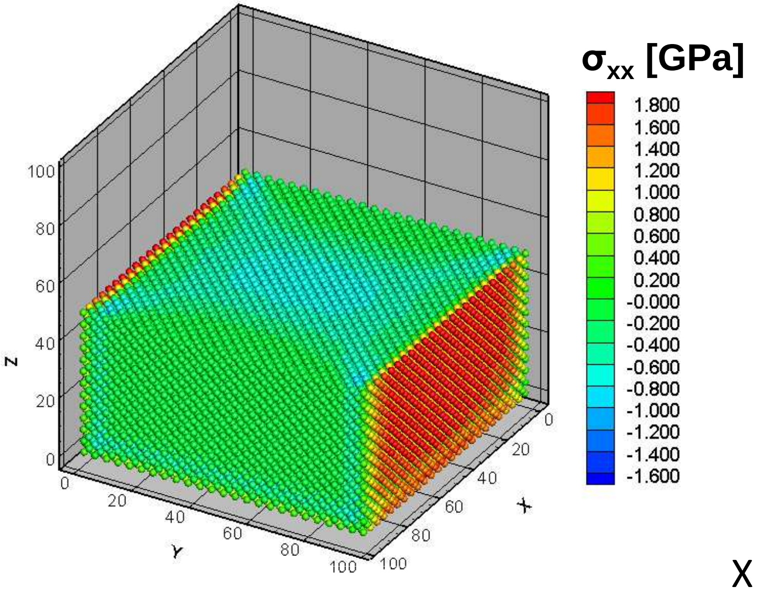

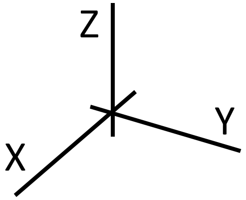

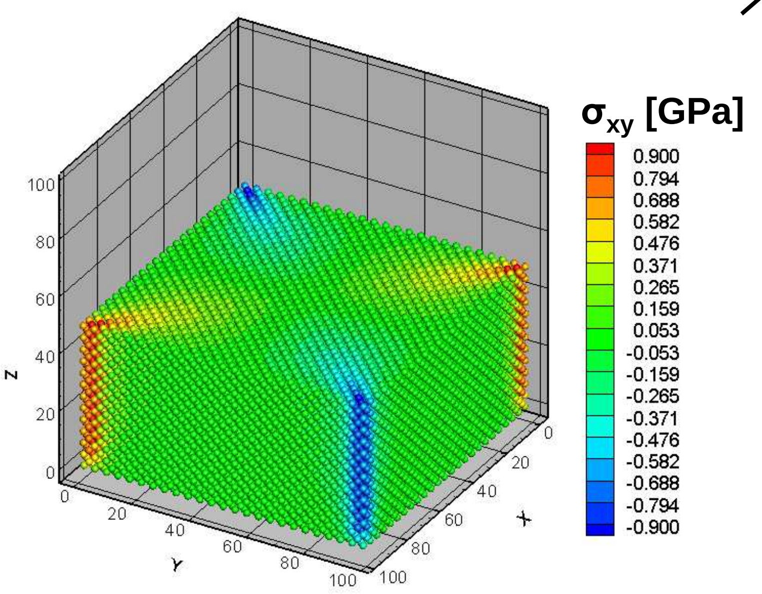

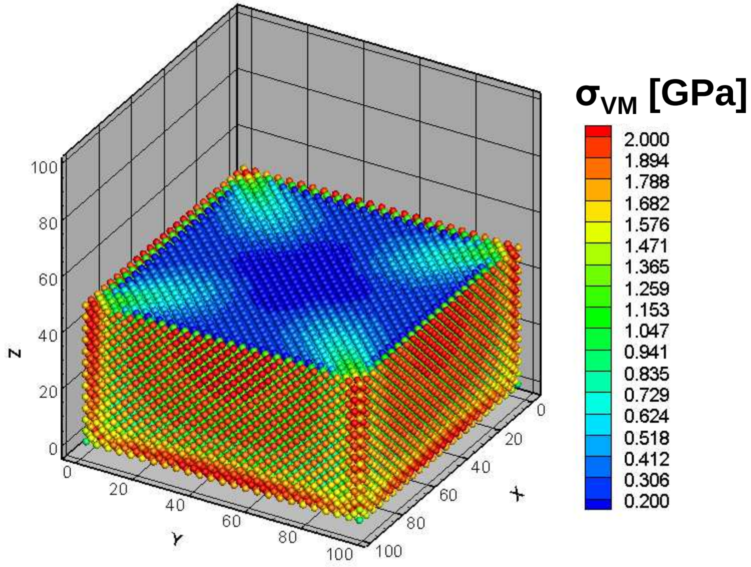

Instabilities in shear and simple shear

Divergence of the Cauchy stress tensor in the reference configuration

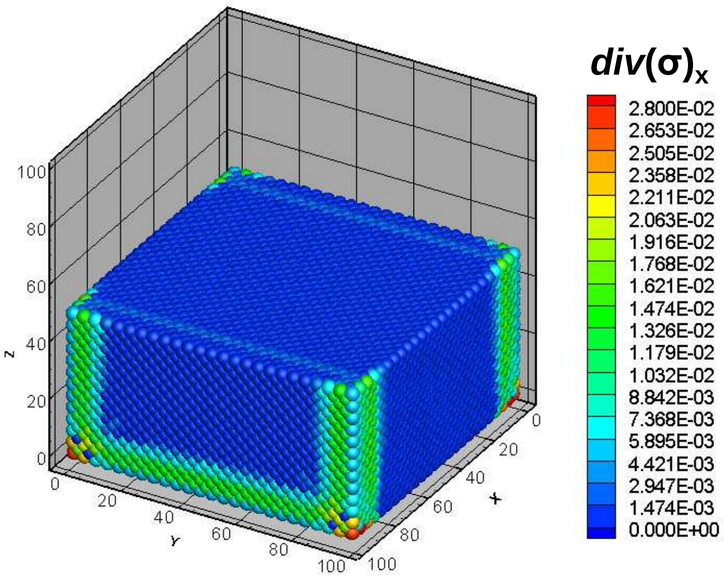

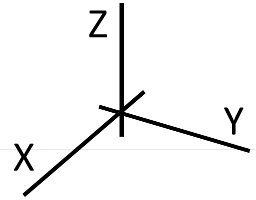

Specimen C

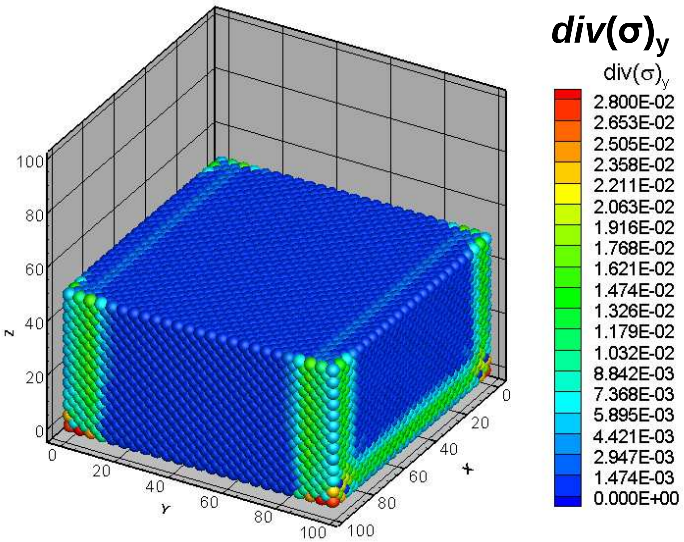

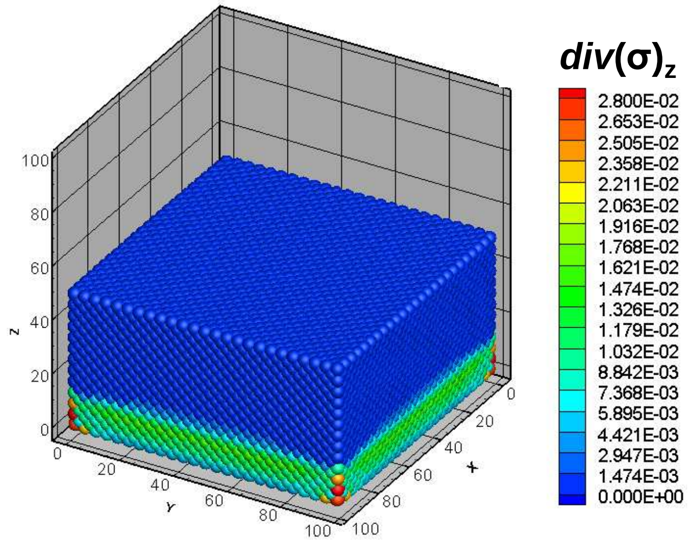

Comparison of shear stress components computed by different methods

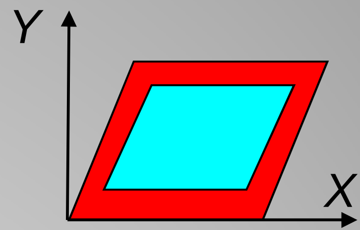

Specimen B

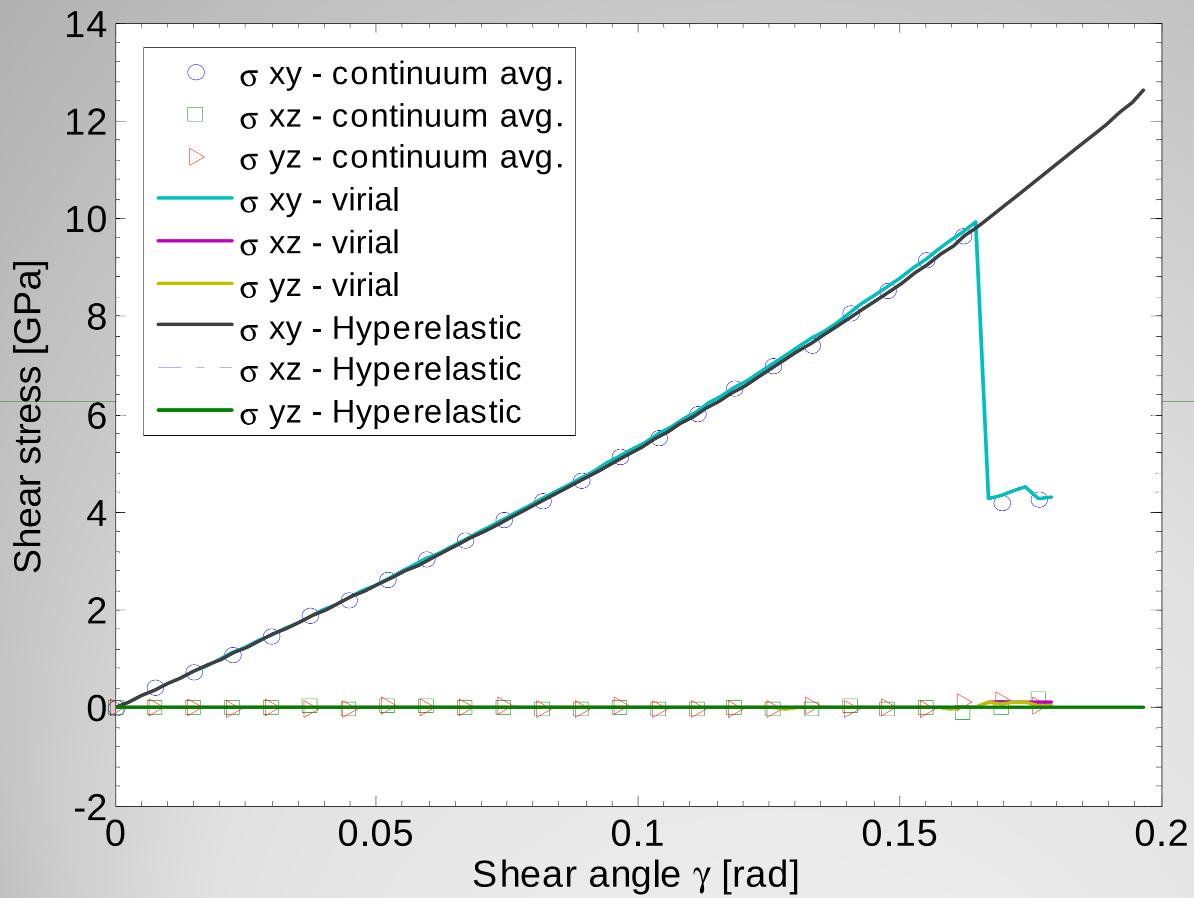

Comparison of normal stress components computed by different methods

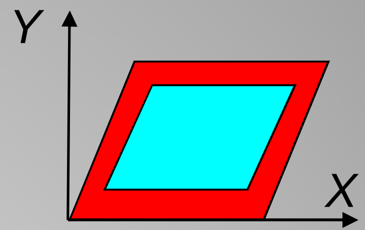

Specimen B

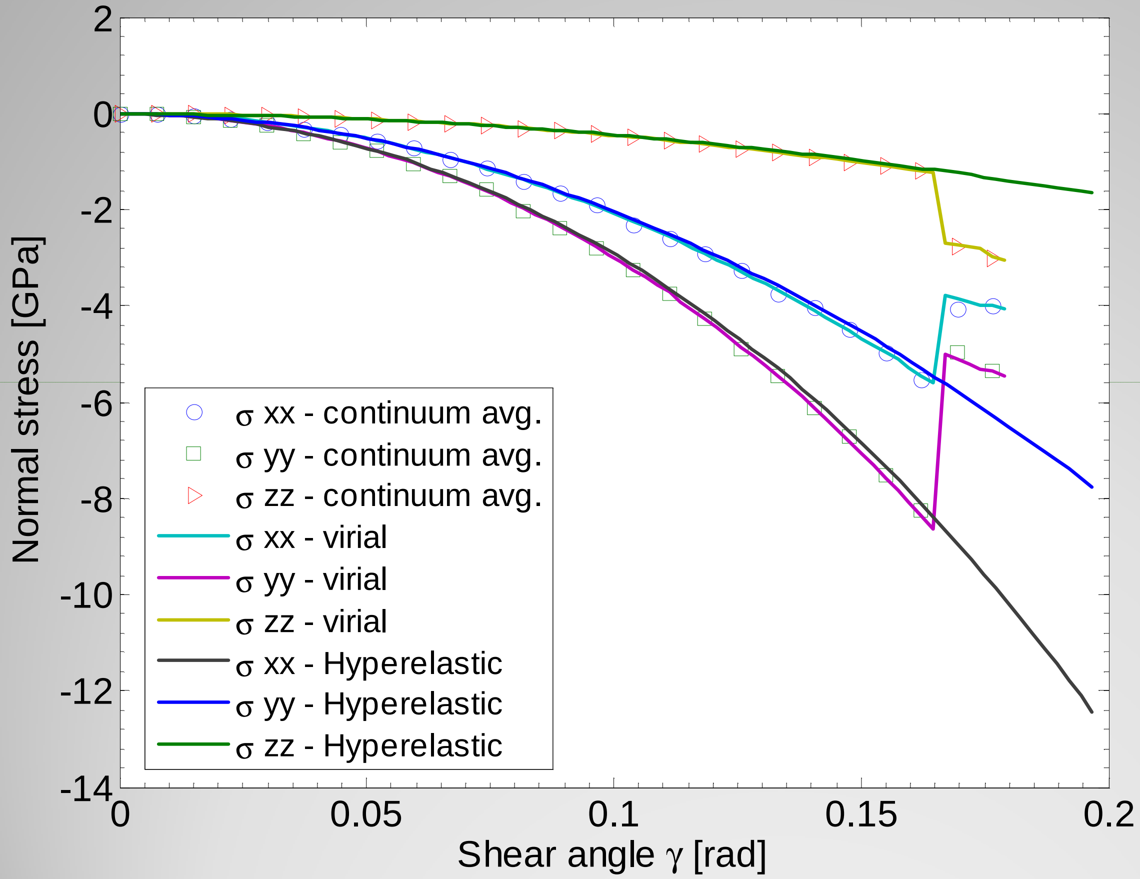

Completed work: instabilities in shear and simple shear deformations of gold crystals

Analysis of instabilities, *Local Instability*

Results of numerical simulations (Local Hessian and CNP distributions)

$\gamma = 0.1655$ **A**

Simple shear test

System C

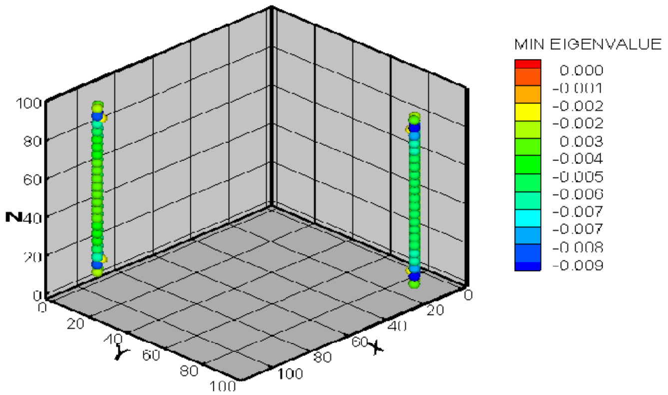

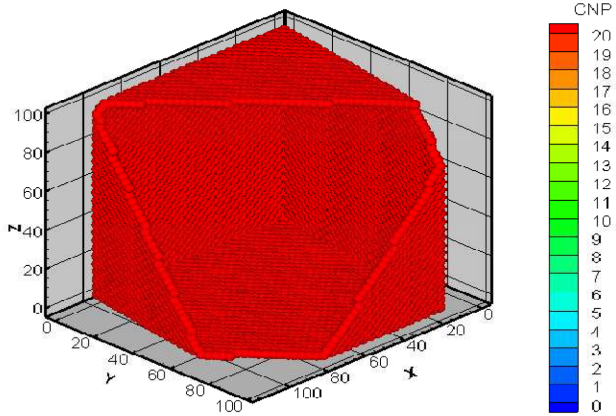

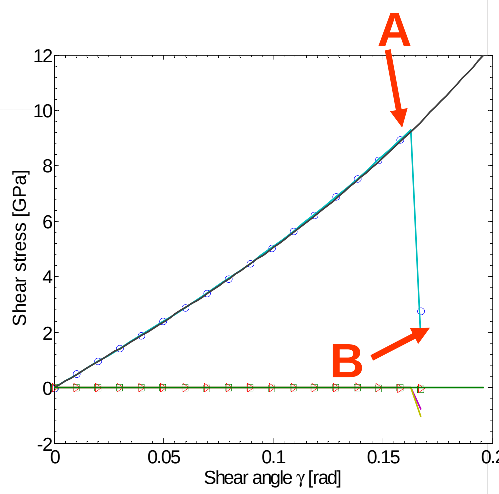

$\gamma = 0.1703$ **B**

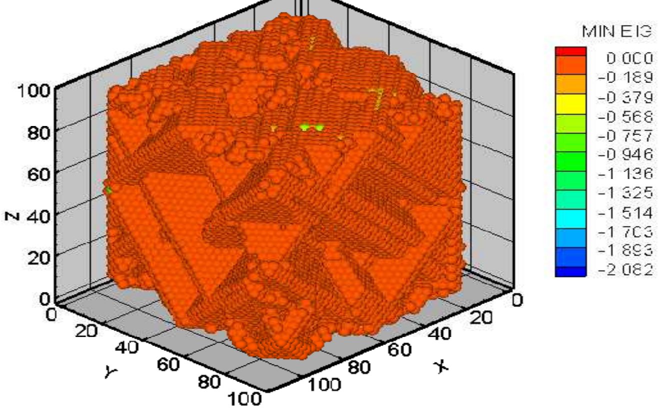

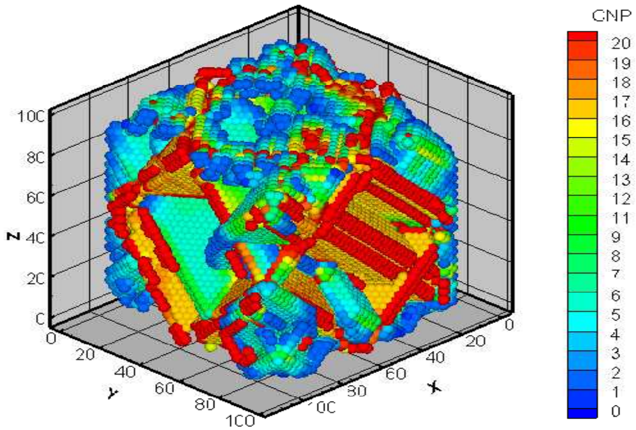

Distribution of the components of the Cauchy stress tensor

$\gamma = 0.0870$

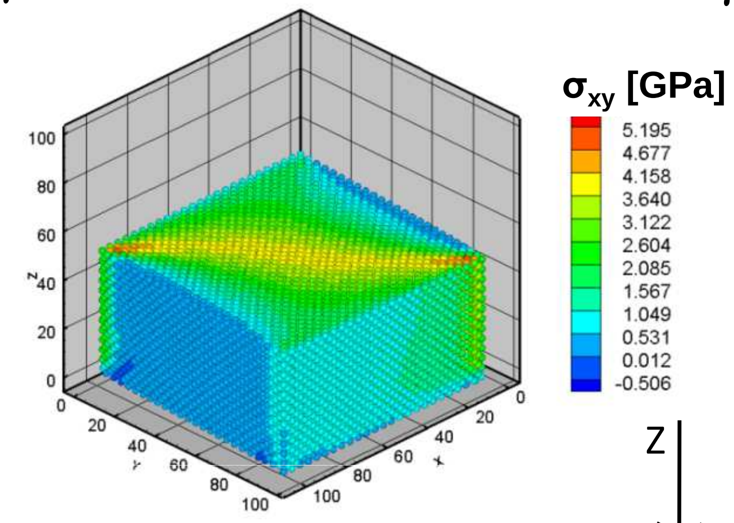

$\gamma = 0.0921$

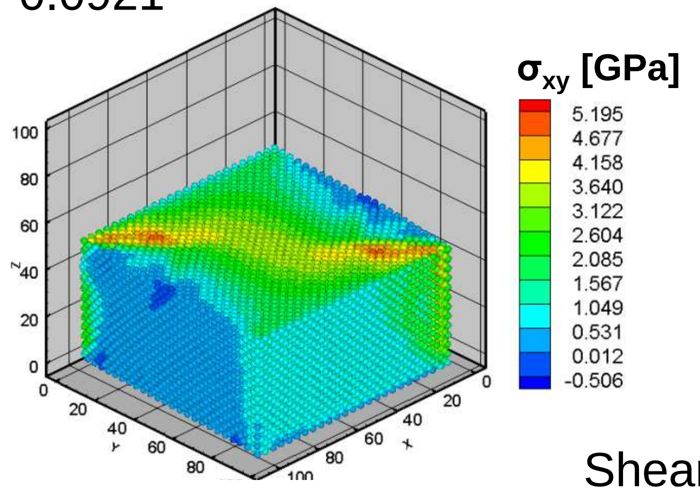

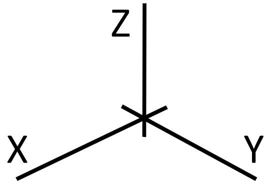

Shear test

Specimen C

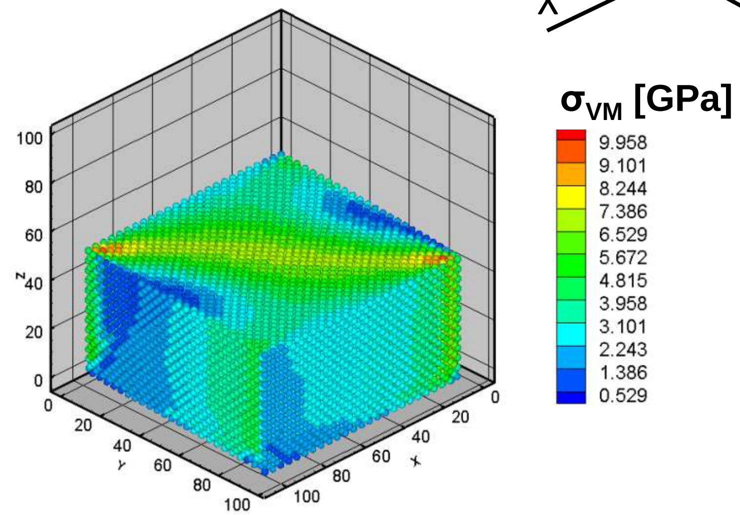

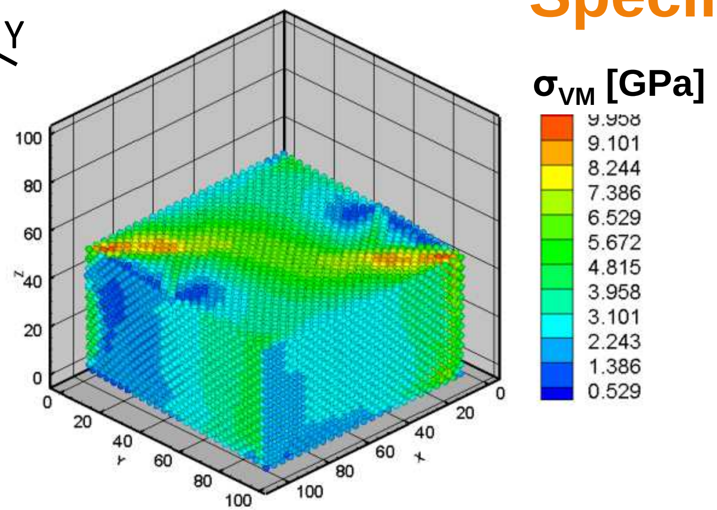

Distribution of the components of the Cauchy stress tensor

$\gamma = 0.1655$

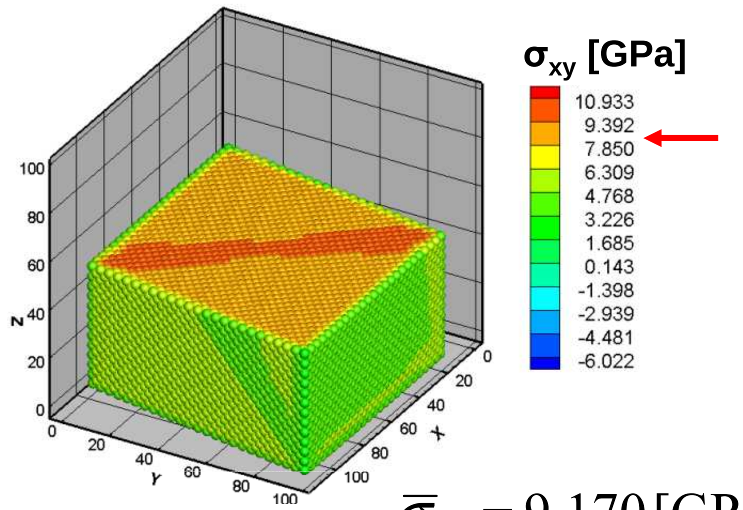

$\overline{\sigma}_{xy} = 9.170\,[\mathrm{GPa}]$

$\gamma = 0.1703$

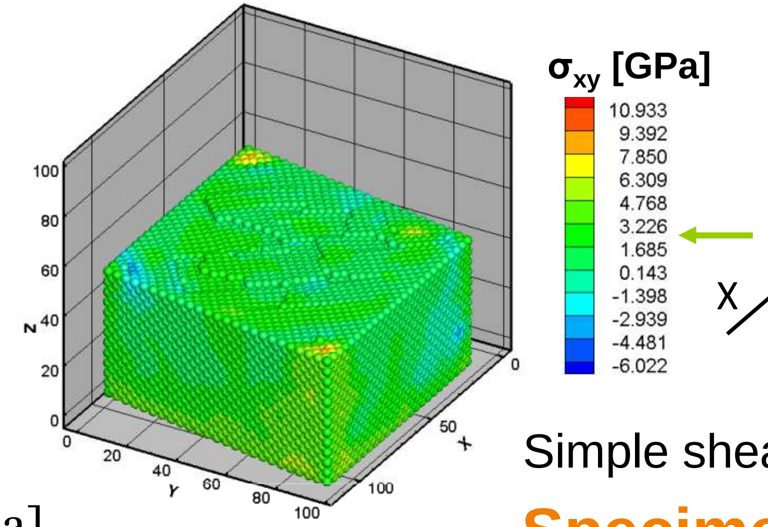

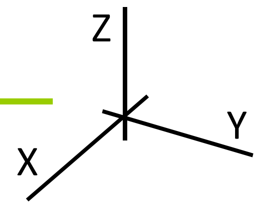

Simple shear test

Specimen C

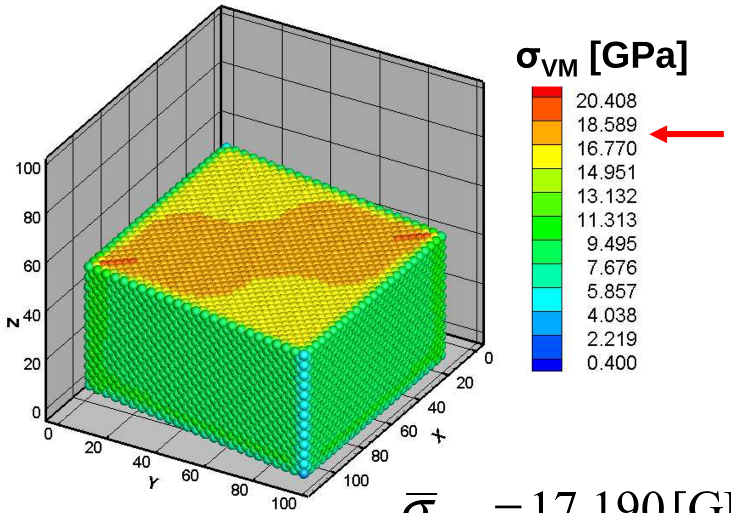

$\overline{\sigma}_{VM} = 17.190\,[\mathrm{GPa}]$

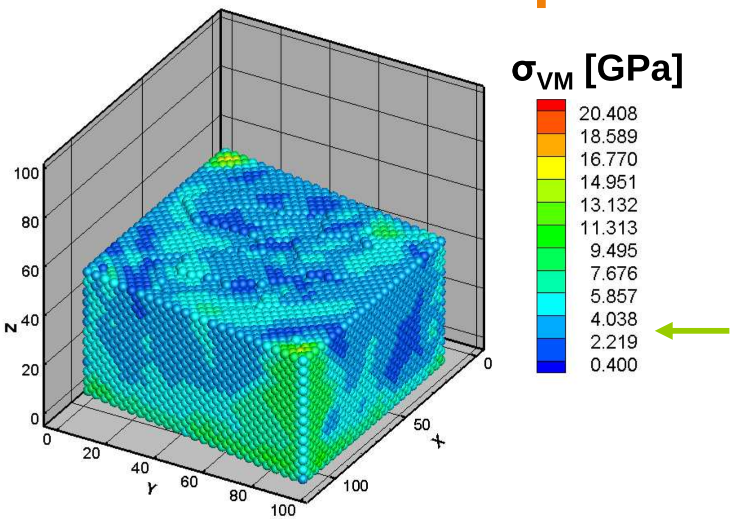

Material instability: stress relaxation

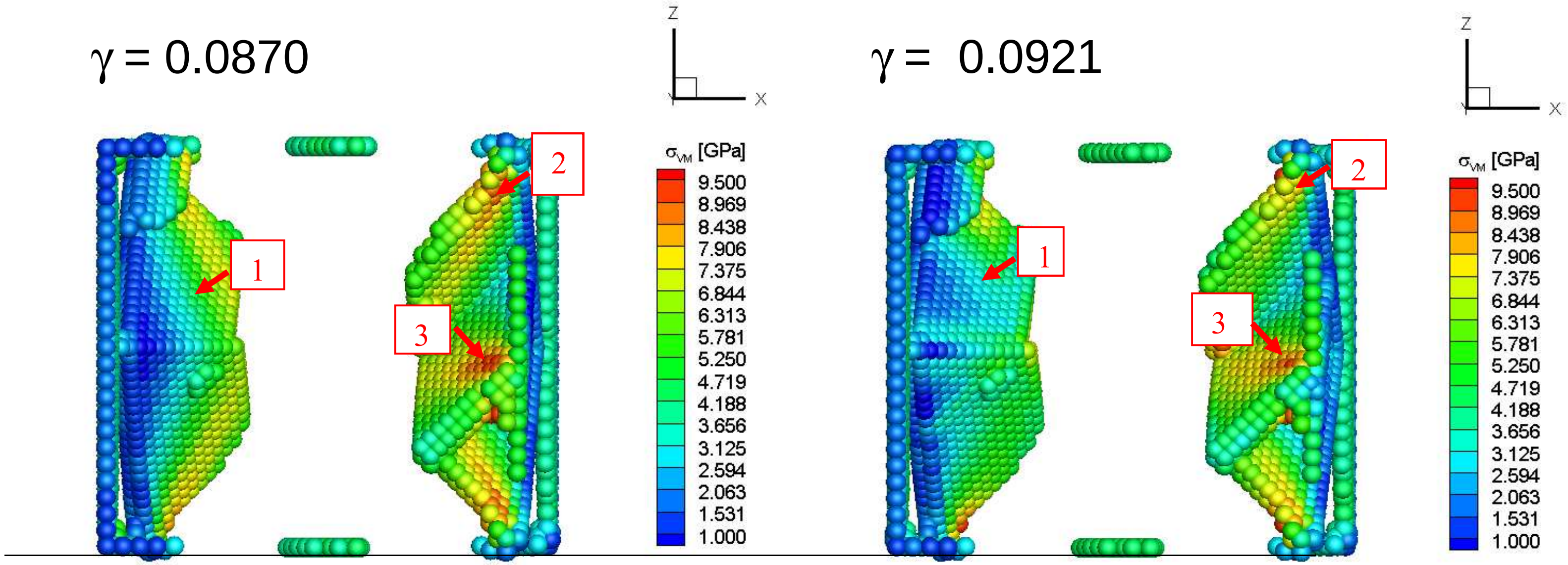

Stress (GPa)	Pre-instability Point 1	Post-instability Point 1	Pre-instability Point 2	Post-instability Point 2	Pre-instability Point 3	Post-instability Point 3
σ_{VM}	6.672	3.364	8.741	7.594	9.038	7.968
σ_{xy}	3.747	1.186	4.043	3.864	4.646	3.512
P_1	-8.004	-3.641	-10.075	-8.386	-11.424	-9.900
P_2	-3.079	-1.701	-4.733	-3.884	-5.691	-4.105
P_3	-0.411	0.243	-0.215	0.381	-1.004	-0.813
$2\tau_{\max}$	7.593	3.884	10.075	8.767	10.419	9.087

Shear test

Specimen C

Instabilities in shear and simple shear

Amorphous metals
-Mechanical properties-

Table . A comparison of properties at room temperature for some metallic glasses and polycrystalline materials.

Alloy	Yield strength σ_y (MPa)	Yield strength σ_y (Ksi)	Density ρ_m (g cm^{-3})	Density ρ_m (lb in^{-3})	Strength to weight ratio	Elongation (%)
Metallic glasses						
$Zr_{41.25}Ti_{13.75}Cu_{12.25}Ni_{10}Be_{22.5}$	1900	275	6.1	0.22	310	2
$Mg_{65}Cu_{25}Tb_{10}$	700	100	4.0	0.14	175	1.5
$Fe_{59}Cr_{6}Mo_{14}C_{15}B_{6}$	3800	550	7.9	0.29	480	~2
Conventional alloys						
Aluminum (7075-T6)	505	73	2.8	0.10	180	11
Titanium (Ti-6Al-4V)	1100	160	4.4	0.16	250	10
Steel (4340)	1620	190	7.9	0.29	206	6
Magnesium (AZ80)	275	400	1.8	0.07	150	7

(From Hufnagel Research Group, Department of Materials Science and Engineering, Johns Hopkins University)

Amorphous metals
-Deformation mechanisms-

Shear transformation zones (STZ)

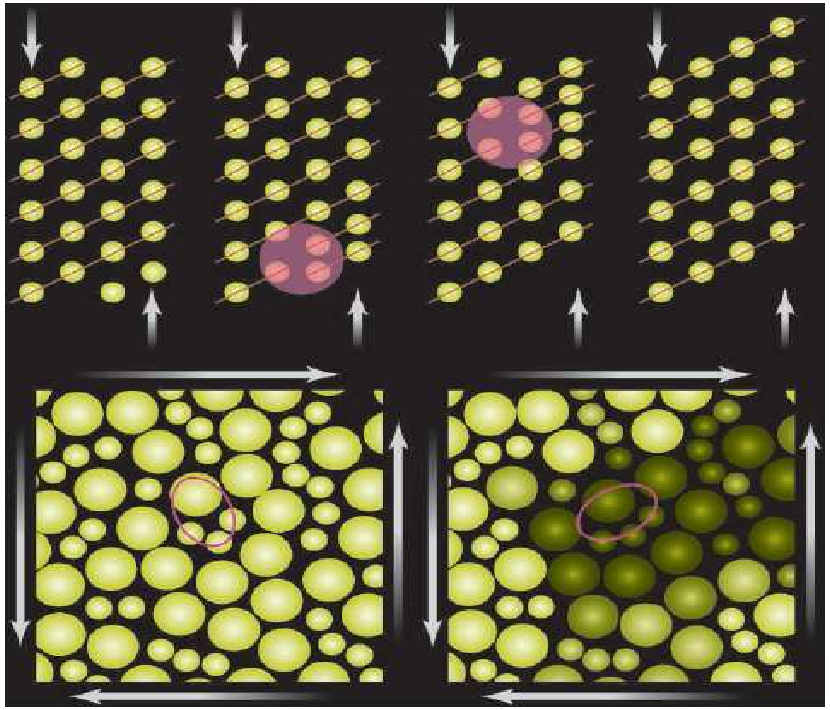

(From Falk, M., 2007)

$$\dot{\varepsilon}_{pl} = \lambda v\left(R_{-}n_{-} - R_{+}n_{+}\right)$$

$$\dot{n}_{\pm} = R_{\mp}n_{\mp} - R_{\pm}n_{\pm} - R_{a}n_{\pm} + R_{c}$$

$\dot{\varepsilon}_{pl}$: plastic strain rate

λ : increment in shear strain

υ : volume of a STZ

$n_{\pm}$: density of STZs $\pm$

$R_{\pm}$: Transformation rate $\pm$

STZs in amorphous Ni

The distortional strain tensors

Tension test

Amorphous Ni

Cauchy strain tensor : $\boldsymbol{C} = \boldsymbol{F}^T \boldsymbol{F}$

Distortional part Cauchy strain tensor : $\tilde{\boldsymbol{C}} = \left(\det[\boldsymbol{F}]\right)^{-2/3} \boldsymbol{C}$.

Second invariant of : $\boldsymbol{II}_{\tilde{\boldsymbol{C}}} = (1/2)\left(\left(trace\ \tilde{\boldsymbol{C}}\right)^2 - trace\left(\tilde{\boldsymbol{C}}^{\boldsymbol{2}}\right)\right)$

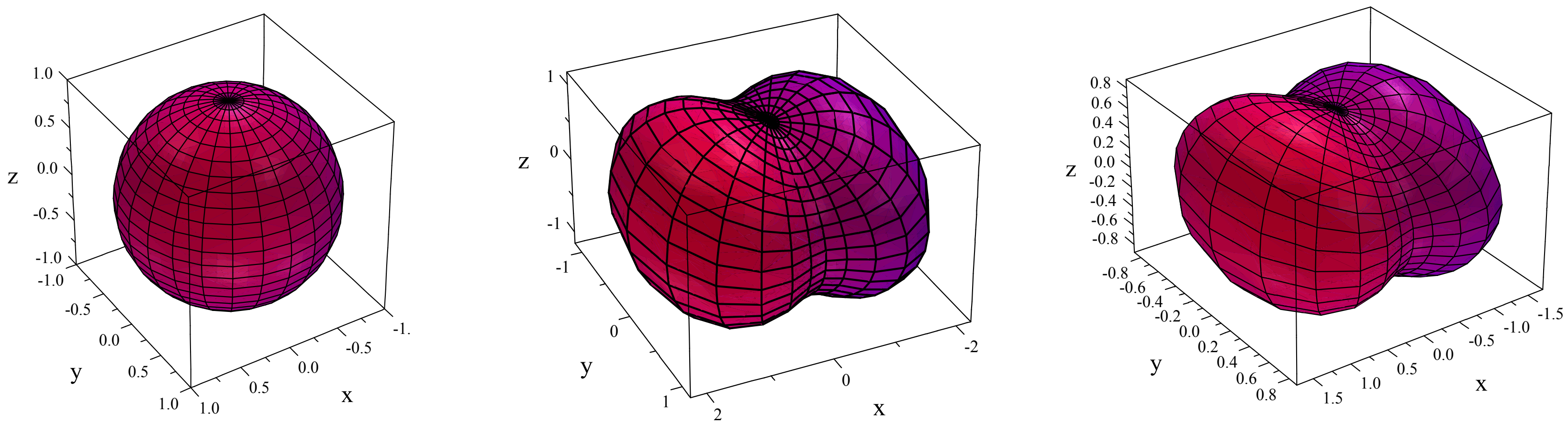

STZs in amorphous Ni

The continuously distributed dislocations and the Nye tensor

$$\boldsymbol{b} = -\int_{A_t} \left(\nabla \times \boldsymbol{F}^{-1}\right) \cdot \boldsymbol{N}_t \, dA_t \qquad \boldsymbol{b} = \int_{A_t} \alpha \cdot \boldsymbol{N}_t \, dA_t$$

$$\boldsymbol{\alpha} = -\left(\nabla \times \boldsymbol{F}^{-1}\right)$$

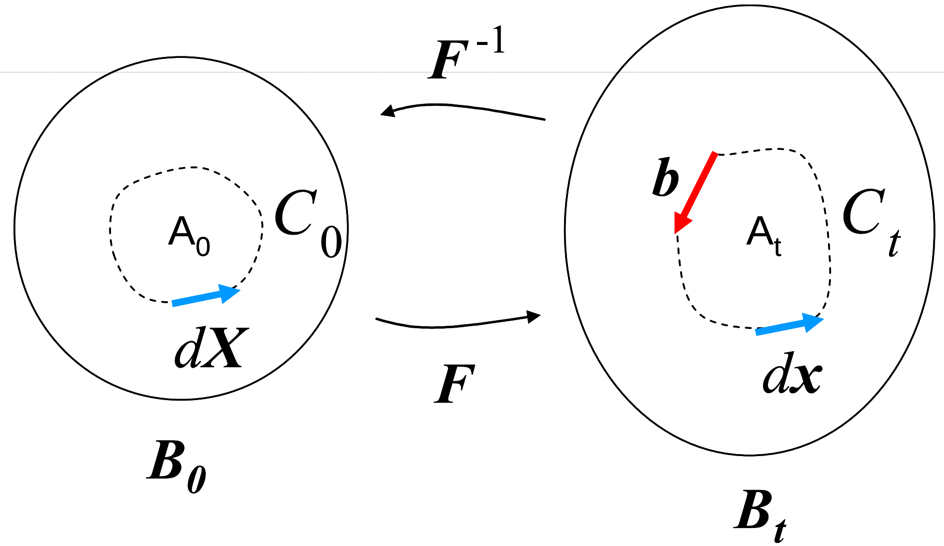

Hartley and Mishin (2005)

STZs in amorphous Ni

Distributions II-CD and STZs

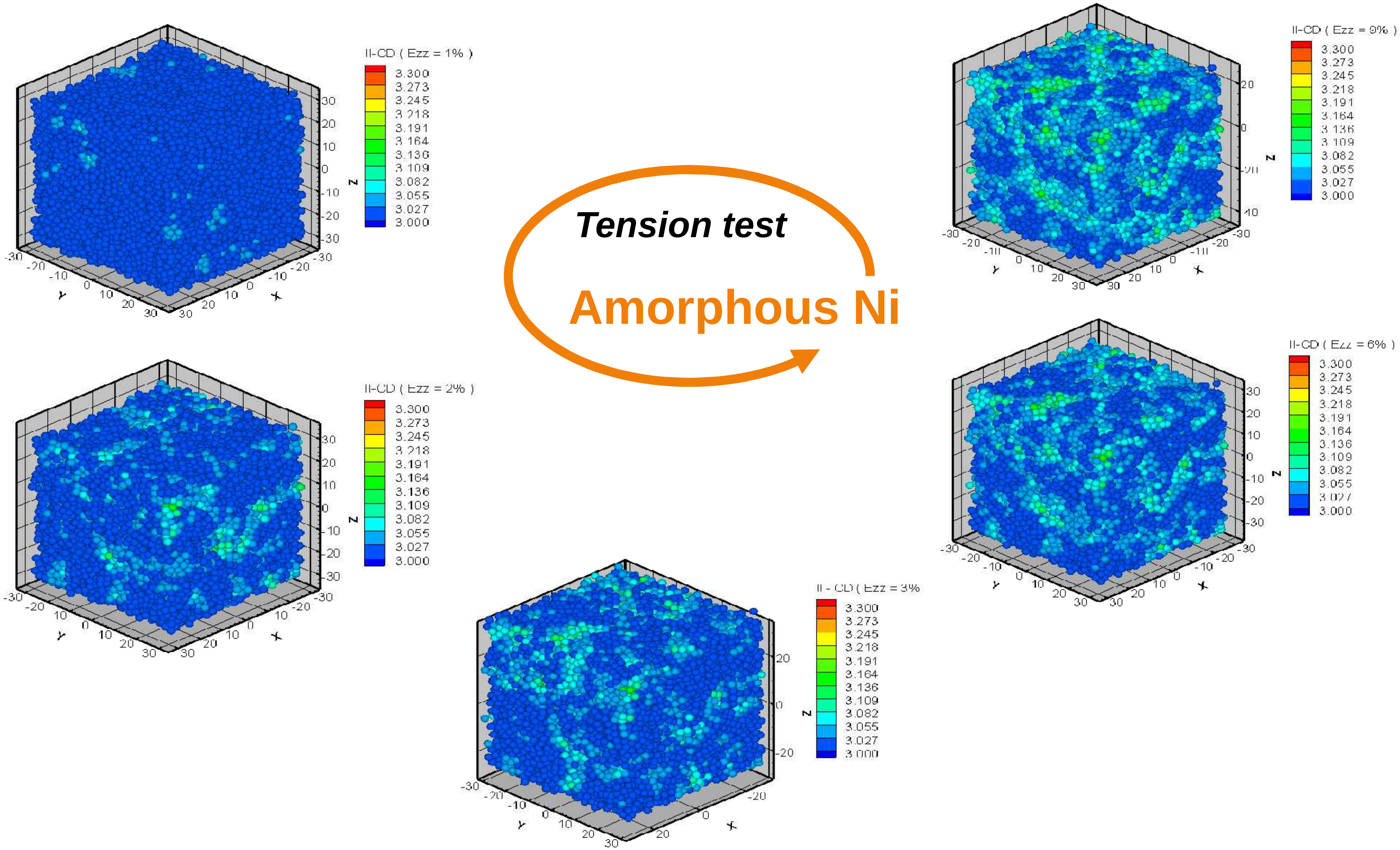

Nanocrystalline materials
-Deformation mechanisms at grain boundaries-

Inverse Hall-Petch

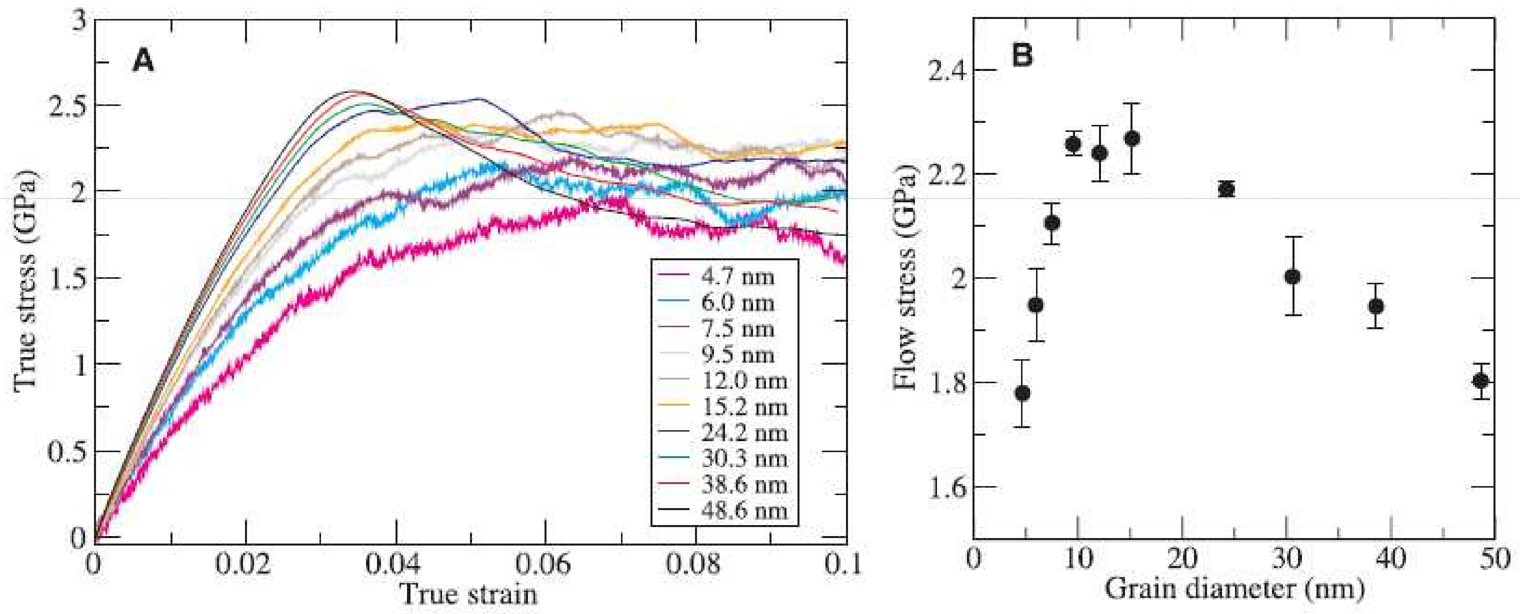

(From Schiøtz and Jacobsen, 2003)

Completed work: Grain boundary deformation in nano-crystalline Ni

Separation of the system in bulk and grain boundaries

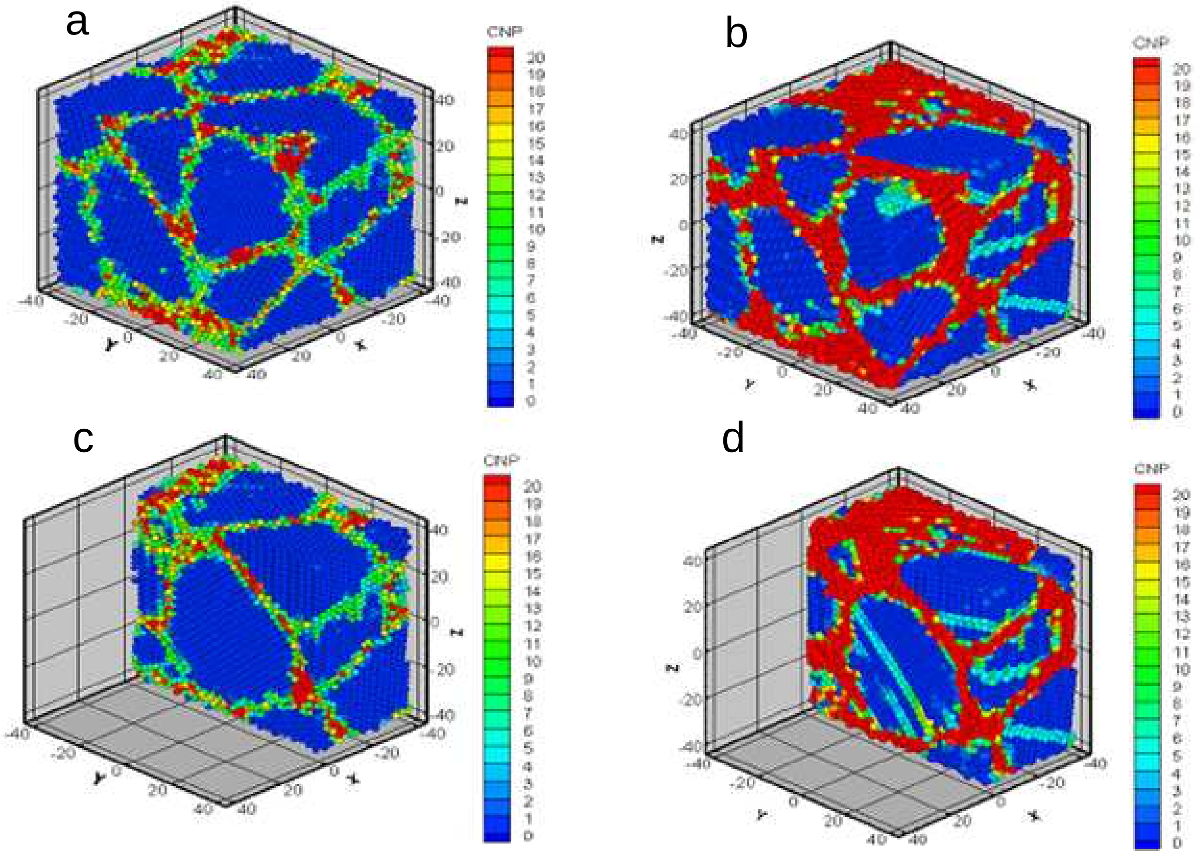

Tension test

nc Ni

(a) ε_{zz} = 1%.
(b) ε_{zz} = 9%.
(c) section x = 0 at ε_{zz} = 1%.
(d) section x = 0 at ε_{zz} = 9%.

Grain boundary deformation in nano-crystalline Ni

Distribution of the Nye tensor

Tension test

nc Ni

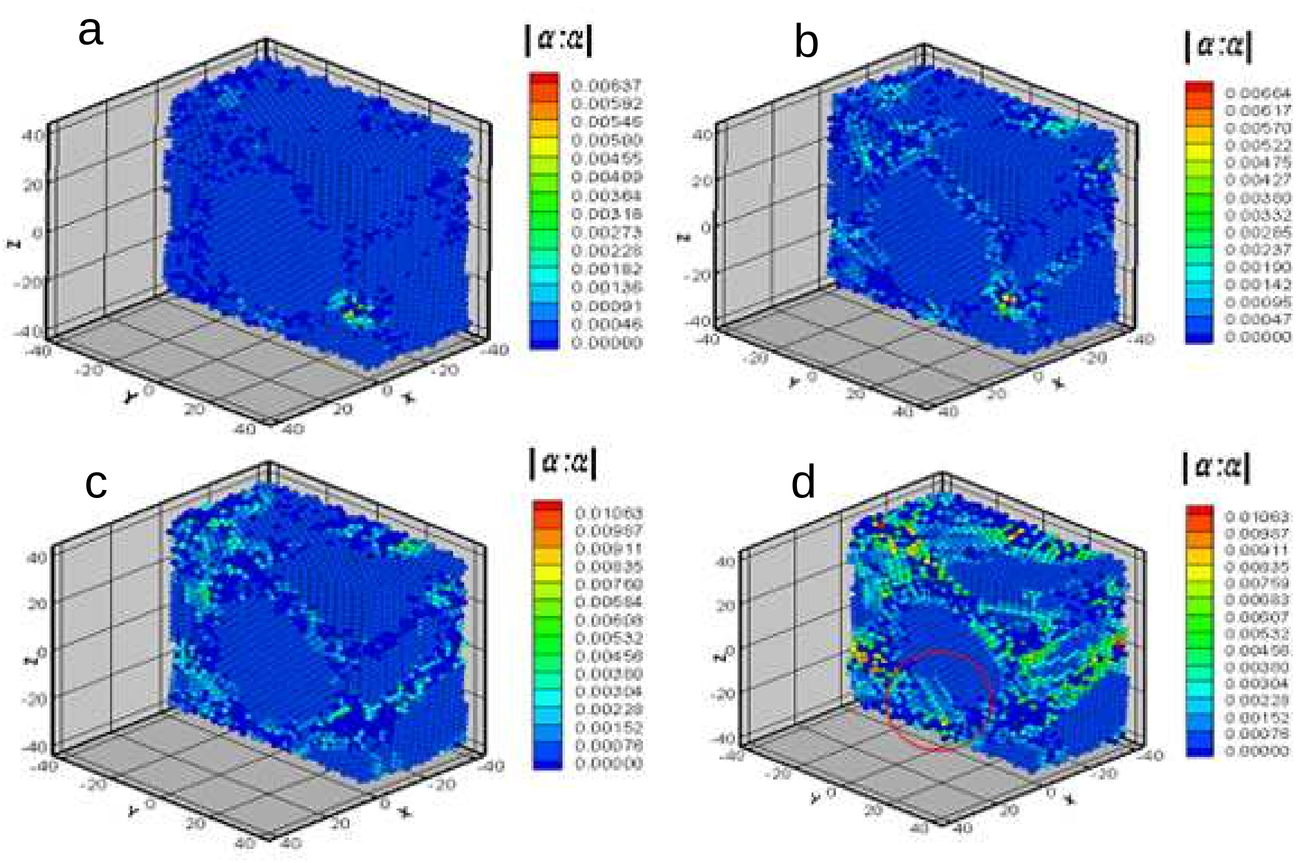

Distribution of the Nye norm for the section x = 0 at different strain levels;
(a) ε_{zz} = 1%, (b) ε_{zz} = 3%,
(c) ε_{zz} = 5%,and (d) ε_{zz} = 7%.

Grain boundary deformation in nano-crystalline Ni

Distribution of the Nye tensor GBs

Tension test

nc Ni

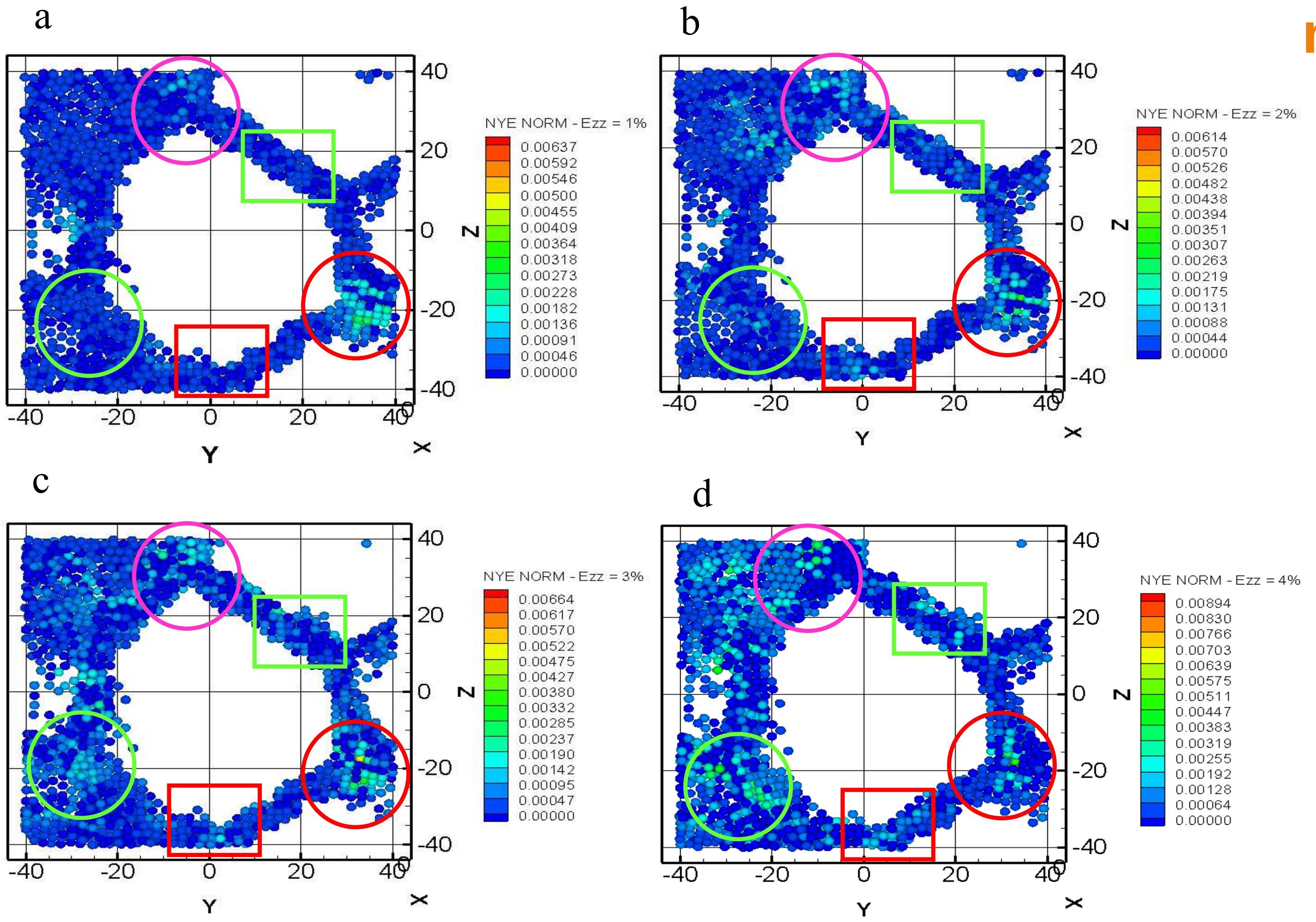

Completed work: Grain boundary deformation in nano-crystalline Ni

Distribution of the Nye tensor section x=0

Tension test

nc Ni

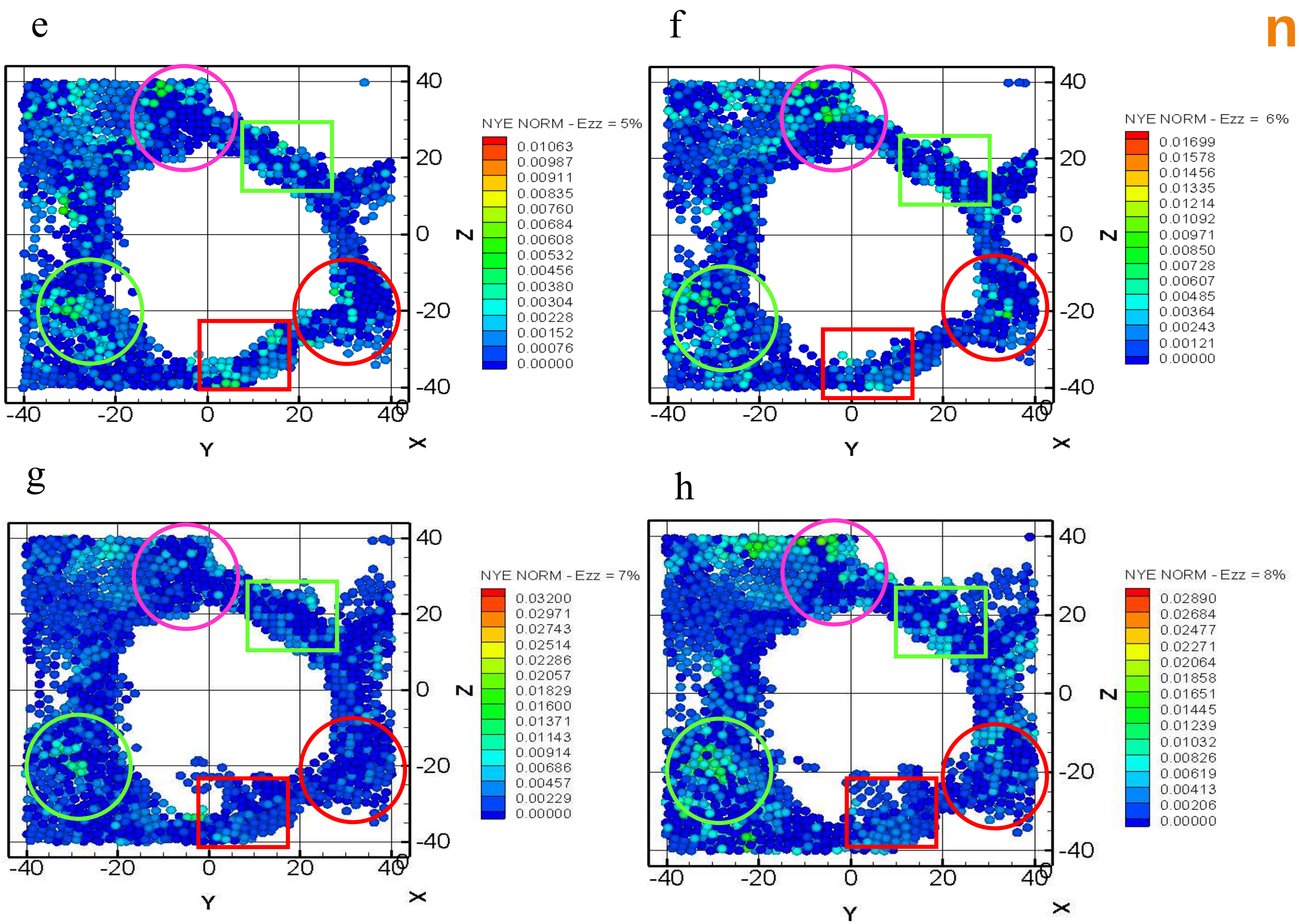

GOLD : MECHANICAL TESTS – FINITE ELEMENT METHOD

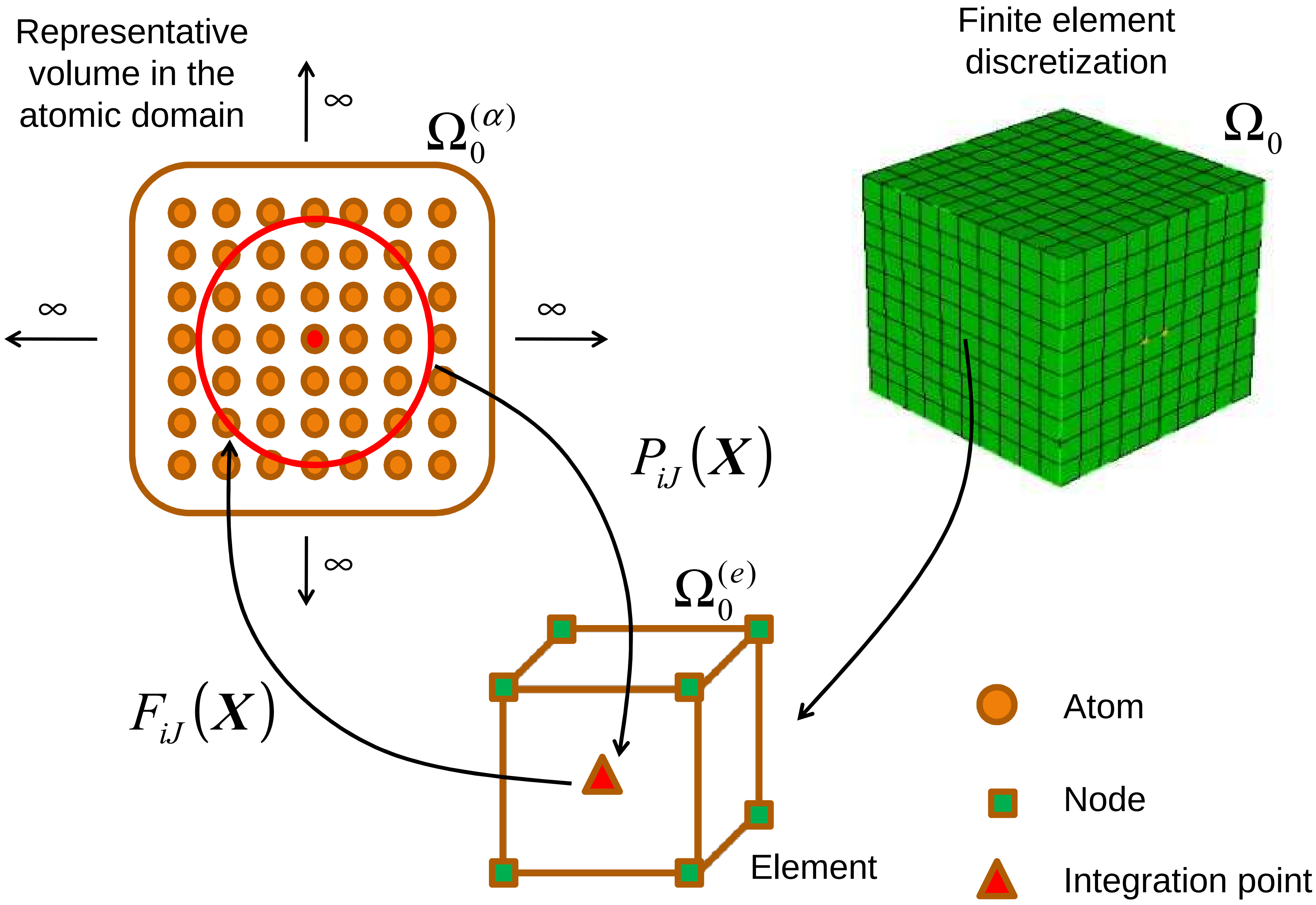

GOLD : MM & FEM - TENSION /COMPRESSION TESTS

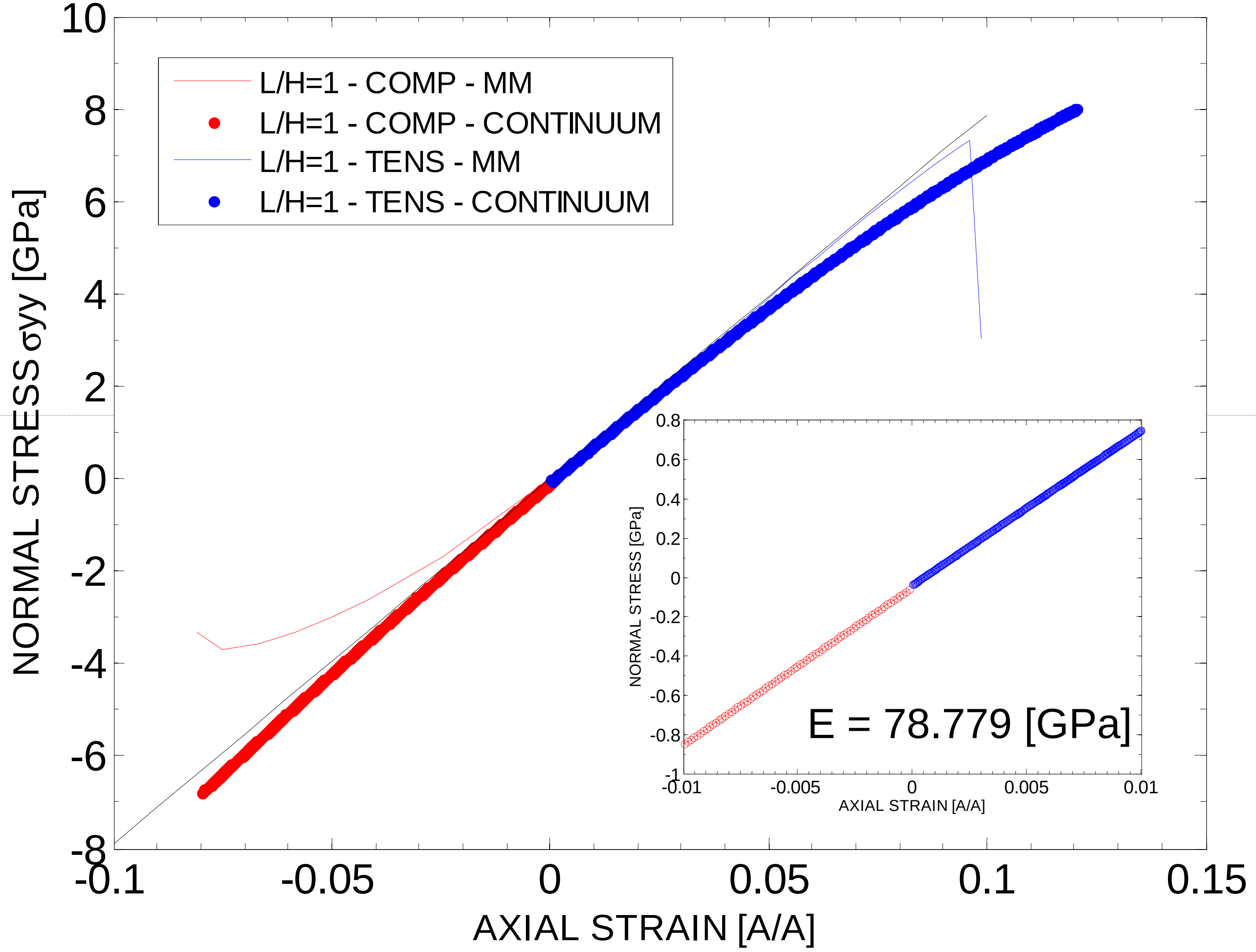

GOLD : TENSION/COMPRESSION TESTS – YOUNG'S MODULUS

BULK Au - FEM VS. MM

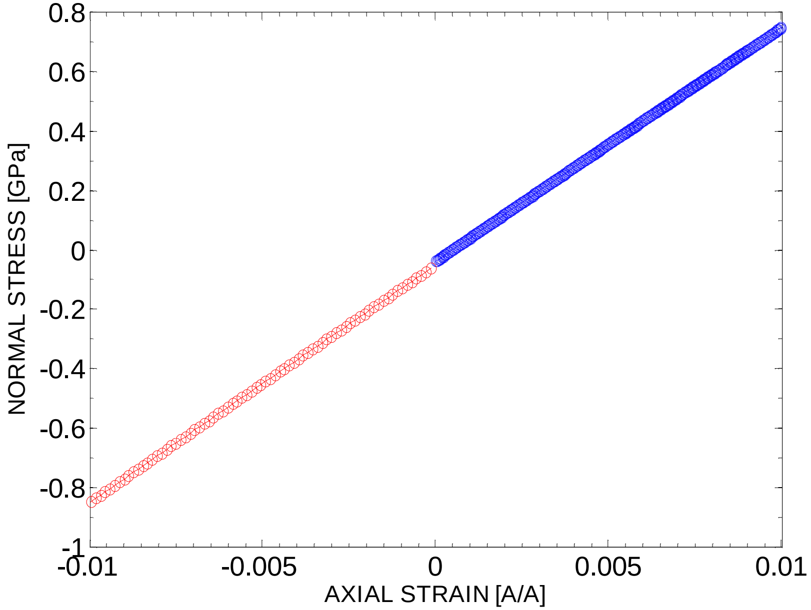

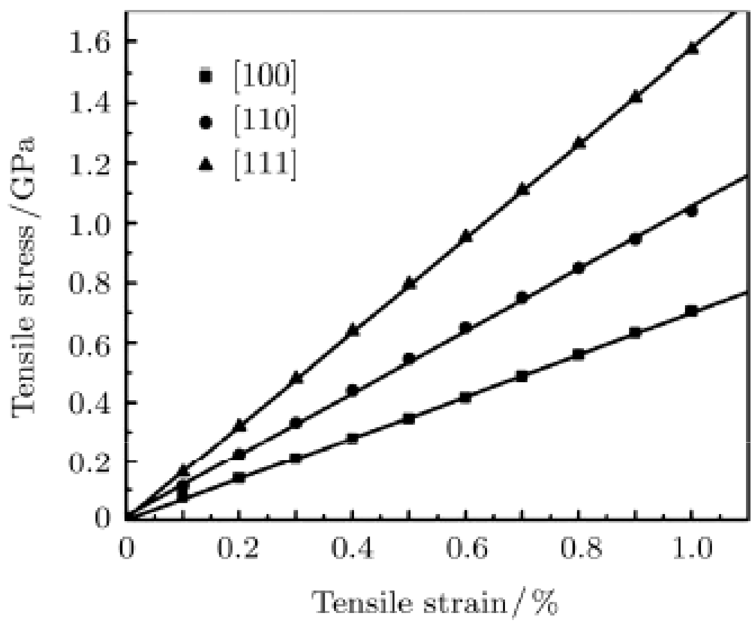

FEM : E = 78.779 GPa

POLYCRYSTAL : E ~ 78 GPa

Fig.2. The elastic response of Au bulk for uniaxial strain applied along [001], [011] and [111] directions under tensile loading.

MM : E = 72.2 GPa

Quantum Corrected Sutton-Chen (Q-SC) potential

Liu, S.S., Wen Y.H., *Zhu Z.Z., 2008.* The elastic properties and energy characteristics of Au nanowires: an atomistic simulation study. Chinese Physics B, Vol. 17 No 7, 2621-2626.

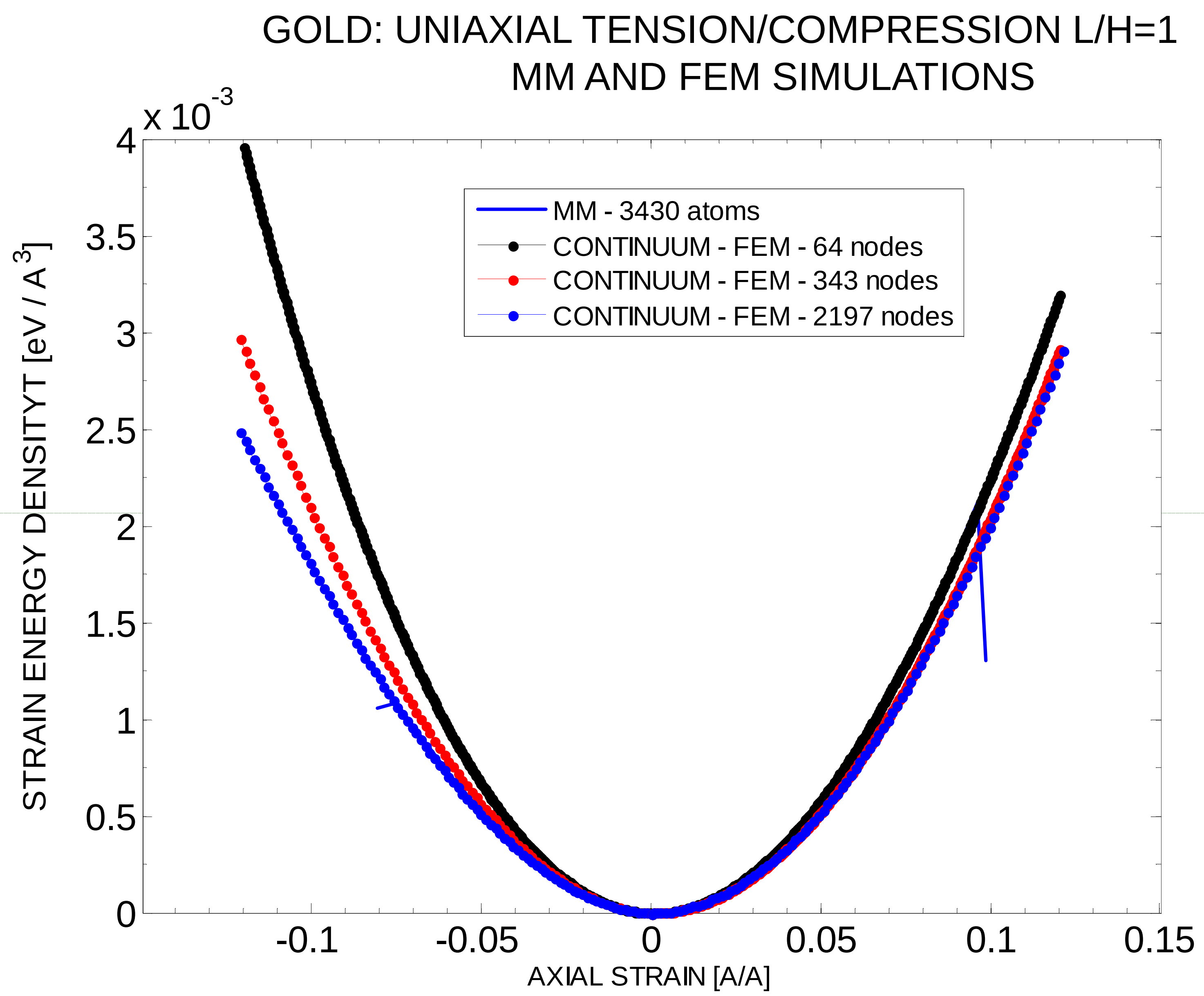
GOLD: UNIAXIAL TENSION/COMPRESSION L/H=1
MM AND FEM SIMULATIONS
x 10^-3
STRAIN ENERGY DENSITYT [eV / A^3]
AXIAL STRAIN [A/A]
MM - 3430 atoms
CONTINUUM - FEM - 64 nodes
CONTINUUM - FEM - 343 nodes
CONTINUUM - FEM - 2197 nodes
0
0.5
1
1.5
2
2.5
3
3.5
4
-0.1
-0.05
0
0.05
0.1
0.15

GOLD: UNIAXIAL TENSION/COMPRESSION L/H=1
MM AND FEM SIMULATIONS

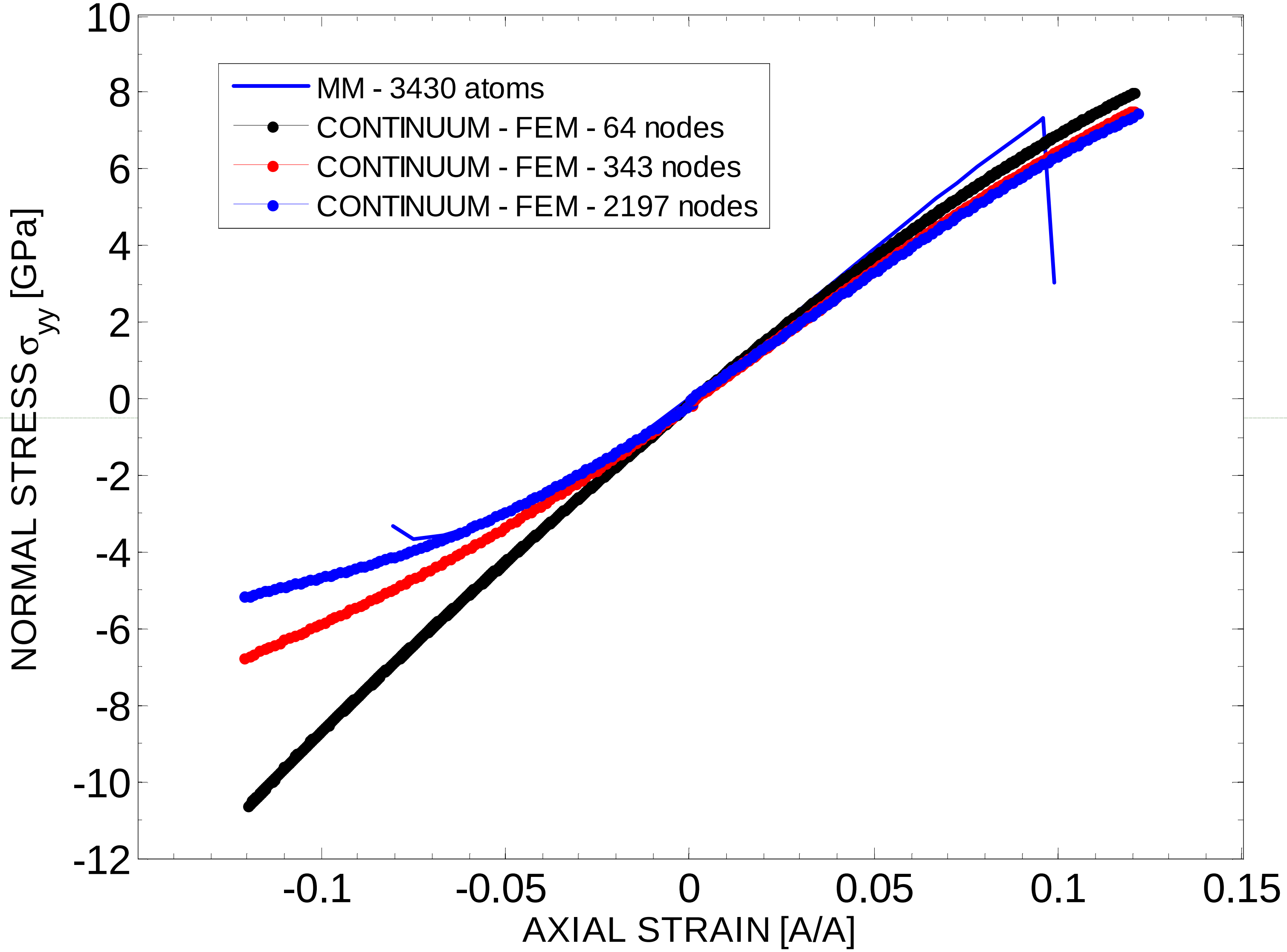

GOLD: UNIAXIAL TENSION/COMPRESSION L/H=1 , MM AND FEM SIMULATIONS
σxy AND σyz DISTRIBUTIONS

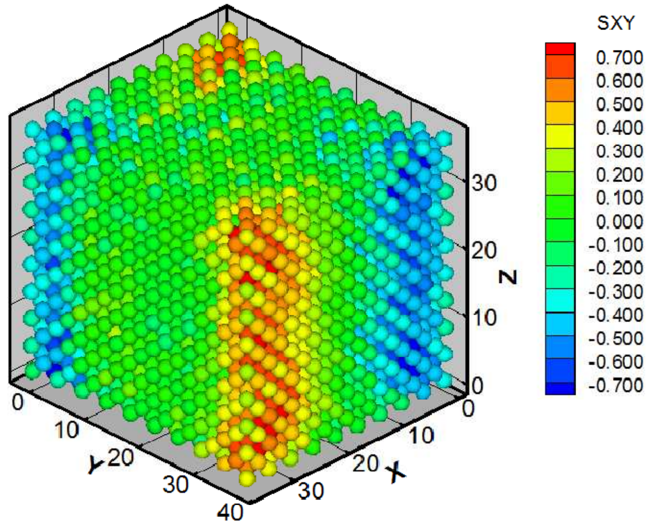

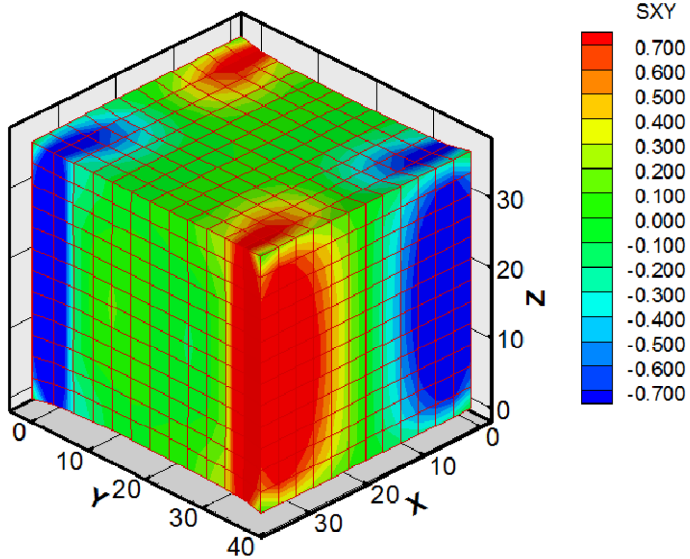

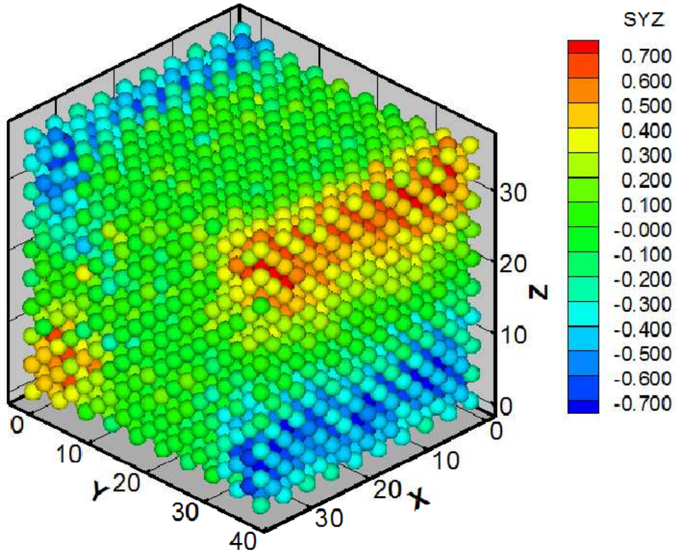

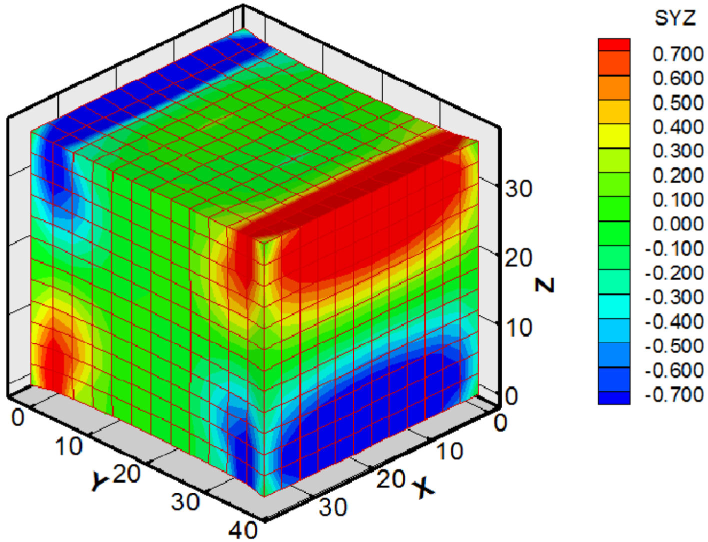

GOLD: UNIAXIAL TENSION/COMPRESSION L/H=1 , MM AND FEM SIMULATIONS
σxz DISTRIBUTIONS

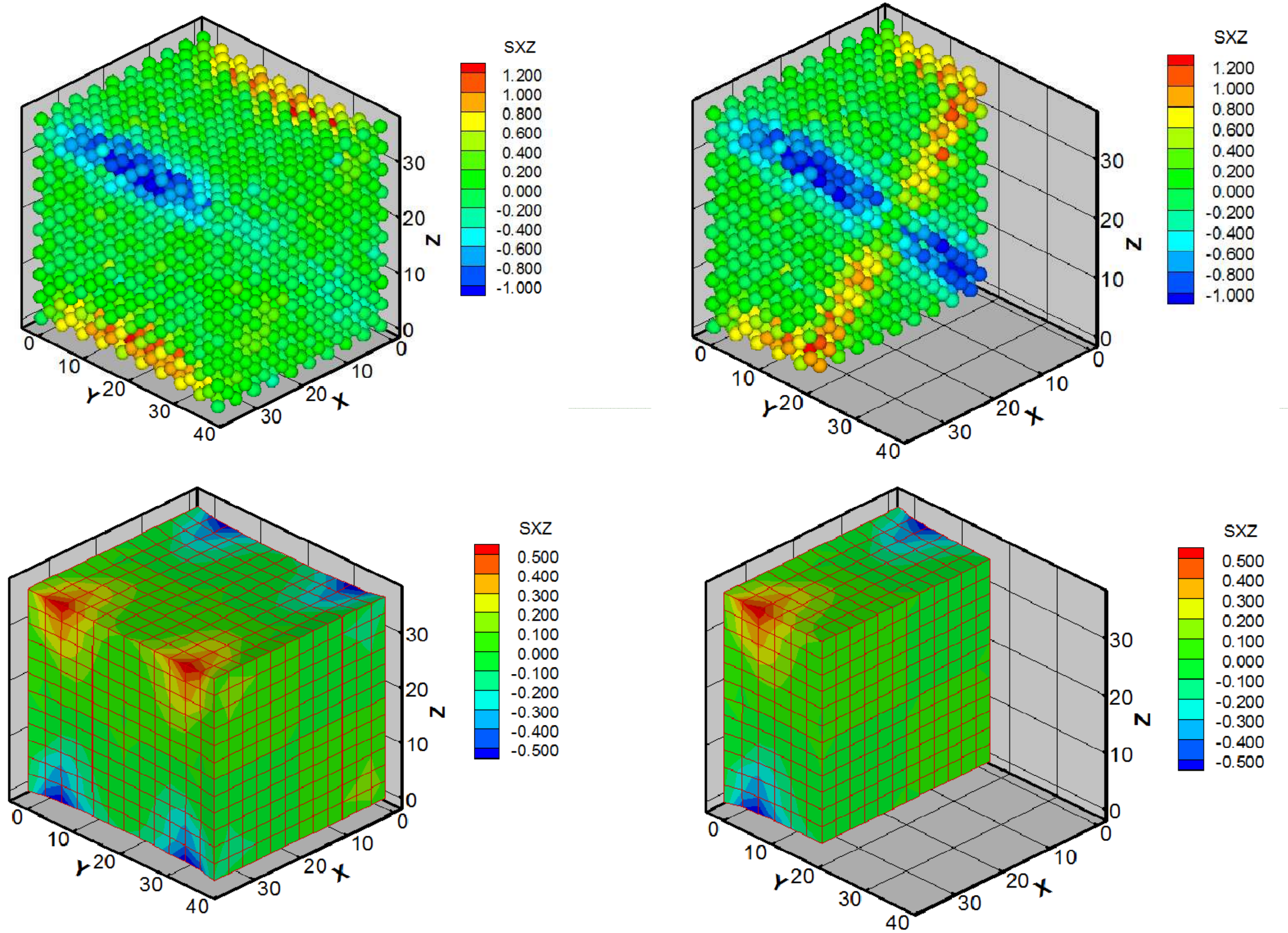

Summary: research topics

Determination of a homogeneous dislocation nucleation criterion based on higher order continuum mechanics theory.

Analysis of structural instabilities by MD+DFT simulation of mechanical tests.

Constitutive relations for amorphous materials based on the nucleation and evolution of the STZs. Implementation of the constitutive theory at macro-scale using homogenization theories.

Analysis of deformation mechanisms for grain boundaries in nano-cristalline materials and formulation of constitutive relations for implementation in multi-scale approaches.

Possibly:
- Constitutive relations for biomaterials, polymers and hydro-gels.
- Analysis of delamination and wear in protective coatings (DFT and MD).

Thank you!

Related publications:

A.A. Pacheco and R. C. Batra, Instabilities in Shear and Simple Shear Deformations of Gold Crystals, *J. of the Mechanics and Physics of Solids*, **56**, 3116-3143, 2008.

R. C. Batra and A. A. Pacheco, Local and Global Instabilities in Nano-size Rectangular Prismatic Gold Specimens, *Computational Materials Science* 46, 960-976.

R. C. Batra and A. A. Pacheco, Changes in internal stress distributions during yielding of square prismatic gold nano-specimens. Acta Materialia, 58 (8), pp. 3131-3161.

Contact information :

Alejandro Pacheco / apacheco@uninorte.edu.co